universität wien

MASTERARBEIT / MASTER'S THESIS

Titel der Masterarbeit / Title of the Master's Thesis

„Is Polyomavirus Middle Tumor Antigen induced cell transformation dependent on a PP2A chaperone?"

verfasst von / submitted by

Michaela Martina Zrelski, BSc

angestrebter akademischer Grad / in partial fulfilment of the requirements for the degree of

Master of Science (MSc)

Wien, 2019 / Vienna 2019

Studienkennzahl lt. Studienblatt / degree programme code as it appears on the student record sheet:	A 066 830
Studienrichtung lt. Studienblatt / degree programme as it appears on the student record sheet:	Masterstudium Molekulare Mikrobiologie, Mikrobielle Ökologie und Immunbiologie
Betreut von / Supervisor:	Ao.Univ.-Prof. Dr Egon Ogris

List of Contents

Abstract

The murine polyomavirus middle T antigen (PyMT) leads to cell transformation and induces a variety of tumors in new-born mice. Association of the catalytic C and structural A subunit of protein phosphatase 2A (PP2A) with PyMT leads to the assembly of the so-called transformation complex and is necessary for transformation. However, it has been shown that catalytically inactive C subunit can associate and build up the transformation complex. In this study, we wanted to investigate whether PTPA, protein phosphatase 2A activator, a protein known to be required for PP2A biogenesis, is involved in PyMT induced transformation. For this purpose we deleted PTPA in two different mouse embryonic fibroblast (MEF) lines using the Cre-Lox system. Additionally, we established stable *Ptpa* knock-out clones of a well-defined PyMT-expressing cell line using a combinatorial CRISPR/Cas9 approach. We investigated the phenotype in both cellular backgrounds and validated the results by re-expression of ectopic myc-tagged PTPA. We could show that the established phenotype of *Ptpa* knock-out could be reproduced. Analysis of the focus formation ability in MEFs lacking PTPA showed that the oncogenic potential of PyMT was impaired and could be rescued by myc-PTPA expression. Through PyMT immunoprecipitation experiments we found that the formation of the transformation complex, such as the association of PP2A A and C subunit as well as src kinase, was increased and not impaired. However, PyMT tyrosine phosphorylation was reduced rather than increased compared to the parental cells. These findings raise the questions how the transformation ability is impaired and whether PP2A and src activity are affected. Investigation of other proteins of the transformation complex, which were not included in this study, might be of future interest to further resolve the underlying mechanisms of cellular transformation and PTPA mediated regulation of PP2A.

Zusammenfassung

Das Middle T Antigen (PyMT) des murinen Polyomaviruses induziert Zelltransformation und verschiedene Tumore in neugeborenen Mäusen. Die Assoziation der katalytischen C und strukturellen A Untereinheit der Protein Phosphatase 2A (PP2A) mit PyMT ist die Grundlage für das Entstehen des sogenannten Transformationskomplexes und ist demnach notwendig für die zelluläre transformation. Interessanterweise kann auch katalytisch inaktive C Untereinheit mit PyMT assoziieren und den Transformationskomplex aufbauen. Ziel dieser Arbeit war es, die Auswirkungen des Protein Phosphatase 2A Aktivator Proteins (PTPA), ein Protein welches für die PP2A Biogenese benötigt wird, auf die von PyMT induzierte Transformation zu untersuchen. Zu diesem Zweck haben wir PTPA in zwei verschiedenen murinen embryonischen Fibroblastenzelllinien (MEF) mittels des Cre-Lox Systems deletiert. Des Weiteren konnten wir, durch die Anwendung eines kombinatorischen CRISPR/Cas9 Ansatzes, stabile *Ptpa* knock-out Klone in einer bereits etablierten PyMT exprimierenden Zelllinie herstellen. Wir haben in beiden zellulären Systemen den Phänotyp der *Ptpa* Deletion rekapituliert und die Resultate durch Reexpression von ektopischem, mit myc markiertem PTPA (myc-PTPA) validiert. Dabei konnten wir zeigen, dass der bereits etablierte Phänotyp der *Ptpa* Deletion reproduzierbar ist. Mittels Fokus Formation Analysen demonstrierten wir, dass in MEFs das onkogene Potential von PyMT beeinträchtigt ist, jedoch durch myc-PTPA Expression wiederhergestellt werden kann. Die Formation des Transformationskomplexes und demnach auch die Assoziation von PP2A A und C Untereinheiten, sowie der src Kinase, war erhöht und nicht beeinträchtigt in der Abwesenheit von PTPA. Im Gegensatz dazu, beobachteten wir jedoch eine Reduktion und nicht etwa einen Anstieg der Tyrosinphosphorylierung an PyMT in den knock-out Zellen. Im Folgenden, stellen sich hier die Fragen wie die Transformationsfähigkeit von PyMT beeinträchtigt und ob im Zuge dessen die Aktivität von PP2A und src beeinflusst wird. Weitere Untersuchungen, auch von weiteren Proteinen des Transformationskomplexes, die nicht Gegenstand dieser Arbeit waren, sind von Größtem Interesse und könnten helfen zukünftig die zugrundeliegenden Mechanismen der zellulären Transformation und der Regulation von PP2A durch PTPA aufzuklären.

1. Introduction

1.1. Protein Phosphatase 2A (PP2A)

A cells ability to react rapidly to external changes or stress is necessary to ensure its survival. Protein regulation via mostly reversible posttranslational modifications (PTM) is one way to respond. The most prominent among so far identified PTMs include ubiquitinylation, acetylation, nitrosilation, glycosylation and phosphorylation (Eichhorn et al. 2009). Phosphorylation was first described in 1932 (Lipmann and Levene 1932), however, it took another 20 years for the discovery of the first enzymatic phosphorylation process (Burnett and Kennedy 1954). Phosphorylation occurs mainly on the three amino acids Serine, Threonine and Tyrosine, at their respective hydroxyl group. Histidine, Lysine, Arginine (at their nitrogen) (Matthews 1995) as well as Cysteine (at its sulfur atom) (Guan and Dixon 1991) and Aspartate (at its acyl group) (Wagner and Vu 2000; Cieśla et al. 2011) have been found to be a target of phosphorylation as well (Buchowiecka 2014). In some studies Glutamate has also been addressed as a target for phosphorylation (Buchowiecka 2014; Lapek et al. 2015), however proteomic studies could not confirm these observations (Cieśla et al. 2011). Due to their labile chemistry and rareness the *in vivo* properties of the phosphorylation of these 5 (or 6) amino acids are largely unknown (Buchowiecka 2014). The addition of phosphate groups is typically catalysed by kinases, their removal by phosphatases. According to the respective modified amino acid, the responsible phosphatases for the removal of the hydroxyl group phosphorylations are grouped into three different categories: (i) serine/threonine phosphatases (PSTPs), (ii) tyrosine phosphatases (PTPs) and (iii) dual specificity phosphatases. The amino acid specificity and the catalytic mechanisms differ depending on the catalytic cores. Hence, PSTPs are metallo-phospho-esterases, requiring metal ions within their catalytic core in order to catalyse dephosphorylation (Burchell and Cohen 1978; Fellner et al. 2003).

Ser/Thr phosphorylation comprises >98 % of the phosphohydroxy-amino acids in proteins (Olsen et al. 2006). More recent studies estimate an even higher percentage, as the occurrence of phosphorylated tyrosine is <1% in typical mammalian cells (Hunter 2014). Surprisingly, while there is a large number of Ser/Thr kinases, only a small number of phosphatases exist (Moorhead et al. 2007). This raised the question of how specific regulation is achieved. The solution to this particular problem can be explained by the multisubunit architecture of these enzymes. A prime example for such an enzyme is protein phosphatase 2A (PP2A), a multisubunit architecture enzyme that is one of the cells major Ser/Thr phosphatases and ubiquitously expressed in all eukaryotic cells. Depending on the cell type it makes up to 0.3%-1 % of the total cellular proteins (Virshup 2000). The high functional importance of this protein is also reflected in terms of amino acid sequence conservation of the catalytic subunit, being over 90% between drosophila and mammals (Orgad et al. 1990).

The multisubunit protein consists of a heterodimeric core enzyme, a scaffolding A subunit (PPP2R1A/B or PR65) a catalytic C subunit (PPP2CA/B or PR36), and one of many regulatory B subunits. Active PP2A is primarily found as trimer, although also AC dimers and possibly a small number of C subunit monomers can be purified (Kremmer et al. 1997; Price and Mumby 2000). PP2A A subunit and C subunits are expressed in two isoforms, α and β. They originate from two highly homologous genes and while they are quite conserved (A 87% sequence similarity (Hemmings et al. 1990), C subunit 97% (Stone et al. 1987), they are functionally non-redundant (Gu et al. 2012; Götz et al. 1998; Zhou et al. 2003).

Regulation of substrate specificity and subcellular localisation is determined by the type of B subunit in the holoenzyme. Up to this point 15 genes for B subunits (Eichhorn et al. 2009) have been found. In contrast to the A and C subunit, those genes lack the high similarity. Hence they were subdivided into four families: B (PPP2R2A-D), B' (PPP2R5A-E), B'' (PPP2R3A-C) and Striatin (STRN1/3/4) (Shi 2009). Considering different isoforms plus additional splice variants, up to 26 different B-type subunits are known. Taking into account that Aβ does associate with only some of B-type subunits (J. Zhou et al. 2003) still a quite large number of PP2A enzymes can be formed, explaining how cells compensate for their apparent lack of phosphatase C subunit genes. As a result, it has been proposed to view PP2A as a family of enzymes rather than a single one (Sents et al. 2013).

PP2A is involved in a large number of signalling pathways, such as cell division, cell cycle regulation, cell survival and death upon many more (Fujiwara et al. 2016), which suggests that dysfunction of PP2A may cause severe diseases. Indeed, PP2A is a major tumor suppressor (Eichhorn et al. 2009), and participates in the pathogenesis of Alzheimer's disease (Sontag and Sontag 2014). The role in cancer development was first shown by the use of okadaic acid, an inhibitor of PP2A. By now mutations of A, B and C subunits have been linked to tumorigenesis and been found in a high percentage of human cancers (Eichhorn et al. 2009; Kiely and Kiely 2015). In other cellular context, however, PP2A can act as a tumor promotor itself (Ruvolo 2016).

In addition to the regulation by the B subunits, PP2A is tightly regulated by posttranslational modifications, most importantly at the far C terminus by phosphorylation and methylation. Reports have identified Thr304 and Tyr307 as phosphorylation sites and suggested that phosphorylation leads to inactivation of the PP2A C subunit (Chen et al. 1992a; Guo and Damuni 1993; Schmitz et al. 2010). Furthermore, various other proteins are involved in the regulation of PP2A, such as alpha4, TIPRL, LCMT-1, PME-1 and PTPA (Sents et al. 2013).

Methylation is catalysed by leucine carboxyl methyltransferase 1 (LCMT-1) at leucine 309 and reversed by phosphatase methylesterase 1 (PME-1). My host lab has compiled a model in yeast in which PPE1,

the yeast orthologue of PME-1, inhibits premature activation of the C subunit. Through the association of RRD2, the yeast orthologue of PTPA, and the methylation by PPM1, the yeast orthologue of LCMT-1, the active PP2A holoenzyme is generated (Hombauer et al. 2007). The current model for the generation of an active holoenzyme of my host lab can be reviewed in (Figure 1). In mammals methylation of PP2A C subunit is a necessary prerequisite for the association with the B subunit and also facilitates the binding of B' subunits, although not absolutely essential (Yu et al. 2001; Longin et al. 2007). Association with PP2A A subunit as well as B'' and STRN does not strictly require a methylated C subunit (Yu et al. 2001; Janssens et al. 2008; Sents et al. 2013). To widen the knowledge on how PP2A biogenesis takes place, my host lab performs diverse analysis on different factors, including the protein PTPA, in the generation of active PP2A.

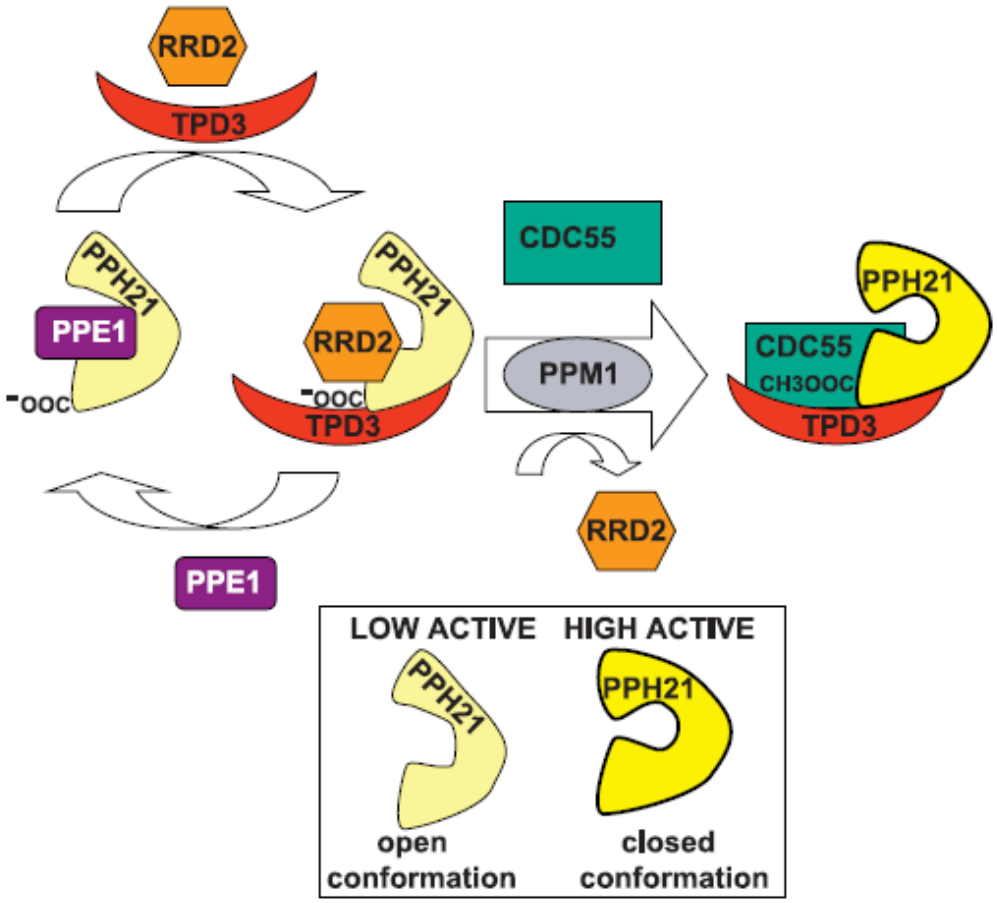

Figure 1 Current model of the generation of active PP2A holoenzyme in yeast. Inactive, low activity C subunit lacks the carboxymethylation at its C terminus. Before an activation can occur, RRD/PTPA needs to associate with the PP2A A and C subunit dimer. This displaces the enzyme PPE1. Through the methylation by PPM1 and the removal of RRD/PTPA the B subunit is recruited to the PP2A dimer. The C subunit is thought to switch into an active conformation (Hombauer et al. 2007).

1.2. Protein Phosphatase 2A Activator Protein (PTPA)

Protein Phosphatase 2A Activator Protein (PTPA), encoded by the *PPP2R4* gene, is a conserved protein from yeast to human. This is resembled by both, their sequence similarity (38% to Rrd1, 37% to Rrd2)

and functional equivalence. Deletion of the two homologues, Rrd1 and Rrd2, in yeast can be partially rescued by the introduction of mammalian PTPA (Fellner et al. 2003). PTPA was originally described as an ATP/Mg^{2+} dependent activator of the basal phosphotyrosine activity of PP2A *in vitro* (Cayla et al. 1990). Our lab first described a role for PTPA *in vivo*. PTPA is needed for proper function of the PP2A C subunit in yeast. Deletion of *Rrd1/Rrd2* leads to an altered substrate specificity, as activity towards pSer/pThr is reduced and enhanced towards a phospho-tyrosine analogue (Fellner et al. 2003). The exact role of PTPA remains elusive so far, but two major proposals have been put forward. A role for PTPA mediated stabilization of the PP2A C subunit during its activation was suggested, where PTPA prevents the misfolding of PP2A C subunit by stabilizing an active conformation and, together with ATP, enabling the loading of two catalytic metal ions into the active site. Crystallization experiments of PTPA, PP2A C subunit and ATP suggest that PTPA and PP2A C subunit form an ATP-binding pocket to orient the γ-phosphate into the active site, where the metal ions are chelated. In the following it was proposed that PTPA is an ATP dependent activating chaperone (Guo et al. 2014). Another model for PP2A activation via PTPA includes the prolyl *cis/trans* isomerase (PPI) activity of PTPA (Magnusdottir et al. 2006). A conserved Proline (Pro190) in PP2A C subunit was identified as the target of the PPI activity of PTPA. The catalysed switch is considered to activate the PP2A C subunit (Jordens et al. 2006). Evidence from Sents et al support this hypothesis, as they have shown that reduced and completely abolished PTPA expression leads to a reduction in PP2A activity (Sents et al. 2017). In contrast, we could not detect a reduction in PP2A activity or C subunit methylation using our model systems (Frohner et al. unpublished data). The importance of PTPA is resembled by the severe phenotypes of the knock-out strains and cells. Double deletion of *Rrd1/Rrd2* in the W303 yeast strain result in synthetic lethality and knock-out in mice is embryonically lethal. Further analysis led to the knowledge, that PTPA is needed for proper proliferation in yeast and in mammals, and proper chromosome separation (nucleus formation) (Frohner et al. unpublished data). An increased amount of apoptotic cells has been detected when PTPA was reduced and/or lost (Fellner et al. 2003). Other studies have reported that PTPA suppression promotes cancer development (Sablina et al. 2010; Sents et al. 2017).

1.3. Polyoma Virus Middle Tumor Antigen (PyMT)

In the 1950s the first tumor inducing viruses in mice were described, among those the murine polyomavirus (Morgan 2014). The diverse family of polyomaviruses owe their name to the first isolated virus causing multiple (*poly*) tumours (*oma*) when injected in new-born mice (Gross 1953). Polyomaviruses are small non-enveloped viruses with a small dsDNA genome infecting invertebrates, fish amphibians, reptiles, birds and mammals (reviewed in Moens et al. 2017). Among the most prominent polyomaviruses are Simian Virus 40 (SV40) and the pathogenic human polyomaviruses BKPyV, JCPyV and MCPyV, which have been attributed to being involved in the formation of cancer

(reviewed in Paoli and Carbone 2013; Delbue et al. 2014; Liu et al. 2019). Especially the Merkel Cell Polyomavirus (MCPyV) has been associated with the formation of highly aggressive tumors (Chang and Moore 2012).

The polyomavirus genome is organized in two regions, early and late. The early region of the small DNA virus encodes at least two tumor antigens, small T (PyST) and large T (PyLT) (Ichaso and Dilworth 2001), that are common to all polyomaviruses and origin from the same pre-mRNA (primary transcript), but different splicing patterns. In the murine and hamster polyoma virus a third tumor antigen (middle tumor antigen, PyMT) arises by differential splicing of the transcript from the early genome region (Moens et al. 2017). All three tumor antigens share a stretch of 79 amino acids at the N terminus, which represents a DnaJ domain. PyST and PyMT have additional 112 amino acids in common, followed by 4 (PyST) or 230 (PyMT) unique amino acids at the C terminus (Schaffhausen and Roberts 2009). Due to their transformation abilities, polyomaviruses such as SV40 and PyMT have proven themselves to be of significant importance in the unveiling of mechanisms of eukaryotic transcription and replication as well as cell growth and its deregulation (Fluck and Schaffhausen 2009). The tumor antigens, large tumor antigen in particular, play a major role in the polyomavirus life cycle. Similar to other viruses, polyomavirus infection starts by attachment and entry. Polyomavirus transcription and replication occurs in the nucleus, with the early genes being transcribed prior to viral DNA replication. The switch from early to late transcripts depends on the large T concentration at the promotor site, but also small T antigen plays a role (Shenk et al. 1976; Berger and Wintersberger 1986; Moens et al. 2017). The late genes are transcribed from the complementary strand in the opposite direction of the early genes. Transcriptional initiation of late genes is mediated by large T binding of cellular basal transcription factors such as TATA-binding protein and TBP-associated factors (Moens et al. 1997). In general, the late region encodes for capsid proteins, VP1 and VP2, which are similar to early genes, transcribed from the same alternatively spliced primary transcript (Smith et al. 1976; Good et al. 1988). The murine polyomavirus encodes for a third capsid protein, VP3 (Treisman and Kamen 1981). VP1 is the major structural capsid protein, arranged in 72 pentamers from 360 proteins into an icosahedral shape; each of those VP1 pentamers associates with either VP2 or VP3 protein, making up the internal cavity (Rayment et al. 1982; Barouch and Harrison 1994). PyLT binds the viral origin of replication and, thereby, initiates DNA replication mainly by recruiting cellular proteins for replication (Valle et al. 2006; DeCaprio and Garcea 2013). DNA replication requires cell cycle progression to the S phase, which is mediated by both, PyLT and PyST (Ogris et al. 1992; Porrás et al. 1999). Large T antigen interacts with retinoblastoma (Rb) family proteins (Ludlow et al. 1989; Ogris et al. 1993) and p53 (Doherty and Freund 1997; Chen et al. 1992b; Moens et al. 2017). Notably, large T Antigens alone can immortalize cells, a feature prominently used in research (Katakura et al. 1998; Maqsood et al. 2013). PyST for example assists PyLT by preventing PP2A-mediated PyLT dephosphorylation and also in the

induction of S-phase (Scheidtmann et al. 1991; Ogris et al. 1992). After virus particle assembly in the nucleus, polyomavirus is released by so far unknown mechanism (Erickson et al. 2012). Both, cell lysis and release from intact cells, have been suggested (Allison and Black 1967; Evans et al. 2015).

Interestingly, although, PyST shows also tumor inducing powers itself (Sontag et al. 1993), **PyMT** is the key to transformation (Fluck and Schaffhausen 2009), as it alone can already induce transformation in immortalized cells (Treisman et al. 1981). PyMT is a membrane localized protein (Carmichael et al. 1982) of 421 amino acids with no known catalytic activity (Fluck und Brian Schaffhausen 2009). It associates with PP2A A and C subunit (Pallas et al. 1990). PyMT does not differentiate between the two A subunit isoforms (Zhou et al. 2003), but it has been shown that PyMT displaces or prevents the binding of B subunits, especially of the B and B' family (Jackson and Pallas 2012). Interestingly, it does not differentiate between methylated or non-methylated C subunit as well (Yu et al. 2001; Ogris et al. 1997). Binding of PP2A allows association and activation of the Src family tyrosine kinases, src, yes and fyn (Courtneidge and Smith 1983; Kornbluth et al. 1987; Horak et al. 1989; Dunant and Ballmer-Hofer 1997). The Src family of nonreceptor protein tyrosine kinases are involved in signal transduction pathways promoting cell survival, growth, division and migration and are classical proto-oncogenes themselves (Juan and Ong 2012; Roskoski 2015). In fact, it was a Src kinase that was first described as oncogene (Stehelin et al. 1976). Src is N-terminally myristoylated and consists of a unique domain, a src-homology 3 (SH3) domain, and a SH2 domain, a SH2-kinase linker domain, a protein-tyrosine kinase domain (SH1) and a C-terminal regulatory segment (Brown and Cooper 1996; Thomas and Brugge 1997). Myristoylation facilitates the insertion of src into membranes (Brown and Cooper 1996). SH3 domains mediate protein-protein interactions with proline rich domains, while SH2 domains serve as binding sites for phosphotyrosines and SH1 domains comprise the catalytically active site (Pawson and Schlessinger 1993). Activity of src kinase is regulated by tyrosine phosphorylation itself, as pY527 phosphorylation characterizes inactive src kinase, while intramolecular autophosphorylation at pY416 leads to kinase activity (Brown and Cooper 1996; Smart et al. 1981; Boggon and Eck 2004).

While the binding of PP2A A and C subunit is absolutely necessary for cell transformation, the catalytic activity of PP2A is not (Ogris et al. 1999); at least not in cis. In turn, src phosphorylates PyMT to further recruit proteins (Ichaso and Dilworth 2001). This suggests, that the PyMT/PP2A complex might act as a scaffolding platform (Figure 2) or it leads to the binding of src, which then phosphorylates tyrosine residues at Y250, Y315 and Y322 (Fluck and Schaffhausen 2009). P-Y250 provides a binding site for the Shc family (Campbell et al. 1994), activating the RAS-RAF-MAP kinase pathway and ultimately leading to enhanced proliferation (Garnett and Marais 2004). The Shc family contains adaptor proteins that provide help to recruit signalling molecules and, thereby, transduce signals, such as the conversion of extracellular to intracellular signals (reviewed in Ahmed and Prigent 2017). P-Y315 leads to binding of the regulatory p85 subunit of Phophoinositide 3-kinase (PI3K) (Kaplan et al. 1987), a lipid kinase family

that phosphorylates the 3'-hydroxyl group of the inositol ring on phosphatidylinositol, resulting in the generation of lipid signalling molecules (Vanhaesebroeck et al. 2010). The activation of this pathway enhances cell growth and survival (Sheridan and Downward 2013). In this specific case, PI3K leads to the activation of AKT kinase (Meili et al. 1998). At the third residue (Y322) binds the phospholipase Cγ1 (PLCγ1) (Su et al. 1995). Mutation of the binding site Y322 did not have an effect on transformation under normal serum conditions, but led to a reduced transformation in low serum conditions (Su et al. 1995). Alongside, a connection to calcium signalling has been proposed. Activation of PLCγ1 leads to the production of the second messenger molecules inositol-1,4,5-triphosphate (IP_3; soluble) and diacylglycerol (DAG; membrane-bound) and ultimately to the activation of the protein kinase C family, which itself is involved in tumor formation (Jang et al. 2018), as shown by a study where PyMT-mediated tumorigenesis was impaired in mice with a protein kinase C beta knock-out (Wallace et al. 2014). However, in comparison to the other two sites (Y250 and Y315), little is known about the consequences of p-Y322 and the subsequent association of PLCγ1 (Schaffhausen and Roberts 2009). Proteins that belong to the 14-3-3 and Heat shock 70 (Hsp70) family are known to associate to PyMT in a PP2A-independent manner (Pallas et al. 1994; Campbell et al. 1995). The 14-3-3 proteins bind to PyMT (Pallas et al. 1994) via phosphoserine 257 (Culleré et al. 1998) and Hsp70 proteins bind at the first 79 amino acids, when PP2A is not bound to PyMT (Pallas et al. 1989; Schaffhausen and Roberts 2009). Parts of the Hippo pathway, such as TAZ (transcriptional coactivator with PDZ-binding motif) and YAP (yes-associated protein) have been shown to associate to PyMT in a PP2A dependent way as both proteins need the formation of the transformation complex beforehand (Tian et al. 2004; Rouleau et al. 2016; Denis et al. 2017). TAZ binds to amino acids 2 to 4 and as this region is part of all three tumor antigens, it is not surprising that an association occurs with PyST, PyMT and PyLT (Tian et al. 2004). The association of YAP was originally identified in context with PyST at the residues 103 and 182 (Hwang et al. 2014), later confirmed to be valid also for PyMT (Rouleau et al. 2016). The Hippo pathway itself is involved in organ size, cell proliferation, and survival as well as stem cell proliferation and maintenance and is considered a major tumor-suppressor pathway (Zhao et al. 2011). A novel study using a proteomics approach identified novel binding partners, such as Lipins, Ran GAP, RanBP1 and the catalytic subunit of Protein Phosphatase 4 (PP4), which were not studied in context with PyMT so far (Rouleau et al. 2016).

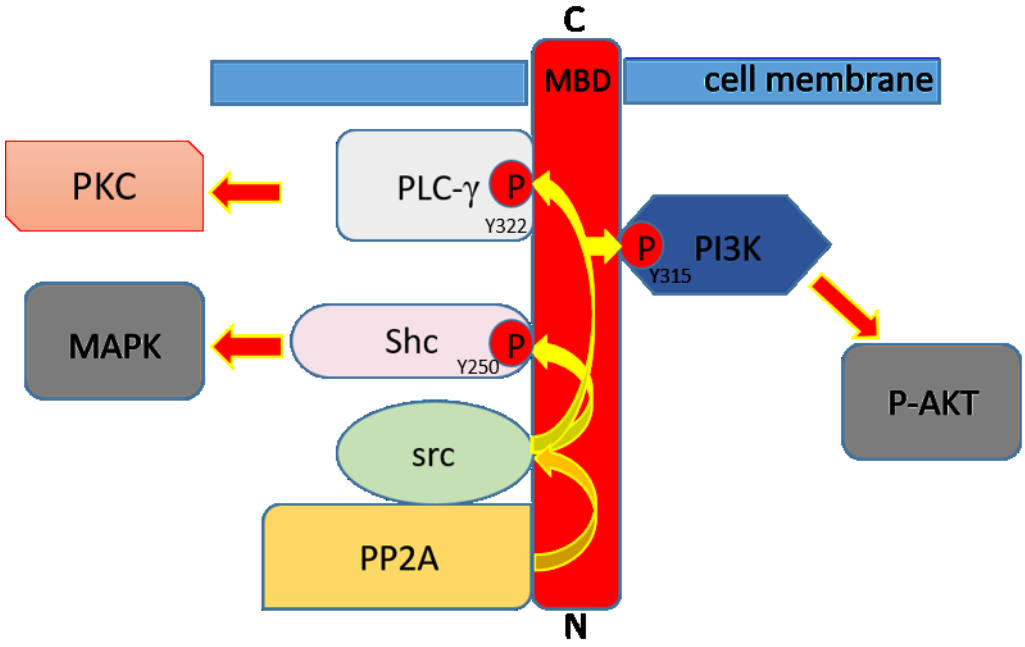

Figure 2 model of the PyMT/PP2A scaffold and connected proteins and downstream targeted pathways. Yellow arrows always indicate the consequence of the protein association and or activity. PP2A (=Protein phosphatase 2A) associates near the N terminus. MBD = membrane binding domain (near the C terminus) is a stretch of 22 hydrophobic amino acids (Soeda et al. 1979). pY250, pY315 and pY322 are the major phosphorylation sites of the src kinases, associated proteins to them are marked.

1.4. Methods for Generation of Knock-Out Cells

1.4.1. Cre-Lox System

Cre is a site-specific recombinase of the P1 bacteriophage (Sternberg and Hamilton 1981). It catalyses the recombination of two *loxP* (locus of crossover in Phage P1) sites, a 34 bp consensus sequence (Janbandhu et al. 2014). This system has been utilized for genome editing in eukaryotes and is nowadays wide-spread (van Duyne 2015). It can be used for a variety of applications, such as mutating or deleting genes, introducing defined chromosomal aberrations or knock-in of genes (Nagy 2000). Within these applications are constitutively active Cre, Cre expressed under the promotor of tissue specific genes or fused to a mutated tamoxifen-responsive hormone-binding domain of the estrogen receptor (Cre-ER^{T}). The later allows the control over Cre recombinase activity, via the localization of the fused estrogen receptor in the cytoplasm. The Cre-ER^{T} fusion protein is only recruited to the nucleus upon tamoxifen administration (Indra et al. 1999; Janbandhu et al. 2014). Depending on the scientific question different approaches can be selected, thereby circumventing possible complications, such as developmental defects or embryonic lethality upon targeting essential genes. The administration of tamoxifen and the subsequent effect are possible to use *in vivo* as well as *in vitro*.

1.4.2. CRISPR/Cas9 System

The Clustered Regularly Interspaced Short Palindromic Repeats (CRISPR) locus in combination with the CRISPR associated (Cas) proteins is a prokaryotic antiviral defence mechanism found in over 50% of bacteria and 90% of archaea (Makarova et al. 2015). The successful story of CRISPR/Cas began with the first identification in *Escherichia Coli* in 1987, where the locus was encountered as unusual sequence element consisting of a series of 29 highly conserved nucleotide repeats with 32 nucleotides spacing in between (Ishino et al. 1987). The biological significance of this finding was only solved 20 years later, when by a combination of computational analysis, genetic and biochemical studies the function of the CRISPR locus together with Cas proteins as an RNA-guided nuclease system involved in the defence against extrachromosomal genetic material was revealed (Bolotin et al. 2005; Makarova et al. 2006; Barrangou et al. 2007; Brouns et al. 2008; Deltcheva et al. 2011). Since then a wealth of information on the various systems utilizing CRISPR/Cas has accumulated.

Up to now six different systems have been found, all of which share the general three steps: (i) spacer acquisition, also referred to as adaptation, (ii) CRISPR RNA (crRNA) biogenesis and (iii) interference (Wright et al. 2016). In all systems upon the encounter of foreign DNA, which originates from bacteriophages or plasmids, a cleavage and integration as novel spacer of 20-50 base pairs into CRISPR locus happens. Those reactions are primarily carried out by Cas proteins (Wright et al. 2016). To avoid the targeting of the own CRISPR locus, a specific 2-5 base pairs long protospacer adjacent motif (PAM) must be located next to the acquired sequence on the foreign DNA piece, but not in the CRISPR locus. Each crRNA, which is later on integrated into an effector complex, is transcribed from the CRISPR locus and processed from a pre-crRNA to the mature crRNA. During the interference phase, the crRNA Watson-Crick base pairs with the complementary foreign DNA, which is then cleaved on both strands by the endonuclease component of the effector complex. This only happens upon recognition of the specific PAM and is in general again performed by Cas proteins (reviewed in Wright et al. 2016).

The different systems are defined by the respective enzymes involved in the immunity process and labelled from Type I to Type VI. Depending on the multi or single subunit effector systems the six CRISPR types are additionally grouped into two classes, namely Class 1 (multi-subunit effector system, Types I, III and IV) or Class 2 (single-subunit effector systems, Type II, V and VI). The type II CRISPR/Cas system needs as single-subunit effector system only the endonuclease Cas9 for performing DNA cleavage plus two small RNAs (crRNA and a trans-acting tracrRNA) (Shmakov et al. 2014; Makarova et al. 2015; Makarova and Koonin 2015).

Through the generation of a chimeric single guide RNA (sgRNA or gRNA) in *Streptococcus pyogenes* it was shown *in vitro* that a piece of DNA could be targeted. Additionally, it was proposed that virtually any DNA could be cleaved and further edited. Targeting of a locus can be achieved by designing a 20

bp seed gRNA complementary to the specific locus, next to a PAM (5'-NGG-3') site. Cas9 endonuclease will then cut the between the 17th and 18th base pair (Jinek et al. 2012). Refinement of this system has made it suitable for application in mammalian cells (Ran et al. 2013b).

The gene editing properties of CRISPR/Cas can be used in cells of model systems to disrupt gene loci and thereby in the simplest case generate knock-outs by introducing a DSB, which is then repaired through non-homologous end joining (NHEJ), the cells natural mechanism to repair DSB. It has been shown that the repair by this error prone, insertions or deletions (indel) forming mechanism is enough to achieve a knock-out (Choi and Meyerson 2014; Singh et al. 2015). Another possibility is to provide the cell with a template, which is included through homology directed repair (HDR). Using this method a more precise editing and further the generation of knock-outs as well as knock-ins is possible (Singh et al. 2015). Cas9 has been mutated to yield a higher specificity in genome editing through a transition from the nuclease to nickase properties, thereby introducing single strand breaks in the DNA (Ran et al. 2013a). Additionally nuclease dead Cas9 (dCas9) has been created, which is viewed as an RNA-guided DNA binding protein and can be used to interfere with the transcriptional and epigenetic regulation of specific loci (Wang and Qi 2016). An overview of current applications can be found in Figure 3.

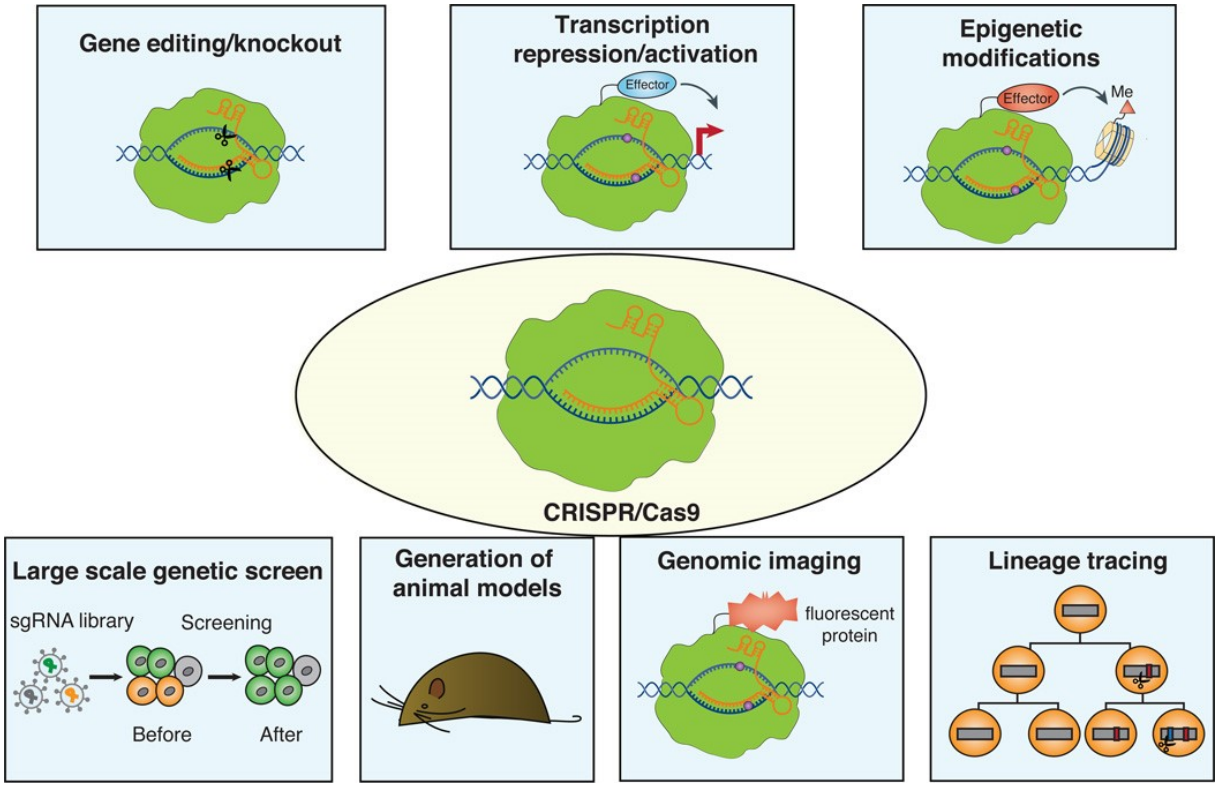

Figure 3 **Applications of CRISPR/Cas9** (F. Wang and L. Qi 2016)

The CRISPR/Cas systems certainly have revolutionized the gene editing field. However, this systems has its limitations, including the appropriate finding of a PAM motif and off-target effects, as Cas9

tolerates a mismatch between the gRNA and the target DNA (Le Cong et al. 2013; Wang and Qi 2016). The limitation of PAM sites is narrow, as the NGG motif appears approximately every 10 base pairs in the human and the murine genome (Ran et al. 2013b; Pelletier et al. 2015) and the variety of different type II CRISPR/Cas systems provide alternatives for the sequence NGG (Wang and Qi 2016). Bioinformatic tools have been designed to calculate the probability of off-target effects, thereby weakening the problem (Listgarten et al. 2018; Lin and Wong 2018).

1.5. Aims of this Study

PP2A is not only crucial for the transforming properties of PyMT (Fluck and Schaffhausen 2009) but also for the pathogenesis of a variety of diseases (Eichhorn et al. 2009; Sontag and Sontag 2014; Kiely and Kiely 2015). However, even after thorough investigation, there are still open questions regarding the role of PP2A, especially in the transformation process. The aim of this project was to investigate whether PP2A needs PTPA to correctly associate with PyMT and whether the transformation ability of PyMT is impaired by *Ptpa* knock-out. In addition, we anticipated, as it was often the case in the past with the combined research of PyMT and PP2A, to learn more about the cellular role of PP2A in the absence of PTPA through studying the impacts on PyMT. Also, as in our lab the study of PTPA is an extensive area of research, we wanted to produce additional evidence for the general phenotype of *Ptpa* knock-out in different cellular backgrounds and with different knock-out methods, being the Cre-Lox and CRISPR/Cas9 system.

2. Results

2.1. Analysis of available Cell Systems for Conducting *Ptpa* Knock-Out Experiments

Initially, the use of mouse embryonic fibroblasts (MEFs) 112 # 4 single clone B6 and 326 # 6 single clone G5 gave hints for an involvement of PTPA in PyMT-induced transformation of MEFs (Stadtmann et al. 2019). However, the phenotype could not be investigated properly up to this point. This was due to certain limitations with both, the G5 and the B6, clones. In earlier studies PTPA was first deleted in G5 cells, which were subsequently transformed with PyMT. However, even the G5 $Ptpa^{fl/fl}$ clone was not efficiently transformed. Thus, the G5 cell line was not included in our experimental set-ups. For the B6 cells we applied a different experimental set-up, where the cells were first transfected with PyMT and then PTPA deletion was induced. Here two complications occurred: Firstly, upon tamoxifen treatment *Ptpa* was not deleted in each and every cell and these $Ptpa^{fl/fl}$ cells outgrew the knock-out cells over time. Therefore, we plated the focus formation assays at the latest 12 days after tamoxifen-induced deletion of PTPA, a time point where the remaining floxed cells had not outgrown the knock-out cells yet. Secondly, we noticed in the focus formation assays that the percentage of PyMT transformed cells increased over the time the PyMT expressing cells were propagated in culture (Stadtmann et al. 2019).

Therefore, we used B6 PyMT cells in two conditions, at early ("young") and late ("old") passage numbers. Young cells had been in culture 30 days post infection with a retroviral PyMT vector (pBabe hygro PyMT), were then frozen and re-thawed for our analysis. Old cells had been in culture for more than 90 post infection with PyMT retrovirus, were frozen and then re-thawed during my Wahlbeispiel, frozen again after approximately 50 days and re-thawed for this analysis. Additionally, we included an empty vector control (pBabe hygro), where the exact timeframe was not monitored strictly. For the empty vector control cells we included only the *Ptpa* floxed and not delta cells, as the phenotype of those knock-out cells had already been established and would not have provided additional information in this specific set-up (Frohner et al. unpublished data). Both PyMT expressing cell lines (old and young) were subjected to tamoxifen treatment (described in 4.4.2) resulting in *Ptpa* knock-out cells. The three cell types were labelled B6 hygro $Ptpa^{fl}$, B6 PyMT $Ptpa^{fl}$ and B6 PyMT $Ptpa^{\Delta}$ for simplicity reasons (Figure 4).

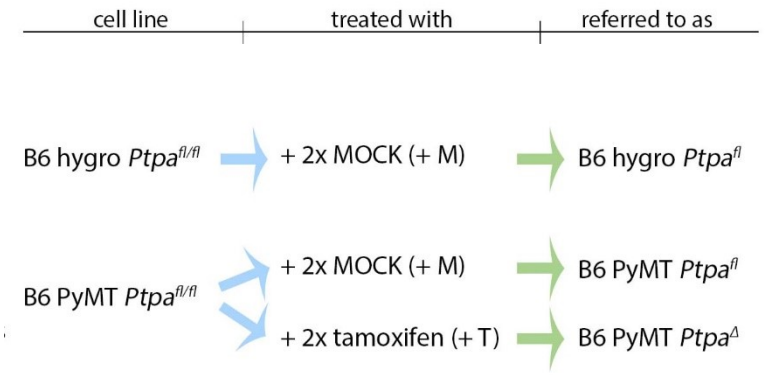

Figure 4 **Overview of B6 Cells and their Labelling** B6 hygro *Ptpa*$^{fl/fl}$ and B6 PyMT *Ptpa*$^{fl/fl}$ were two times mock-treated (+ M) or two times tamoxifen-treated (+ T).

We started our experiments with old B6 PyMT (detailed schedule see table 1a) and moved on to young B6 PyMT cells to overcome the limitation of older cells to incompletely delete *Ptpa* (detailed schedule see table 1b).

Table 1 **Time schedule of assays with B6 Cells.** Days post infection (= d.p.i) with retroviral supernatant carrying PyMT are indicated, in violet the day post PyMT at the date of thawing. FFA = Focus Formation Assay, IP = immunoprecipitation

a B6 PyMT *Ptpa*$^{fl/fl}$ cells (thawed 140 days post PyMT infection)

treated with tamoxifen/MOCK		**FFA plated**	**duration FFA**	**IP performed**
1st time	**2nd time**			
145 d.p.i.	**147** d.p.i.	**152** d.p.i.	**15 days**	**154** d.p.i.
147 d.p.i.	**149** d.p.i.	**154** d.p.i.	**15 days**	
149 d.p.i.	**152** d.p.i.	**156** d.p.i.	**14 days**	**159** d.p.i.
170 d.p.i.	**173** d.p.i.	**180** d.p.i.	**16 days**	

b B6 PyMT *Ptpa*$^{fl/fl}$ cells (thawed 30 days post PyMT infection)

treated with tamoxifen/MOCK		**FFA plated**	**duration FFA**	**IP performed**
1st time	**2nd time**			
37 d.p.i.	**38** d.p.i.	**46** d.p.i.	**19 days**	**48** d.p.i.
39 d.p.i.	**40** d.p.i.	**51** d.p.i.	**16 days**	**51** d.p.i.
51 d.p.i.	**52** d.p.i.	**60** d.p.i.	**50 days**	
53 d.p.i.	**54** d.p.i.	**65** d.p.i.	**45 days**	**66** d.p.i.
61 d.p.i.	**62** d.p.i.			**75** d.p.i.

We monitored *Ptpa* deletion by PCR and Western blot. The PCR setup enables a differentiation between three states of the *Ptpa* locus, wild type (wt), floxed (fl) and delta (Δ) (+/fl/Δ PCR). In our set-up we determined whether cells were floxed or delta, hence the PCR should either give a 366 bp fragment (fl) or 509 bp fragment (Δ). Time course experiments by Ingrid Frohner showed that over

90% of the *Ptpa* locus were deleted upon the first tamoxifen treatment (Frohner et al. unpublished data). The second treatment was performed within the following three days to make sure that *Ptpa* was deleted.

In the **old B6 cells** the PCR gave a band at the size of ~350 bp (fl) in B6 PyMT *Ptpa*^{fl} cells, which correlated with the calculated size of the PCR product when the loxP sites are still present (fl). In the PCR of B6 hygro *Ptpa*^{fl} and B6 PyMT *Ptpa*$^{\Delta}$ there was a strong band detectable at the size of ~500 bp, correlating with the calculated size of the knock-out (Δ) PCR product, and a weaker floxed band (Figure 5a). Western blot analysis revealed that approximately one quarter of B6 PyMT *Ptpa*$^{\Delta}$ cells still expressed PTPA (Figure 5b). From this data we deduced that the mock-treated B6 hygro *Ptpa*^{fl} cells had undergone *Ptpa* deletion, although no tamoxifen was added. This was not observed for B6 PyMT *Ptpa*^{fl} cells. Deletion of the *Ptpa* locus had occurred approximately 60-80% of in the tamoxifen treated B6 PyMT *Ptpa*$^{\Delta}$ cells.

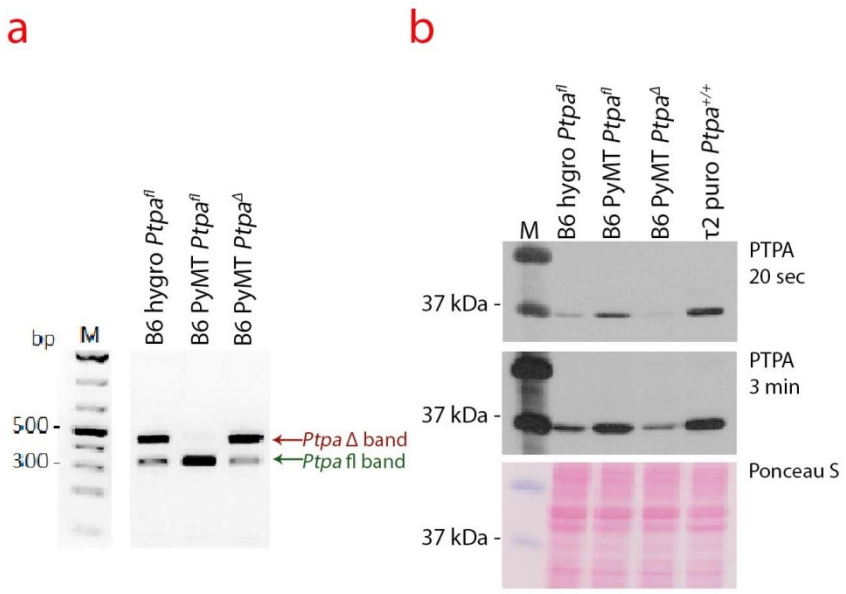

Figure 5 **PCR and Western blot analysis of Old B6 PTPA (*Ptpa*^{fl}) and *Ptpa* Knock-Out Cells (*Ptpa*$^{\Delta}$) (a)** Genotyping PCR to determine the configuration of the *Ptpa* locus in B6 cells. B6 hygro *Ptpa*^{fl} and B6 PyMT *Ptpa*^{fl} cells were treated with MOCK, B6 PyMT *Ptpa*$^{\Delta}$ cells were treated with tamoxifen. Products of PCR were separated by electrophoresis on a 1.4% Agarose gel. Marker and samples were separated on the same gel but not adjacent to another, indicated by the gap. **(b)** Analysis of PTPA expression. Whole cell lysates of B6 hygro *Ptpa*^{fl}, B6 PyMT *Ptpa*^{fl}, B6 PyMT *Ptpa*$^{\Delta}$ and τ2 puro *Ptpa*$^{+/+}$ cells were tested for PTPA expression. τ2 puro *Ptpa*$^{+/+}$ cells were used as positive control (*Ptpa* wild-type locus).

In the **young B6 cells** the PCR gave a band at the size of ~350 bp (fl) in B6 hygro *Ptpa*^{fl} and B6 PyMT *Ptpa*^{fl} cells. PCR of B6 PyMT *Ptpa*$^{\Delta}$ samples resulted in a strong Δ band (~500 bp) and a faint floxed band (~350 bp). In B6 PyMT *Ptpa*$^{\Delta}$ cells PTPA protein levels were reduced to almost undetectable amounts, as showed in Western blot analysis (Figure 6b). Thus, *Ptpa* deletion was more efficient in young than in old B6 cells, but still incomplete. Here the control B6 hygro *Ptpa*^{fl} cells were fl and not Δ cells. Next, we examined the PTPA expression by Western blot analysis.

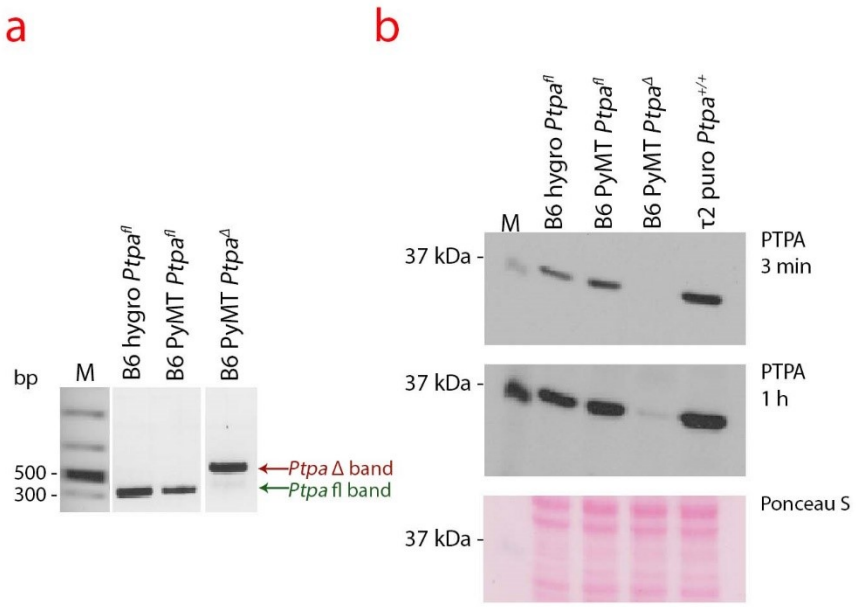

Figure 6 **PCR and Western blot analysis of Young B6 Cells Expressing PTPA (*Ptpa*^{fl}) and *Ptpa* Knock-Out Cells (*Ptpa*$^{\Delta}$) (a)** Genotyping PCR to determine the configuration of the *Ptpa* locus in B6 cells. B6 hygro *Ptpa*^{fl} and B6 PyMT *Ptpa*^{fl} cells were treated with MOCK, B6 PyMT *Ptpa*$^{\Delta}$ cells were treated with tamoxifen. Products of PCR were separated by electrophoresis on a 1.4% Agarose gel. Marker and samples were separated on the same gel but not adjacent to another, indicated by the gap. **(b)** Analysis of PTPA expression. Whole cell lysates of B6 hygro *Ptpa*^{fl}, B6 PyMT *Ptpa*^{fl}, B6 PyMT *Ptpa*$^{\Delta}$ and τ2 puro *Ptpa*$^{+/+}$ cells were tested for PTPA expression. τ2 puro *Ptpa*$^{+/+}$ cells were used as positive control (*Ptpa* wild-type locus).

To investigate whether *Ptpa* deletion had an effect on the transformation efficiency of PyMT we performed focus formation assays with young and old B6 cells. While non-transformed cells stop proliferating as soon as a monolayer is formed, transformed cells keep on proliferating and form foci (Alvarez et al. 2014). We plated 200, 100 and 50 cells of old PyMT *Ptpa*^{fl} and *Ptpa*$^{\Delta}$ together with a layer of B6 hygro *Ptpa*^{fl} cells. All dark violet spots distinguishable by eye were defined as foci and counted (Figure 7a). I performed a single factor analysis of variances (ANOVA) to test whether the means of the focus percentages were similar. As the necessary criteria were met (F<F crit.), I could combine the results (Supplementary Figure 1). With an efficiency of 29%±3% PyMT *Ptpa*^{fl} formed significantly more foci than PyMT *Ptpa*$^{\Delta}$ cells did (20%±7%) (Figure 7b).

To have a second, more unbiased analysis we also measured the colour density of the plates (Guzmán et al. 2014). In contrast to the counted foci, the area analysis showed no significant difference between PyMT floxed and delta cells (Figure 7c).

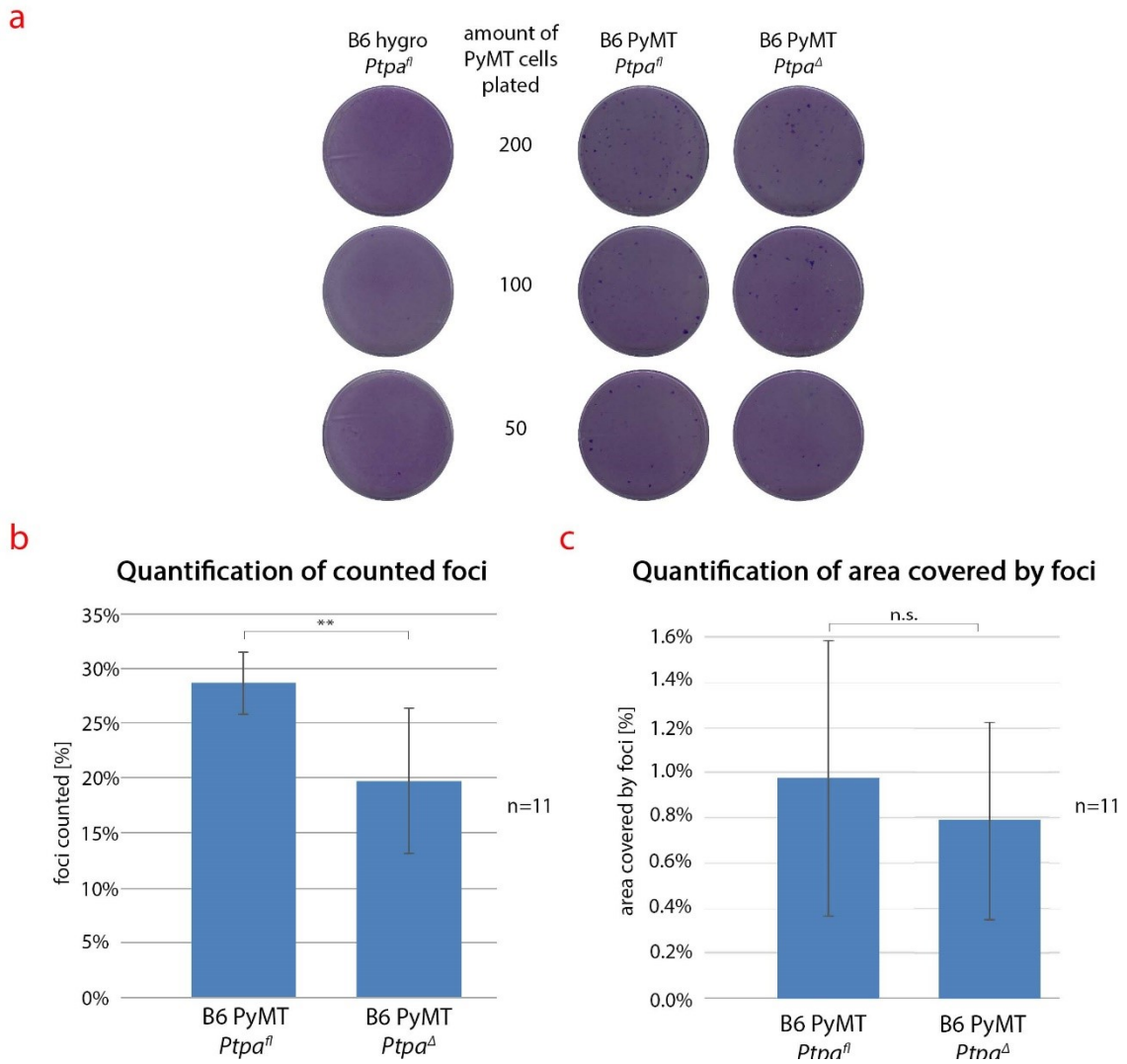

Figure 7 **Analysis of the Transformation Ability of Old B6 Cells Expressing PTPA (*Ptpa*^{fl}) and B6 *Ptpa* Knock-Out Cells (*Ptpa*$^{\Delta}$)** **(a)** Representative scans of focus formation assay. B6 *Ptpa*^{fl} cells expressing only the empty vector (hygro) were plated together with 200, 100 or 50 cells of B6 PyMT cells either *Ptpa*^{fl} or *Ptpa*$^{\Delta}$. *Ptpa* knock-out was induced 7-10 days before plating. Foci were stained after 14-16 days. Graphical representation of the **(b)** percentage of foci counted and **(c)** average area covered by foci. Data in are representative of four independent assays with 11 experimental values (n=11). Standard deviation and statistical significance are indicated. Statistical significance was calculated using Student's T-Test (two tailed, unpaired, unequal variance) with P values * < 0.05; ** < 0.01; *** < 0.001

Next we examined the **young B6 PyMT** cells, where we plated 500, 200 and 100 cells of young PyMT *Ptpa*^{fl} and *Ptpa*$^{\Delta}$ with a layer of B6 hygro *Ptpa*^{fl} cells. Higher cell numbers were plated because of the lower transformation efficiency of younger cells (Zrelski et al. unpublished data). As the first preliminary results showed no focus formation after an incubation period of 16-19 days (data not shown), we wondered whether longer incubation of the plates would lead to an increase in focus formation and therefore incubated the follwoing assays, under constant monitoring and change of medium, up to 50 days. This was however not the case (Figure 8a) and, due to the high variability within the data, our results were inconclusive (Figure 8b and c). Also here we combined the values from all floxed and delta cells after performing an ANOVA (Supplementary Figure 2).

In conclusion, we could recapitulate our observations on reduced focus formation in PyMT *Ptpa*$^{\Delta}$ in the old B6 PyMT cells, but with a drastically less severe phenotype than in our previous data, and in generally reduced focus formation in young cells (Stadtmann et al. 2019; Zrelski et al. unpublished data).

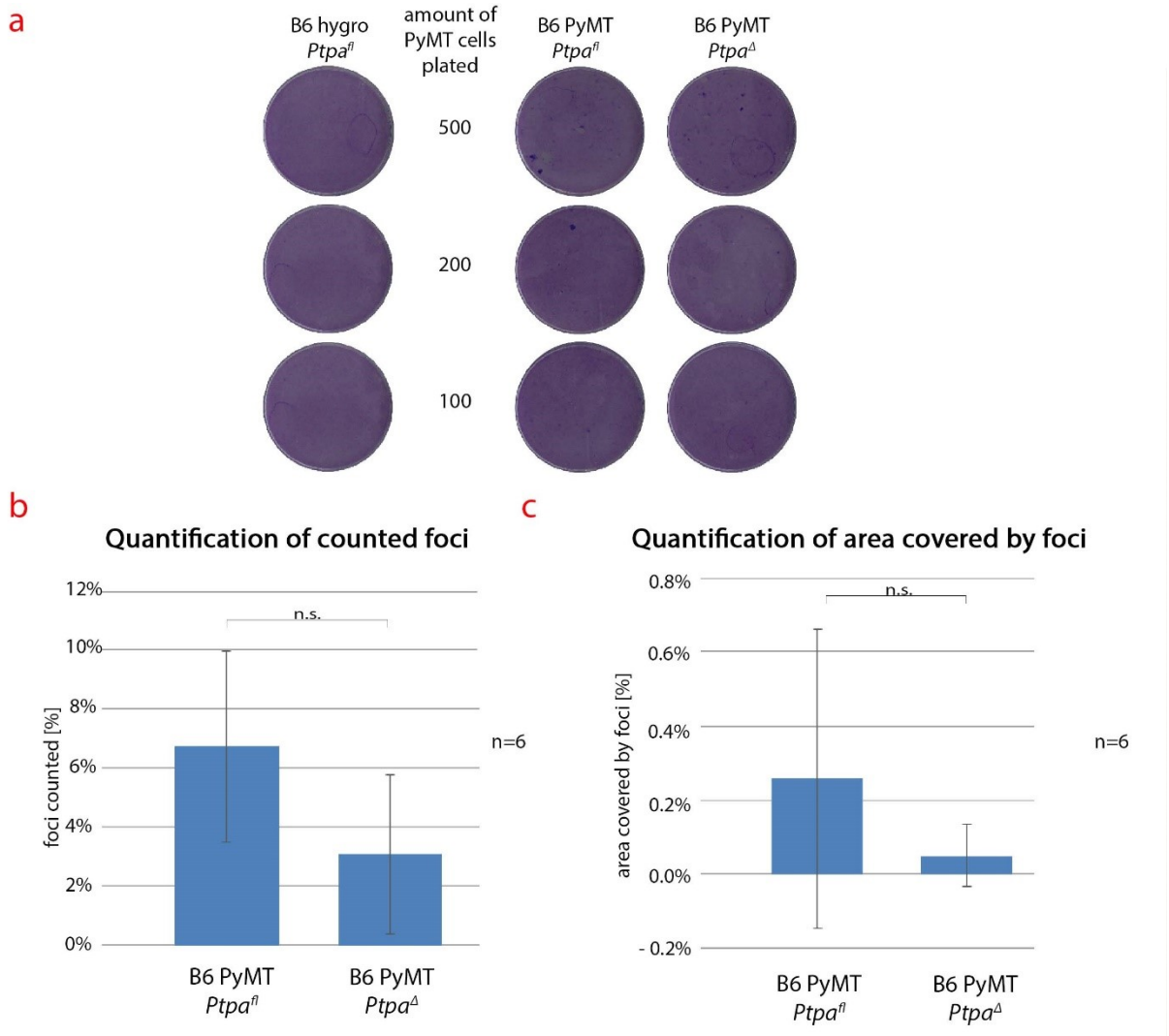

Figure 8 **Analysis of the Transformation Ability of Young B6 Cells Expressing PTPA (*Ptpa*^{fl}) and B6 *Ptpa* Knock-Out Cells (*Ptpa*$^{\Delta}$) (a)** Representative scans of focus formation assay. B6 *Ptpa*^{fl} cells expressing only the empty vector (hygro) were plated together with 500, 200 or 100 cells of B6 PyMT cells either *Ptpa*^{fl} or *Ptpa*$^{\Delta}$. *Ptpa* knock-out was induced 9-12 days before plating. Foci were stained after 16-50 days. Graphical representation of the **(b)** percentage of foci counted and **(c)** average area covered by foci. Data in are representative of four independent assays with 12 experimental values (n=12). Standard deviation and statistical significance are indicated. Statistical significance was calculated using Student's T-Test (two tailed, unpaired, unequal variance) with P values * < 0.05; ** < 0.01; *** < 0.001

In parallel to the focus formation experiments, we performed **immunoprecipitations** via PyMT in old and young B6 cells to find out whether PyMT transformation complex formation was altered in *Ptpa* knock-out cells.

In the lysate of **old B6 cells** we detected not only full-length PyMT (56 kDa) but also a shorter fragment of approximately 40 kDa, which was three times more abundant than the full-length protein (Figure 9, left panels). Expression of PP2A A subunit, PP2A C subunit and src kinase was not different between

Ptpa^{fl} and *Ptpa*$^{\Delta}$ cells. As expected, pY416 tyrosine phosphorylation of src kinase, a modification that upregulates src activity was increased in PyMT expressing cells. PTPA was detected in lysates of PyMT *Ptpa*^{fl} as well as PyMT *Ptpa*$^{\Delta}$, providing an explanation for the small (if at all) differences between floxed and delta cells observed in the focus formation assays (Figure 7b and c).

Interestingly, it appears that full-length PyMT was slightly better immunoprecipitated by the PyST antibody than the 40kDa species. The reason for this is unknown. Further, the expression of PyMT was slightly increased in PyMT *Ptpa*$^{\Delta}$ cells. In both cell types PyMT was able to form a complex with PP2A and active src kinase, as demonstrated by the co-immunoprecipitations. We observed tyrosine phosphorylation of full-length PyMT, but less tyrosine phosphorylation on the shorter fragment (Figure 9, right panels).

In the lysates of young B6 cells both fragments of PyMT were present, however approximately half of the total protein amount was made up of the 40 kDa protein (Figure 10a, left panels). Thus it seems that formation of the 40 kDa fragment increases over time. Otherwise overall protein expression was similar to old B6 cells, with the exception of PTPA. PTPA was well detected in floxed but hardly in delta cells.

According to the IP results we concluded that in both cell types, fl and delta, PyMT could equally initiate the building of the transformation complex via PP2A and src kinase (Figure 10b). PyMT was tyrosine phosphorylated to a similar extent and again, the smaller PyMT protein was phosphorylated less (Figure 10a).

In summary, we could not find a distinctive difference between B6 PyMT *Ptpa*^{fl} and *Ptpa*$^{\Delta}$ cells, with the exception of the ratio between the full-length protein and the 40 kDa fragment. Because of the observed limitations, such as incomplete *Ptpa* deletion, of the B6 clone we decided not to use the B6 cells any further and developed two approaches to generate new cell lines for future approaches.

On the one hand, we generated new *Ptpa* knock-out cells using the Cre-Lox system with a new vector construct; on the other hand, we used CRISPR/Cas9 using two guide RNAs targeting the *Ptpa* locus.

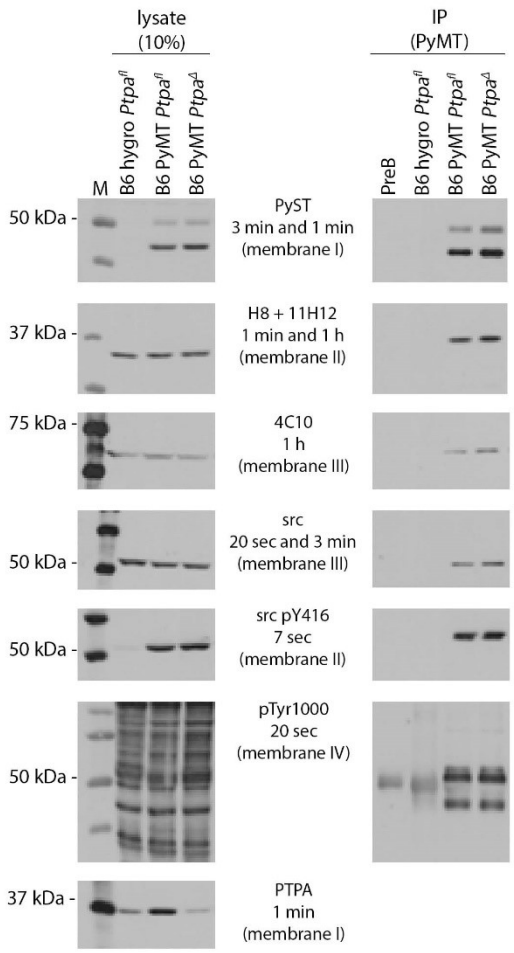

Figure 9 **Interaction between PyMT and its Associated Proteins in Old B6 Cells Expressing PTPA (*Ptpa*^{fl}) and B6 *Ptpa* Knock-Out Cells (*Ptpa*$^{\Delta}$)** Immunoprecipitation was performed via PyMT, using the rabbit polyclonal anti-PyST antibody. Empty vector (B6 hygro *Ptpa*^{fl}) and preimmune serum (PreB, incubated with PyMT *Ptpa*^{fl} lysates) were used as negative control. 10% of the protein amount of the IP were loaded for the lysates (left panel). Samples were separated on a 10% SDS-PAGE. Membranes were incubated in the following order: Membrane I: PyST (PyMT) and PTPA, Membrane II: H8+11H12 (PP2A C Subunit) and pY416 src, Membrane III: 4C10 (PP2A A Subunit) and src, Membrane IV: pTyr1000. For the detection of Co-IPs of PP2A A and C subunit as well as src 20% ECL select was used. Blots are representative of 2 independent experiments.

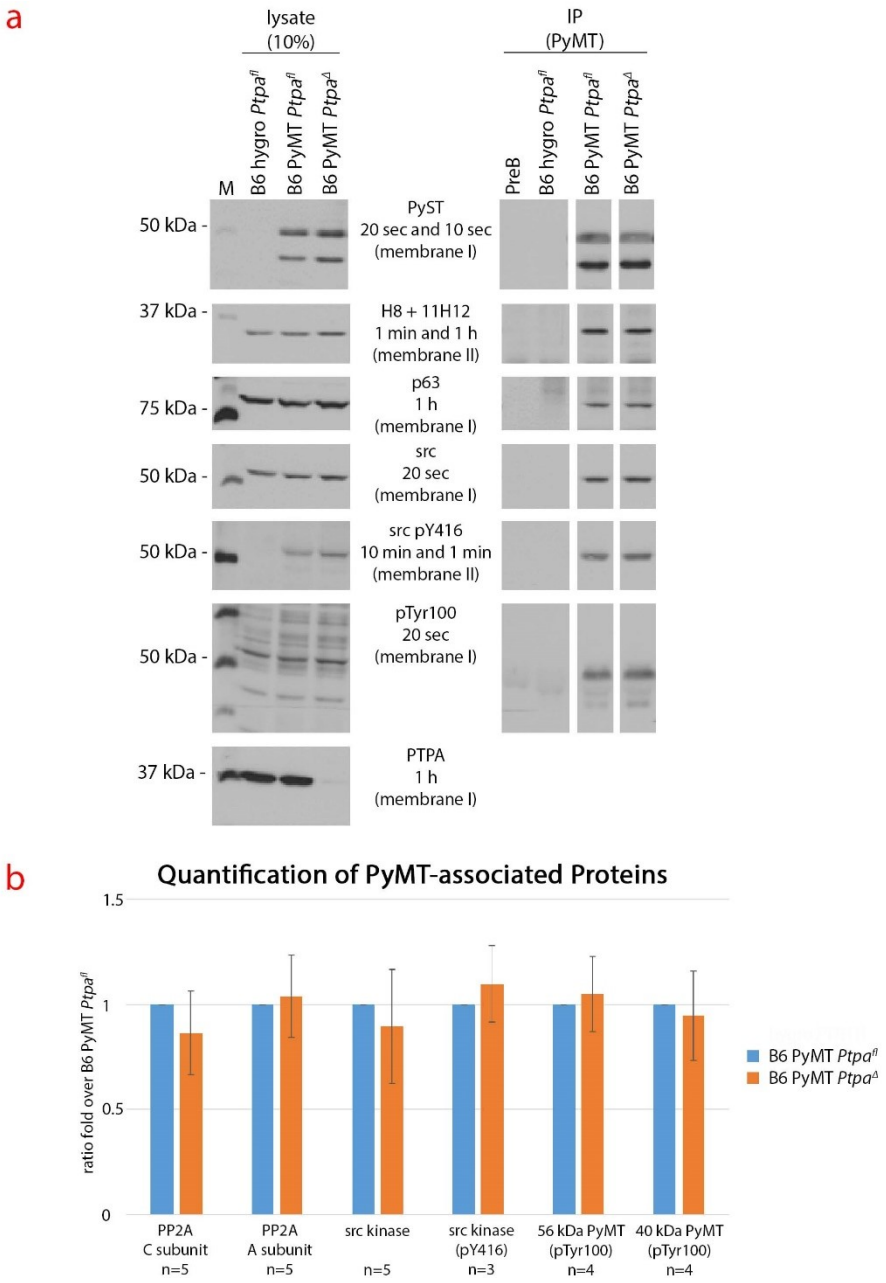

Figure 10 **Interaction between PyMT and its Associated Proteins in young B6 Cells Expressing PTPA (*Ptpa*^{fl}) and B6 *Ptpa* Knock-Out Cells (*Ptpa*$^{\Delta}$)**. **(a)** Immunoprecipitation was performed via PyMT, using the rabbit polyclonal anti-PyST antibody. Empty vector (B6 hygro *Ptpa*^{fl}) and preimmune serum (PreB, incubated with PyMT *Ptpa*^{fl} lysates) were used as negative control. Since overall expression of PyMT was increased in delta cells, 66% of PyMT were loaded. 10% of the protein amount of the IP were loaded for the lysates (left panel). : Membrane I: p63 (PP2A A subunit), pTyr100, src, PyST (PyMT) and PTPA, Membrane II: H8+11H12 (PP2A C subunit) and pY416 src. For the detection of Co-IPs of PP2A A and C subunit as well as src 20% ECL select was used. Blots are representative of 5 independent experiments. **(b)** Quantification of PyMT-associated proteins normalized to the immunoprecipitated, full-length PyMT. Number of values 5 independent experiments (n=5, for pY416 src kinase (n=3), for tyrosine phosphorylation of PyMT n=4) and standard deviations, that were calculated using the Excel function, are indicated.

2.2. Generation of *Ptpa* Knock-Out Cells Using Cre Recombinase

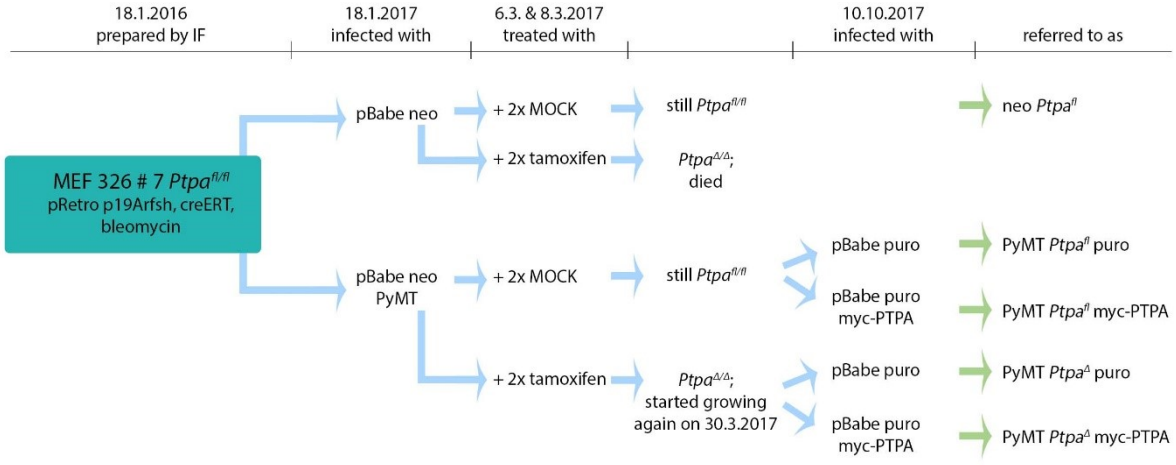

Figure 11 **Overview and time line of 326 MEF # 7 cell line** Isolation and infection with pRetro bleo and pBabe neo were performed by Ingrid Frohner. Tamoxifen was administrated twice, two days apart. Time line lacks the different freezing and thawing cycles in between. Infection with retroviral supernatant of pBabe puro with or without myc-PTPA was only performed with PyMT expressing cells (lower path).

We established a new MEF cell line using a novel cre-ER^T expression vector that enabled complete deletion of *Ptpa*. For this purpose, a new vector construct was designed, carrying p19Arfsh for immortalisation together with Cre recombinase fused to a bleomycin resistance over a cleavable T2A linker (Lange et al. 2012). The generated cells were only resistant to bleomycin when simultaneously expressing cre-ER^T.

In total, we immortalized five primary MEFs. 326 MEFs # 7 (326 # 7) were infected with a retroviral supernatant carrying either pBabe neo or pBabe neo PyMT. Further, those cells were treated with tamoxifen twice (Figure 11). Upon treatment with tamoxifen we observed a severe reduction in proliferation (data not shown). Treated 326 # 7 neo cells died, while 326 # 7 PyMT cells experienced a growth arrest, however, after 22 days in culture some PyMT expressing cells started to grow again. For simplicity reasons, cells were labelled neo *Ptpa*^{fl} (326 # 7 pBabe neo *Ptpa*$^{fl/fl}$), PyMT *Ptpa*^{fl} (326 # 7 pBabe neo PyMT *Ptpa*$^{fl/fl}$) and PyMT *Ptpa*$^{\Delta}$ (326 # 7 pBabe neo PyMT *Ptpa*$^{\Delta/\Delta}$), as depicted in Figure 11.

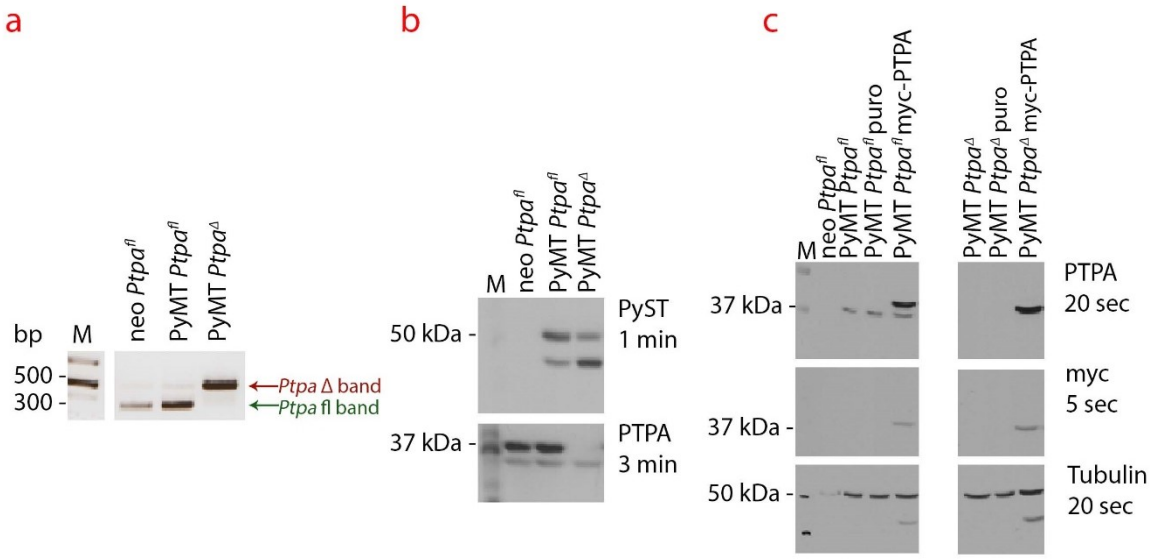

Figure 12 **Analysis of 326 # 7 Cells Expressing PTPA (neo *Ptpa*^{fl}, PyMT *Ptpa*^{fl}) and *PTPA* Knock-Out (PyMT *Ptpa*^{Δ}) Cells (a)** Genotyping PCR to determine the configuration of the *Ptpa* locus in 326 # 7 cells. Cells were tested more than 7 days post treatment. Products of PCR were separated by electrophoresis on a 1.4% Agarose gel. Marker and samples were separated on the same gel but not adjacent to another, indicated by the gap. **(b)** Analysis of PTPA and PyMT expression of neo *Ptpa*^{fl}, PyMT *Ptpa*^{fl} and PyMT *Ptpa*^{Δ} cells after a 10% SDS-PAGE. **(d)** Analysis of myc-PTPA expression in PyMT *Ptpa*^{fl} (left panels) and *Ptpa*^{Δ} (right panels) cells. Whole cell lysates were separated on a 10% SDS-PAGE and analysed for PTPA and myc expression (two separate membranes). Tubulin was used as control and incubated after PTPA.

We monitored *Ptpa* deletion with PCR and Western blot analysis. In the **neo *Ptpa*^{fl} and PyMT *Ptpa*^{fl} cells** the PCR gave a band at the size of ~350 bp (fl). PyMT *Ptpa*^{Δ} cells produced a band of ~500 bp (Δ) (Figure 12a). Immunoblot analysis of the 326 # 7 protein lysates showed PTPA expression in neo *Ptpa*^{fl} and PyMT *Ptpa*^{fl} but not in PyMT *Ptpa*^{Δ} cells, indicating a complete *Ptpa* knock-out (Figure 12b). The signal at 36 kDa in all three lanes corresponded to PP2A C subunit derived from a previous incubation with PP2A C subunit antibody. PyMT expression was similar in PyMT *Ptpa*^{fl} and PyMT *Ptpa*^{Δ} cells and we again observed the 40 kDa fragment. Interestingly, in PyMT *Ptpa*^{fl} the full-length protein was twice as much as the 40 kDa fragment, in PyMT *Ptpa*^{Δ} it was vice versa.

Timo Schwab (a Wahlbeispiel student) evaluated the new cell lines and showed that Cre recombinase was approximately four to five times overexpressed in comparison to our previous models. In addition he also revealed that upon treatment with tamoxifen all tested cell lines (*Ptpa*$^{+/+}$, *Ptpa*$^{fl/+}$, *Ptpa*$^{fl/fl}$) were affected in terms of proliferation rate, growth arrest and micronucleus formation (Schwab et al. unpublished data). This was quite problematic, as the phenotypes of *Ptpa* deletion and Cre overexpression were not clearly distinguishable. To distinguish between the PTPA knock-out and Cre dependent phenotype we included control cell lines expressing myc-PTPA (PyMT *Ptpa*^{fl} myc-PTPA and PyMT *Ptpa*^{Δ} myc-PTPA, Figure 11) and tested whether those could rescue the observed phenotypes. Expression check showed that ectopically expressed myc-PTPA was at least four times overexpressed

compared to endogenous PTPA (Figure 12c). Tubulin was included as loading control unveiling that scarcely any protein was loaded in neo *Ptpa*^{fl} samples.

2.2.1. Analysis of the *Ptpa* Deletion Phenotype versus Cre Induced Phenotype

2.2.1.1. Exogenous Expression of myc-PTPA Rescued Micronucleus Phenotype

Enhanced micronucleus formation has been shown to be a consequence of either *Ptpa* deletion (Frohner et al. unpublished data) or DNA damage by Cre overexpression (Loonstra et al. 2001; Janbandhu et al. 2014). Thus we asked whether the effect of enhanced micronucleus formation could be reversed in PyMT *Ptpa*$^{\Delta}$ cells by re-expressing myc-PTPA (Figure 13a).

In the PyMT *Ptpa*$^{\Delta}$ puro cells the percentage of cells with normal nuclei were reduced compared to floxed levels (83.0%±2.3%). The number of cells with one micronucleus (12.5%±3.1%), two micronuclei (2.0%±1.4%) and more than two micronuclei (2.6%±1.7%) was significantly higher than in floxed cells (6.1%+1.2%, 0.5%±0.6% and 0.5%±0.4%) (Figure 13b). Expression of myc-PTPA restored normal nucleus morphology (94.0%±1.5%). Hence, we concluded, that the observed phenotype of abnormal nucleus formation was indeed caused by *Ptpa* deletion.

Overexpression of PTPA in PyMT *Ptpa*^{fl} cell lines did not affect nuclear morphology (Figure 13b). Surprisingly, also neo *Ptpa*^{fl} cells, which were used as PyMT negative control, had showed enhaced formation of abnormal nuclei. 11.1%±4.8% showed one micronucleus, 1.7%±1.6% two micronuclei and 1%±0.8% more than two micronuclei. In accordance the number of normal cells was reduced to 86.2%±6.8% (Figure 13b).

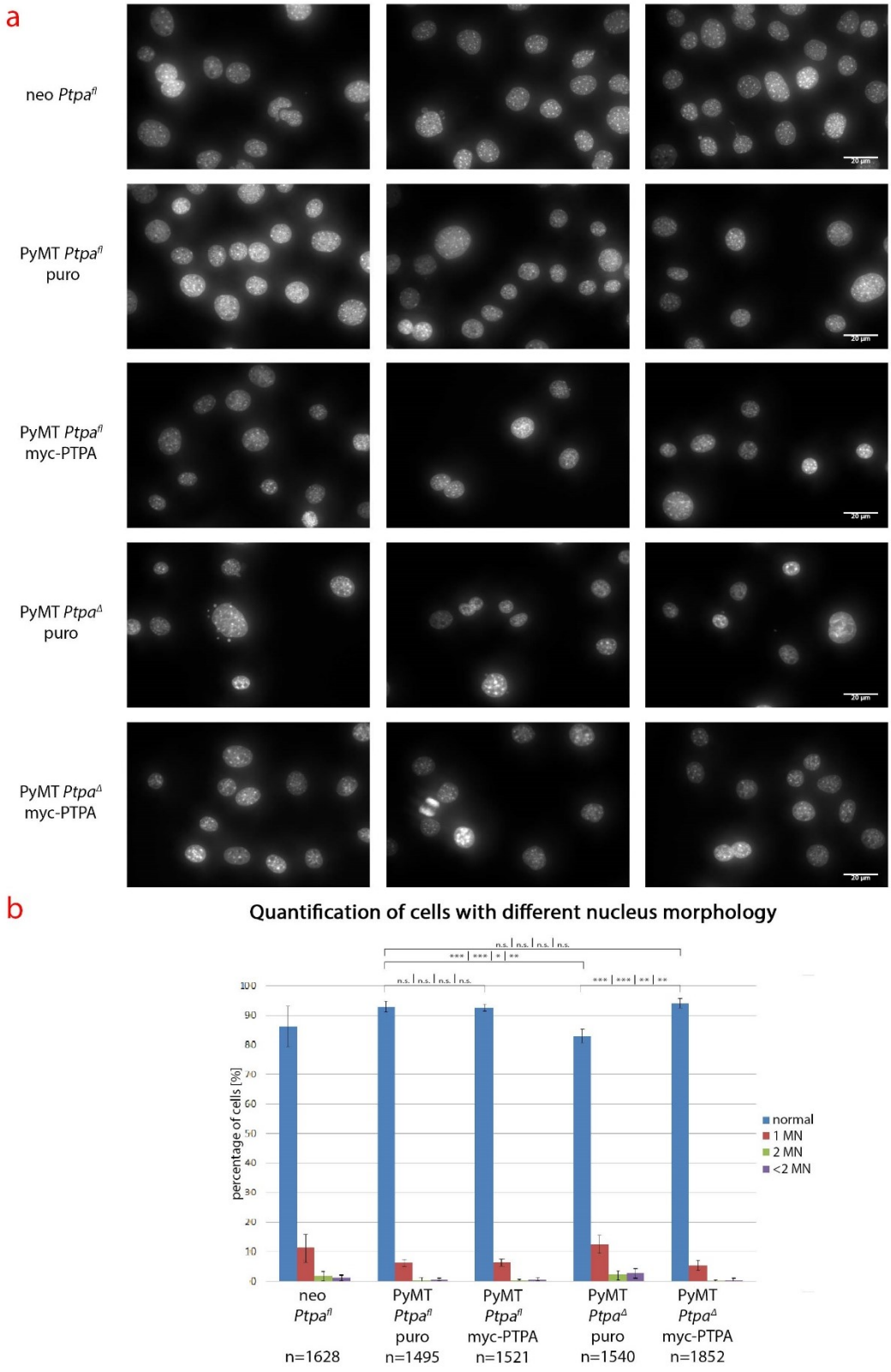

Figure 13 **Micronucleus Analysis of 326 # 7 Cells Expressing PTPA and/or myc-PTPA and *Ptpa* Knock-Out Cells (a)** Representative pictures of DAPI staining of neo *Ptpa*^{fl}, PyMT *Ptpa*^{fl} puro, *Ptpa*^{fl} myc-PTPA as well as PyMT *Ptpa*$^{\Delta}$ puro and *Ptpa*$^{\Delta}$ myc-PTPA. Pictures were recorded with Zeiss "ApoTome", 40x magnification. Cells during mitosis were not taken into account. Scale bar = 20 µm **(b)** Quantification of cells. In blue cells with normal nuclei, red showing the ones with one micronucleus (1 MN), green two (2 MN) and violet more than two (<2 MN. Amount of counted cells is indicated below each cell line. Statistical significance was calculated using Student's T-Test (two tailed, unpaired, unequal variance). P values * < 0.05; ** < 0.01; *** < 0.001

2.2.1.2. *Ptpa* Deletion Led to Altered Proliferation of the Cells

In addition to enhanced micronucleus formation, we also observed that overexpression of Cre recombinase led to reduced proliferation rates, especially after tamoxifen induction (Schwab et al. unpublished data).

The proliferation of PyMT $Ptpa^{\Delta}$ puro cells was reduced compared to the PyMT floxed cells, but exceeded the proliferation of neo $Ptpa^{fl}$ (Figure 14a and b). However, this reduction was within standard deviation. The total cell number increased similarly in the PyMT floxed in all time points, but the doubling time differed at 96 hours. Ectopic expression of myc-PTPA could increase the proliferation rate to floxed levels in *Ptpa* knock-out cells, even superseding them (Figure 14b). In comparison to PyMT expressing cells, neo $Ptpa^{fl}$ cells showed a typical growth curve that flattened after cells reached confluency after 72 hours (Figure 14a). This was also reflected by the calculation of the doubling time tending towards infinity (851 hours; Figure 14c). Notably, all tested cell lines kept proliferating towards the 168h time point, even though cells had already reached confluency. *Ptpa* knock-out leads to enlarged cells (Frohner et al. unpublished data). PyMT expressing cells that lack *Ptpa* and neo $Ptpa^{fl}$ cells were approximately 2 µm larger than PyMT cells expressing PTPA (Figure 14d). In general, we observed that a correlation between cell density and cell size existed, since cell size was reduced on denser plates (Figure 14d).

a

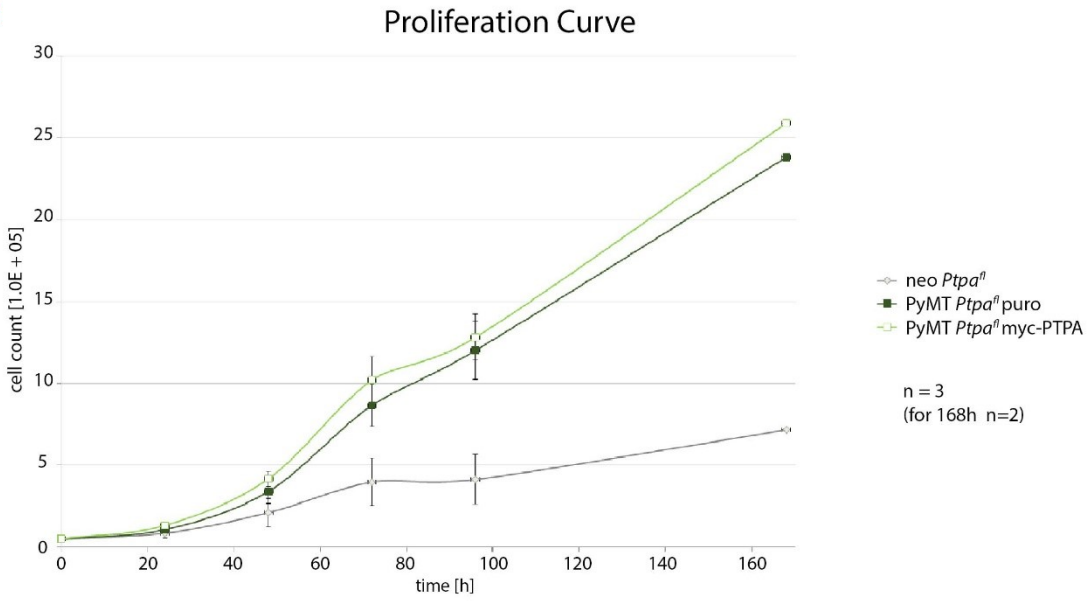

b

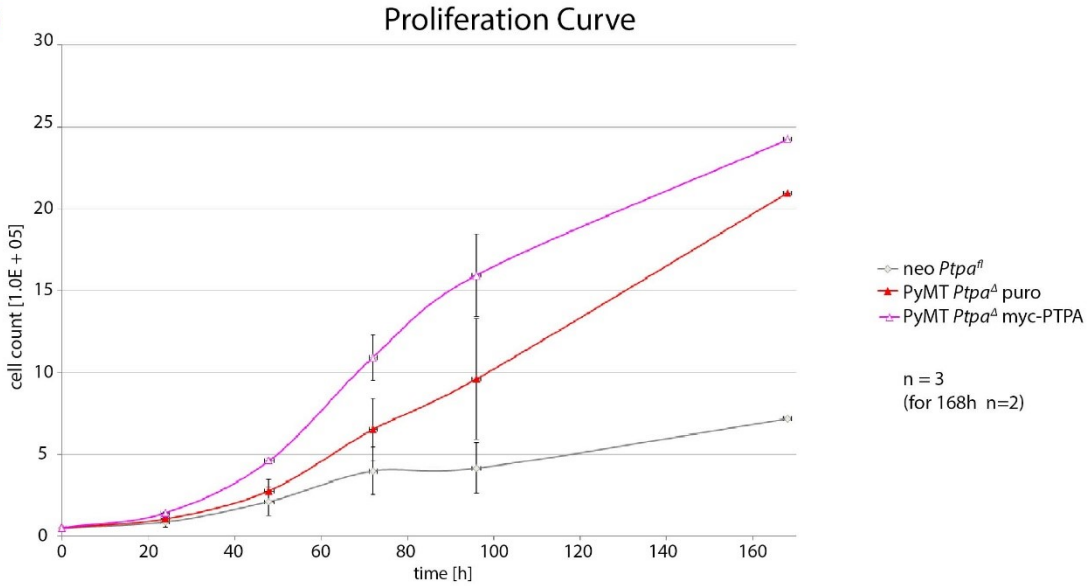

c

time point	24 hours	48 hours	72 hours	96 hours
neo *Ptpa*^{fl}	39.5 ± 19.9	20.2 ± 3.6	27.4 ± 3.4	851.0 ± 1412.9
PyMT *Ptpa*^{fl} puro	21.6 ± 6.1	14.9 ± 1.0	18.6 ± 1.7	47.6 ± 2.5
PyMT *Ptpa*^{fl} myc-PTPA	15.5 ± 2.4	15.1 ± 0.3	19.5 ± 0.7	68.3 ± 8.0
PyMT *Ptpa*^{Δ} puro	24.2 ± 10.3	17.6 ± 0.9	21.2 ± 3.9	44.8 ± 9.5
PyMT *Ptpa*^{Δ} myc-PTPA	14.6 ± 1.8	14.6 ± 0.8	20.3 ± 1.5	41.9 ± 4.5

d

after	24 hours [µm]	48 hours [µm]	72 hours [µm]	96 hours [µm]	168 hours [µm]
neo *Ptpa*^{fl}	23.1 ± 0.6	22.0 ± 1.3	22.2 ± 1.6	22.8 ± 1.6	21.2 ± 0.0
PyMT *Ptpa*^{fl} puro	20.9 ± 0.1	20.3 ± 0.2	19.6 ± 0.2	19.6 ± 0.1	18.5 ± 0.3
PyMT *Ptpa*^{fl} myc-PTPA	20.8 ± 0.2	20.0 ± 0.3	19.4 ± 0.2	18.8 ± 0.8	18.4 ± 0.1
PyMT *Ptpa*^{Δ} puro	23.3 ± 0.7	22.5 ± 0.6	22.1 ± 0.7	21.7 ± 0.5	20.6 ± 0.3
PyMT *Ptpa*^{Δ} myc-PTPA	21.5 ± 0.4	20.6 ± 0.4	20.2 ± 0.5	19.9 ± 0.2	18.9 ± 0.2

Figure 14 **Analysis of Proliferation of 326 # 7 Cells Expressing PTPA and/or myc-PTPA and Ptpa Knock-Out Cells** Proliferation over 7 days. 5 x 10^4 cells were plated each in duplicates. Neo *Ptpa*^{fl} cells were included as negative control. Results were split for easier display. For time points 24 hours to 96 hours n=3, for time point 168 hours n=2. **(a)** Curves from neo *Ptpa*^{fl}, PyMT *Ptpa*^{fl} puro and myc-PTPA cells. **(b)** Curves from neo *Ptpa*^{fl}, PyMT *Ptpa*^{Δ} puro and myc-PTPA cells. **(c)** Calculated doubling times of the five different cell lines after 24 hours each (see 4.6.1). **(d)** Average size of each cell line at each time point in µm.

We then asked for the reason causing the reduced cell count within the first 24 hours. Therefore, we performed a propidiumiodide staining to determine the number of dead cells. The count of dead cells rose from 4% (cells expressing PTPA) to over 8% percent in PyMT *Ptpa*^{Δ} puro cells (Figure 15).

Extrapolations using the cell count, doubling times and the apoptotic cells showed, that the increased death rate did not make up for the difference observed in the proliferation curve (Material and Methods 4.6.1). Due to a limitation in time, we performed the propidiumiodide staining only once, which limited the value of the obtained data.

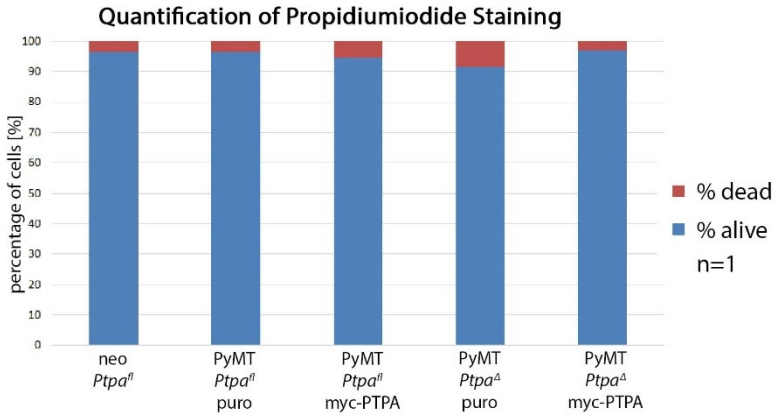

Figure 15 Propidiumiodide staining of cells after 24 hours. Blue part of the bar represents percentage of alive cells, red of dead ones. Cells were sorted using FACS Calibur, n=1.

Here we found a trend for reduced proliferation rate in the *Ptpa* knock-out cells. However, due to the high standard deviations no distinctive statement could be given here. Interestingly, complementation with myc-PTPA showed the lowest doubling times (Figure 14c). It seems that myc-PTPA could reverse the phenotype created by *Ptpa* deletion. Expression of PyMT induced a rapid acceleration in proliferation speed, even in *Ptpa* knock-out cells, which significantly outgrew neo $Ptpa^{fl}$ cells, an observation which we had also seen in cell culture and with the B6 clone (data not shown).

2.2.2. Analysis of PyMT Phenotype in *Ptpa* Knock-Out Cells

2.2.2.1. Cells Lacking PTPA could not Form Foci

Previous experiments indicated that cells expressing PyMT but lacking PTPA were not able to form foci on a layer of non-oncogenic cells (Stadtmann et al. 2019; Zrelski et al. unpublished data). We wanted to determine whether and to what extent this applied for the 326 # 7 cell lines.

Both PyMT expressing floxed cell lines had a focus formation efficiency of 50% to 65% (Figure 16a and b). Focus formation was nearly completely abolished in PyMT $Ptpa^{\Delta}$ puro cells (1%). Complementation with myc-PTPA restored the focus formation ability to almost floxed levels (35% to 45%). Similarly, the area covered by foci was reduced from around 13%/10%/5% (500/250/125 cells plated) in floxed puro cells to 0.5%/0.3%/0.3% (500/250/125 cells plated) in delta puro and then again elevated to almost floxed levels in PyMT $Ptpa^{\Delta}$ myc-PTPA cells (Figure 16c). In contrast to the B6 cells, the criterion for a combination of all values (F < F crit) in an ANOVA was not met here.

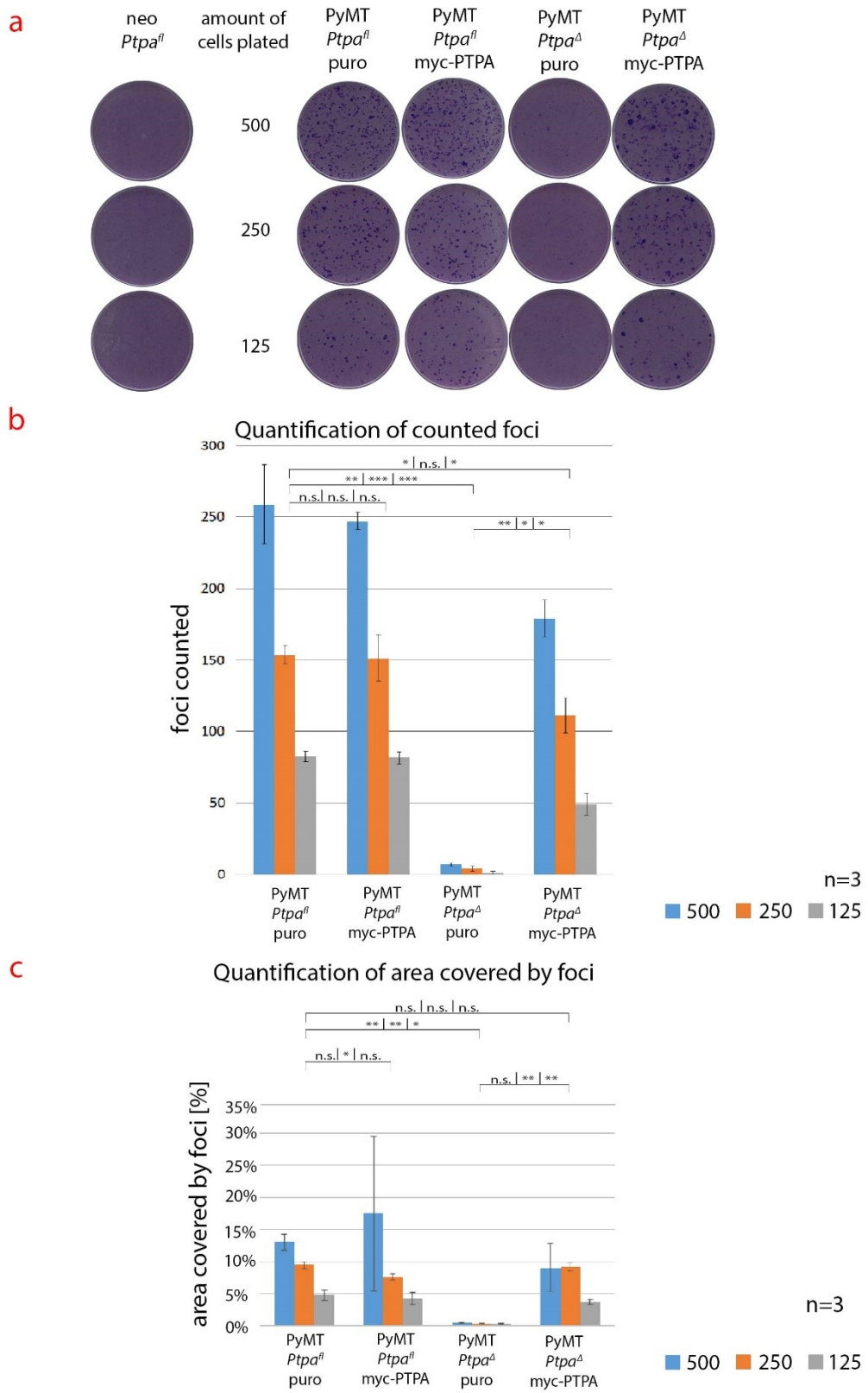

Figure 16 **Analysis of the Transformation Ability of PyMT in 326 # 7 Cells Expressing PTPA and/or myc-PTPA and *Ptpa* Knock-Out Cells (a)** Representative scans of focus formation assay. Neo *Ptpa*^{fl} cells expressing only the empty vector (neo) were plated together with 500, 250 or 125 cells of PyMT cells either *Ptpa*^{fl} puro, *Ptpa*^{fl} myc-PTPA, *Ptpa*^{Δ} puro or *Ptpa*^{Δ} myc-PTPA. Foci were stained after 14 days. Graphical representation of the **(b)** counted foci and **(c)** of area covered by foci. Data in (b) and (c) are representative of three independent assays. Standard deviation and statistical significance are indicated. Statistical

significance was calculated using Student's T-Test (two tailed, unpaired, unequal variance) with P values * < 0.05; ** < 0.01; *** < 0.001

2.2.2.2. Lack of PTPA Resulted in Differential Assembly of the Transformation Complex

Next we asked whether the PyMT transformation complex assembly was affected by *Ptpa* deletion. PyMT-immunoprecipitations were performed with lysates of 326 # 7 PyMT $Ptpa^{fl}$ puro and myc-PTPA, PyMT $Ptpa^{\Delta}$ puro and myc-PTPA, and τ2 $Ptpa^{+/+}$ cells, as positive control for PyMT detection and for quantification (

Supplementary Figure *3*).

Expression levels of the full-length and the 40 kDa protein of PyMT were different in cells with different *Ptpa* locus configurations (Figure 17a, left panels). In 326 # 7 PyMT cells expressing PTPA half of the PyMT amount was made up of full-length, in PyMT $Ptpa^{\Delta}$ puro cells this was reduced to one third. No 40 kDa fragment was detected in τ2 $Ptpa^{+/+}$. Overall expression of PP2A A and C subunit and src kinase was within the same range in the PyMT cells but less in neo $Ptpa^{fl}$. pY416 tyrosine phosphorylation of src kinase was most increased in τ2 $Ptpa^{+/+}$ cells and lowest in the control cells (neo $Ptpa^{fl}$). pY527 tyrosine phosphorylation, which is a marker for inactive src (Boggon and Eck 2004; Smart et al. 1981; Fluck and Schaffhausen 2009), was increased in neo $Ptpa^{fl}$ and PyMT $Ptpa^{\Delta}$ puro cells. No PTPA was detected in the $Ptpa^{\Delta}$ puro and no endogenous PTPA in $Ptpa^{\Delta}$ myc-PTPA cells (Figure 17a).

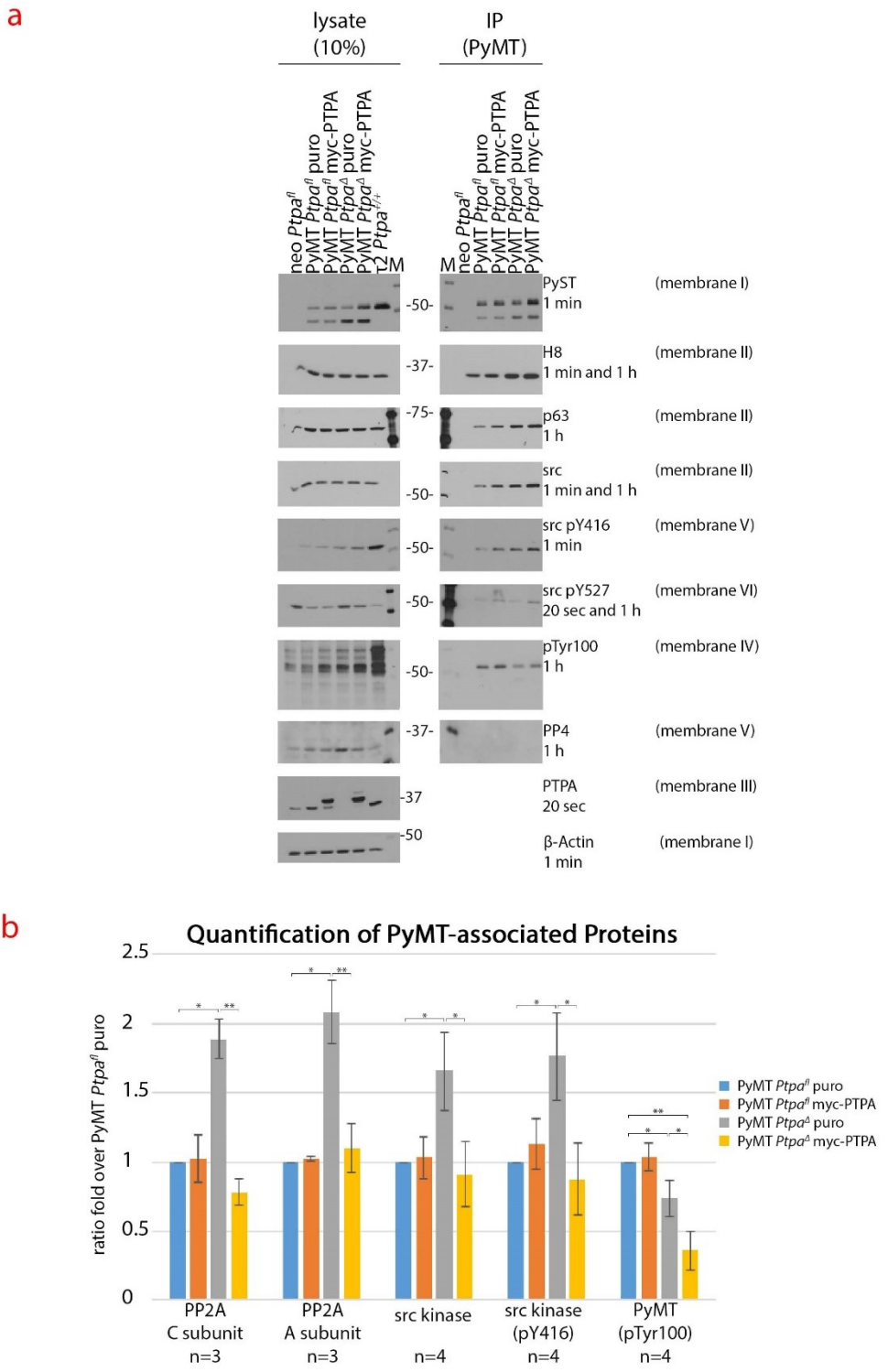

Figure 17 **Interaction of PyMT and its Associated Proteins in 326 # 7 Cells Expressing PTPA and/or myc-PTPA and *Ptpa* Knock-Out Cells (a)** Immunoprecipitation was performed via PyMT, using the rabbit polyclonal anti-PyST antibody. Empty vector (326 # 7 neo *Ptpa*^{fl}) was used as negative control. 326 # 7 cells expressing PyMT (*Ptpa*^{fl} puro, *Ptpa*^{fl} myc-PTPA, *Ptpa*^{Δ} puro and *Ptpa*^{Δ} myc-PTPA) were analysed. τ2 *Ptpa*$^{+/+}$ were included as positive control. 10% of the protein amount of the IP were loaded for the lysates (left panel). Proteins were separated on a 10% SDS-PAGE and transferred to 6 nitrocellulose membranes. Membranes were incubated with antibodies in the following order: Membrane I: PyST (PyMT), β-Actin; Membrane II: H8 (PP2A C Subunit), src, p63 (PP2A A Subunit); Membrane III: PTPA; Membrane IV; pTyr100; Membrane V: pY416; PP4; Membrane VI: pY527. For the detection of pY416 src kinase 5% ECL Select was used, for the detection of the Co-IPs of PP2A A and C subunit, src kinase, pY527 src kinase and PP4 15% ECL Select were used. Blots are representative of 4 independent experiments. **(b)** Quantification of PyMT-associated proteins normalized to the amounts of immunoprecipitated full-length PyMT. Quantification was performed using ImageJ (for algorithm see 4.6.2). Analysis was done of 4 independent

experiments (n=4). For PP2A C and A subunit three values were obtained (n=3). Standard deviations are indicated and were calculated using the Excel function. Statistical significance was calculated using Student's T-Test (two tailed, unpaired, unequal variance) with P values * < 0.05; ** < 0.01; *** < 0.001

The transformation complex (PP2A and active src kinase) was formed in all PyMT expressing cells. Interestingly, the association of PP2A C subunit, PP2A A subunit and (active, pY416 phosphorylated) src kinase was even more in PyMT *Ptpa*$^{\Delta}$ puro cells. In contrast, tyrosine phosphorylation of PyMT full-length protein was significantly reduced (Figure 17b). Ectopic expression of myc-PTPA restored the levels of co-immunoprecipitated proteins to floxed values. However, the amount of tyrosine phosphorylated PyMT was even further reduced in those cells. Hardly any tyrosine phosphorylation of the 40 kDa fragment was detected. The amount of inactive src kinase (pY527) was negligible.

A recent publication found that PP4, a phosphatase closely related to PP2A, interacts with PyMT as well (Rouleau et al. 2016). As our lab has showed that PTPA is involved in PP4 activity as well, we tested whether PP4 association was altered in *Ptpa* knock-out cells. PP4 was detected in all lysates, but not in the PyMt immunoprecipitates. This could, however, have been due to the overall weak signal with the PP4 antibody.

2.2.3. Summary

Indeed, we could show that *Ptpa* deletion resulted in a phenotype in the 326 # 7 cells, manifesting itself in enhanced micronucleus formation and a trend in the reduction of proliferation as well as reduced cell viability in comparison to their floxed counterparts. The empty vector control was significantly slower and showed also an enhanced micronucleus formation. While the reduction in proliferation speed was not surprising to us, the result from the micronucleus formation was. It could be that, similar to old B6 cells, neo *Ptpa*^{fl} cells did undergo a certain amount of *Ptpa* deletion although no tamoxifen was added. This is supporated by the PCR were in the beginning of the screening a slight delta band could be observed (Figure 12a).

Here we could also define a PyMT specific phenotype. Focus formation in 326 # 7 PyMT *Ptpa* knock-out cells was nearly completely abolished. Interestingly, also an effect on protein level could be detected, as the number of transformation complexes rose between 1.5 and 2 times in the *Ptpa* knock-out cells. Stunningly, the overall tyrosine phosphorylation of PyMT was reduced in these cells.

Rescue experiments with ectopically expressed myc-PTPA (PyMT *Ptpa*^{fl} myc-PTPA; PyMT *Ptpa*$^{\Delta}$ myc-PTPA) confirmed our hypothesis that the observed phenotypes in PyMT *Ptpa* knock-out cells were indeed due to the *Ptpa* deletion. With the PyMT *Ptpa*^{fl} myc-PTPA cells we could show that overexpression of myc-PTPA did not influence cells in our experiments. In PyMT *Ptpa*$^{\Delta}$ puro cells, myc-PTPA rescued all observed phenotypes, with the only exception being the tyrosine phosphorylation of PyMT in the immunoprecipitation experiments. Here even less tyrosine phosphorylation than in the

Ptpa knock-out cells was observed. The source and background of this phenomenon remains to be elucidated.

2.3. Generation of *Ptpa* Knock-Out Cells Using CRISPR/Cas9

To generate a cell line with stable *Ptpa* deletion, we decided to use a CRISPR/Cas9 approach with two guide RNAs (strategy depicted in Figure 18). From previous data we hypothesized, that PyMT might help cells lacking PTPA to survive, therefore we transfected two cell lines, NIH 3T3 Tom Roberts $Ptpa^{+/+}$ and τ2C3C1 neo $Ptpa^{+/+}$, expressing PyMT from a neo vector. Transfected cells were selected by addition of puromycin and singularized by minimal dilution (Figure 18). Screening for *Ptpa* knock-out cells was performed by PCR of the genomic locus, immunoblotting against PTPA and sequencing of the genomic DNA and isolated mRNA.

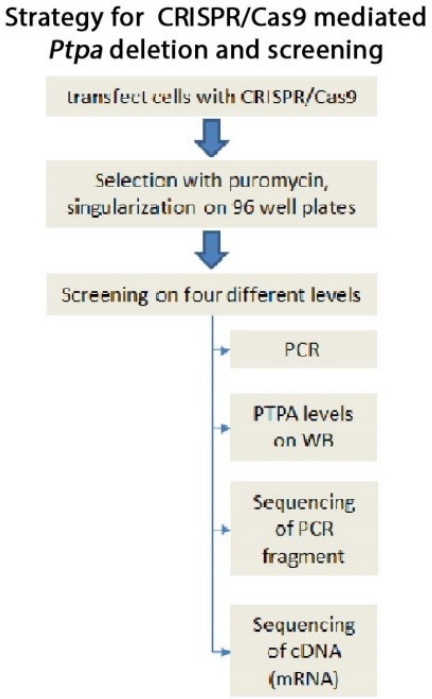

Figure 18 Strategy for generation and screening of *Ptpa* knock-out via CRIPSR/Cas9 in NIH 3T3 Tom Roberts and τ2C3C1 neo (PyMT expressing) cells.

First screening by PCR was performed on the mixed clones of the transfected cell lines. We used three different PCR setups, with primers for the locus of c1, c2 and a combination of both primers ($c1_f$+$c2_r$). Wild type fragments of c1 and c2 were calculated to be approximately 250 and 210 base pairs in size. The PCR of the third setup was expected not to work for wild type samples, because the intronic region between exon 1 and 2 is stretched out over 10 000 base pairs. A deletion of the region between exon 1 and 2 would lead to a fragment in the $c1_f$+$c2_r$ PCR and a lack of the c1 and c2 product. This would be the expected result if Cas9 had at both guide RNAs simulatenously. Lysates of 326 # 7 PyMT $Ptpa^{fl}$ cells were used as positive (c1, c2) and negative ($c1_f$+$c2_r$) control.

PCR of τ2c3c1 neo mixed clones was unsuccessful (Figure 19a). However, of originally 192 plated τ2C3C1 cells, 34 were tested in PCR, 24 in Western blot analysis (for statistics see Supplementary Figure 4) and we obtained seven clones that were likely *Ptpa* knock-outs and were further tested by sequencing the genomic locus (T1F4, T1F5, T2A7, T2C5, T2C6, T2G9, T2H6) (Figure 19b). For NIH 3T3 cells (obtained from Tom Roberts, DFCI, Boston) the PCR of the mixed clones directly after transfection was promising, as the third PCR setup ($c1_f$+$c2_r$) also gave a band of approximately 240 bp (Figure 19a). However, of the 35 clones that were tested in immunoblot analysis, no knock-out clones were obtained, but three of those (N1C7, N1G8, N2G4) had significantly reduced PTPA protein levels (example of N1C7 in Figure 19c). Three still expressed Cas9, including N1C7. The other 18 clones had died during expansion.

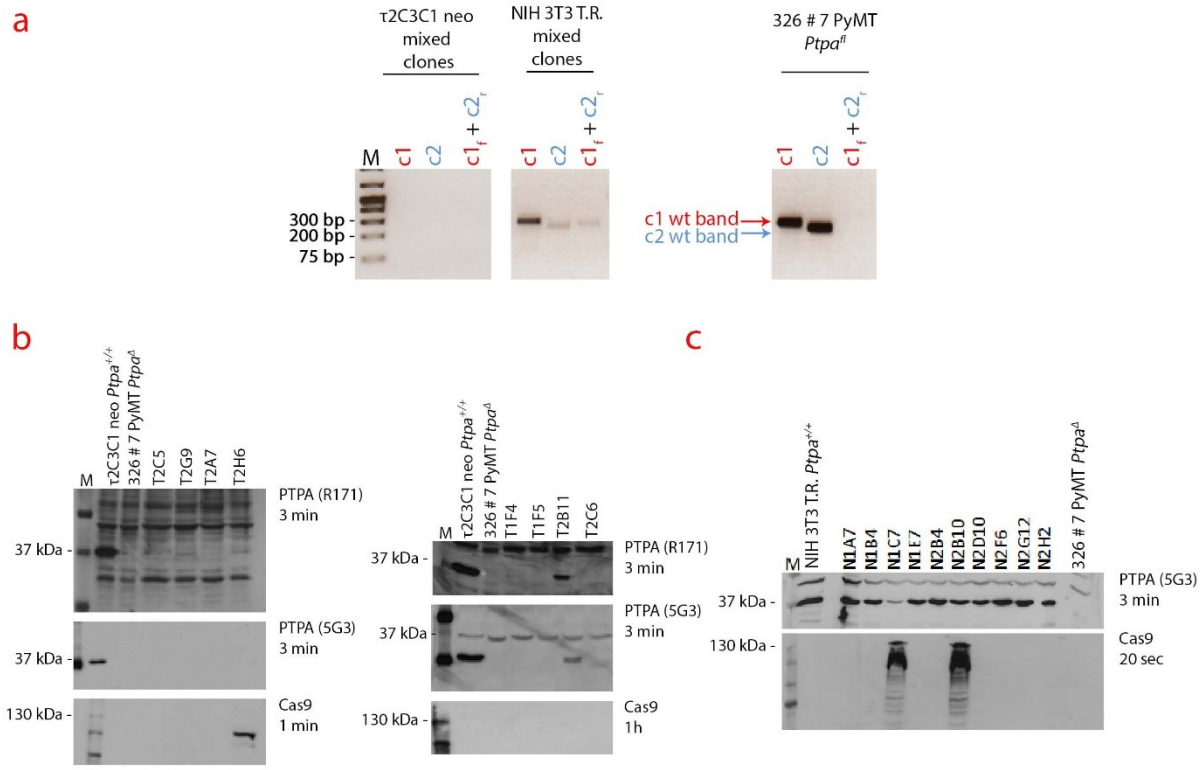

Figure 19 **Screening of CRISPR/Cas9 generated *Ptpa* Knock-Outsτ2C3C1 neo and NIH 3T3 Tom Roberts (T.R.) Cells (a)** Screening PCR of mixed clones of τ2C3C1 neo and NIH 3T3 T.R. cells, harvested 18 hours after CRISPR/Cas9 transfection. 326 # 7 *Ptpa^{fl}* cells were used as positive control for the c1 and c2 PCRs and as negative control for the $c1_f$+$c2_r$ PCR. Wild-type fragments are indicated by arrows (c1 ~ 250 bp, c2 ~ 210 bp) Products of PCR were separated by electrophoresis on a 1.4% Agarose gel. Samples were separated on the same gel but not adjacent to another, indicated by the gap. **(b)** Analysis of PTPA expression of protein level of τ2C3C1 neo single clones. Whole cell lysates were separated on a 10% SDS-PAGE and tested for PTPA using polyclonal rabbit R171 (membrane I) and monoclonal mouse 5G3 (membrane II) antibodies and subsequently Cas9 (membrane II). **(d)** Analysis of PTPA expression of protein level of NIH 3T3 T.R. single clones. Whole cell lysates were separated on a 10% SDS-PAGE and tested for PTPA and Cas9 expression.

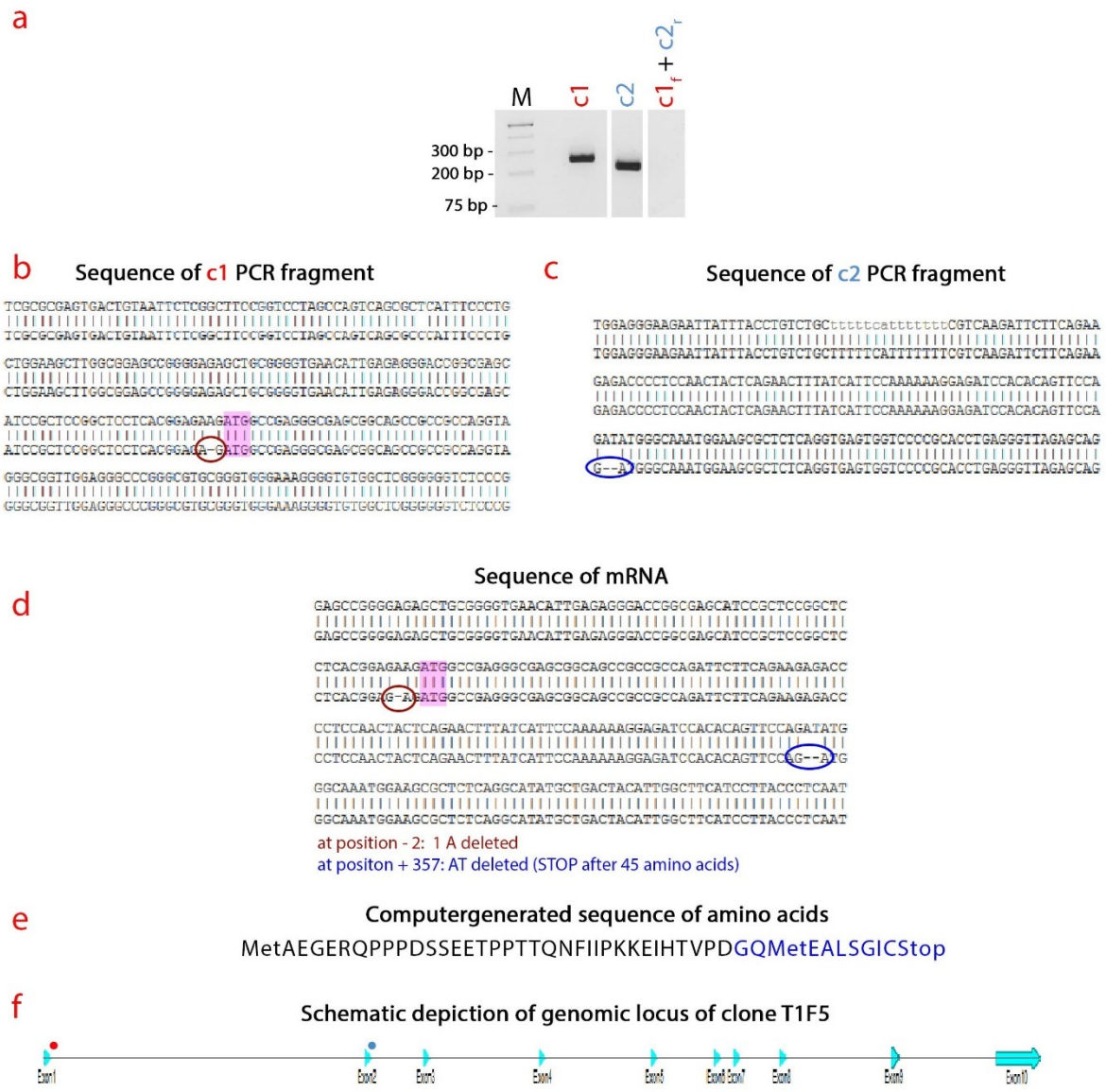

Figure 20 **Screening of Single Clone T1F5 (a)** Screening PCR of single clone T1F5. PCR products were separated by electrophoresis on a 2% Agarose gel, on the same gel but not adjacent to another, indicated by the gap. **(b**) Sequence obtained from c1 PCR fragment of single clone T1F5. Deletion is marked by red ellipse. ATG is indicated by pinkish bubble. **(c)** Sequence obtained from c2 PCR fragment of single clone T1F5. Deletion is marked by blue ellipse. **(d)** Sequence of cDNA obtained by reverse transcription of mRNA of single clone T1F5. Alterations are marked according to colours (b) and (c). ATG is indicated by pinkish bubble) **(e)** Predicted amino acid sequence of (d). Mutated amino acids are indicated in blue colour. **(f)** Schematic setup of the genomic *Ptpa* locus. Exons are marked by turquoise arrows. Red and blue dots indicate detected alterations in the genomic locus.

In seven single τ2C3C1 clones I did not detect PTPA on protein level (Figure 19b). Clone **T1F5** was the most promising, because PCR analysis gave one fragment in both PCRs (c1 ~ 250 bp, c2 ~ 210) and no PCR product was generated with $c1_f$+$c2_r$ primers indicating that no large deletion had occurred (Figure 20a). Sequencing of the genomic locus and the cDNA of the mRNA revealed that one adenine before the ATG and two nucleotides (adenine at position 356, thymidine at position 357) in exon 2 were deleted, resulting in a frameshift and ultimately in a premature stop codon (Figure 20b and c). The

resulting fragment was 45 amino acids long, of which 10 amino acids (GQMEALSGIC) at the C terminus were not PTPA related due to the frame shift at position 356 (Figure 20d and e). Thus, we were confident that single clone T1F5 was a full *Ptpa* knock-out clone (overview of the locus in Figure 20f, full sequence can be found in appendix, chapter 6.6).

The other six clones were tested by sequencing of genomic locus. T2A7 and T2H6 were excluded as the sequencing of T2A7 was inconclusive and T2H6 still expressed Cas9 (Figure 19b). Next I analysed the reversely transcribed *Ptpa* cDNA of four (T1F4, T2C5, T2C6, T2G9) clones. In the clone T2C5 we found that among a variety of different mutations also one sequence of fully functional *Ptpa* mRNA was present. Therefore also this clone was excluded from further analysis. The cDNA sequence of single clones T1F4, T2C6 and T2G9 showed no functional coding sequence for PTPA (sequence of T2C6 can be found in the appendix, chapter 6.7).

The generation of *Ptpa* knock-out clones using CRISPR/Cas9 was largely unsuccessful, resulting in no *Ptpa* knock-out clones in NIH 3T3 T.R. and only four clones in τ2C3C1 neo cells. Analysis of metaphase spreads opened up a possible explanation for this behaviour, as we found that NIH 3T3 T.R. had a total chromosome count of 73, τ2C3C1 neo of 68 (Figure 21a), while the karyotype of a normal diploid murine cell is 40. We could not identify the chromosomes that were multiplied (Figure 21b and c). Still, it was likely that the number of chromosome 2 and therefore the *Ptpa* locus were overrepresented in comparison to normal murine cells. Determination of the karyotype beforehand would be prudent in the future.

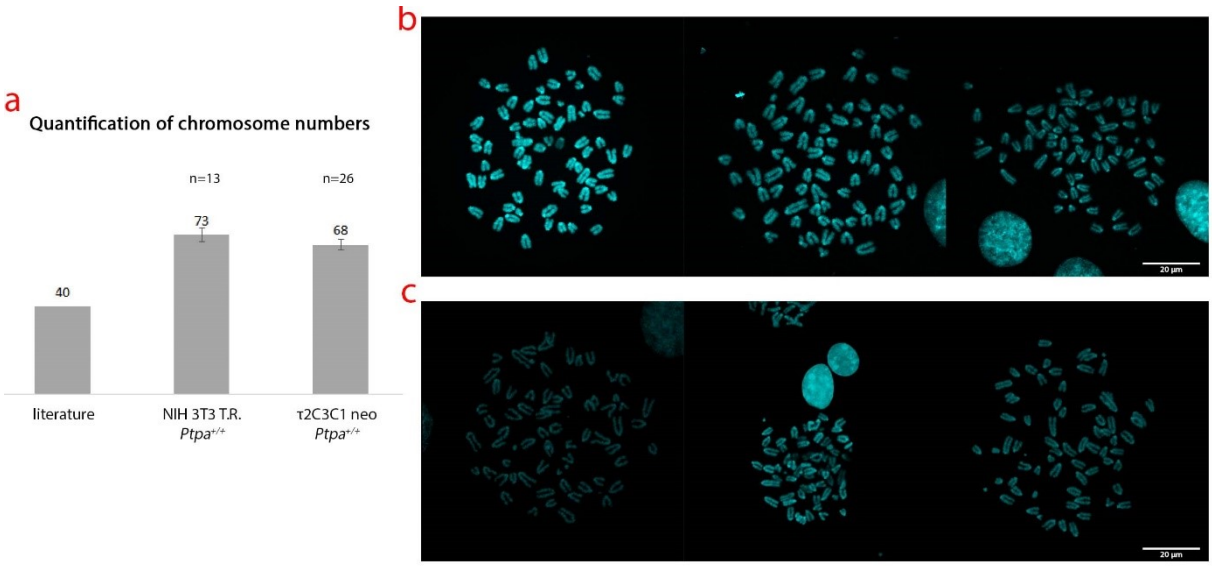

Figure 21 **Determination of the Karyotype of NIH 3T3 Tom Roberts *Ptpa*$^{+/+}$ and τ2C3C1 neo *Ptpa*$^{+/+}$ Cells (a)** Quantification of chromosomes. For NIH 3T3 T.R. *Ptpa*$^{+/+}$ 13 cells were analysed, for τ2C3C1 neo *Ptpa*$^{+/+}$ 26. Three representative pictures of **(b)** NIH 3T3 T.R. *Ptpa*$^{+/+}$ and **(c)** τ2C3C1 neo *Ptpa*$^{+/+}$. Pictures were taken with 100x magnification with Zeiss LSM700. Scale bar = 20 µm

2.3.1. Determination of Phenotype of τ2C3C1 neo *Ptpa* Knock-Out Cells

After testing for *Ptpa* knock-out we infected τ2C3C1 *Ptpa*$^{+/+}$, T1F5 and T2C6 with retroviral supernatants carrying either pBabe puro or pBabe puro myc-PTPA, to determine the phenotype of knock-out cells and whether it could be rescued by exogenous PTPA. Swiss 3T3 *Ptpa*$^{+/+}$ were included as non-transformed control cell line. Immunoblot analysis showed that all four *Ptpa*$^{+/+}$ cell lines expressed a similar amount of endogenous PTPA and myc-PTPA was about 2-4 fold overexpressed (Figure 22a). In myc-PTPA transfected cells additional bands at the height of 45 kDa and 37 kDa were found. However, these additional bands were only detected in cell lines transfected with the pBabe puro myc-PTPA vector and not in the pBabe puro lysates (Figure 22a). For simplicity reasons labelling was shortened again, as depicted in Figure 22b.

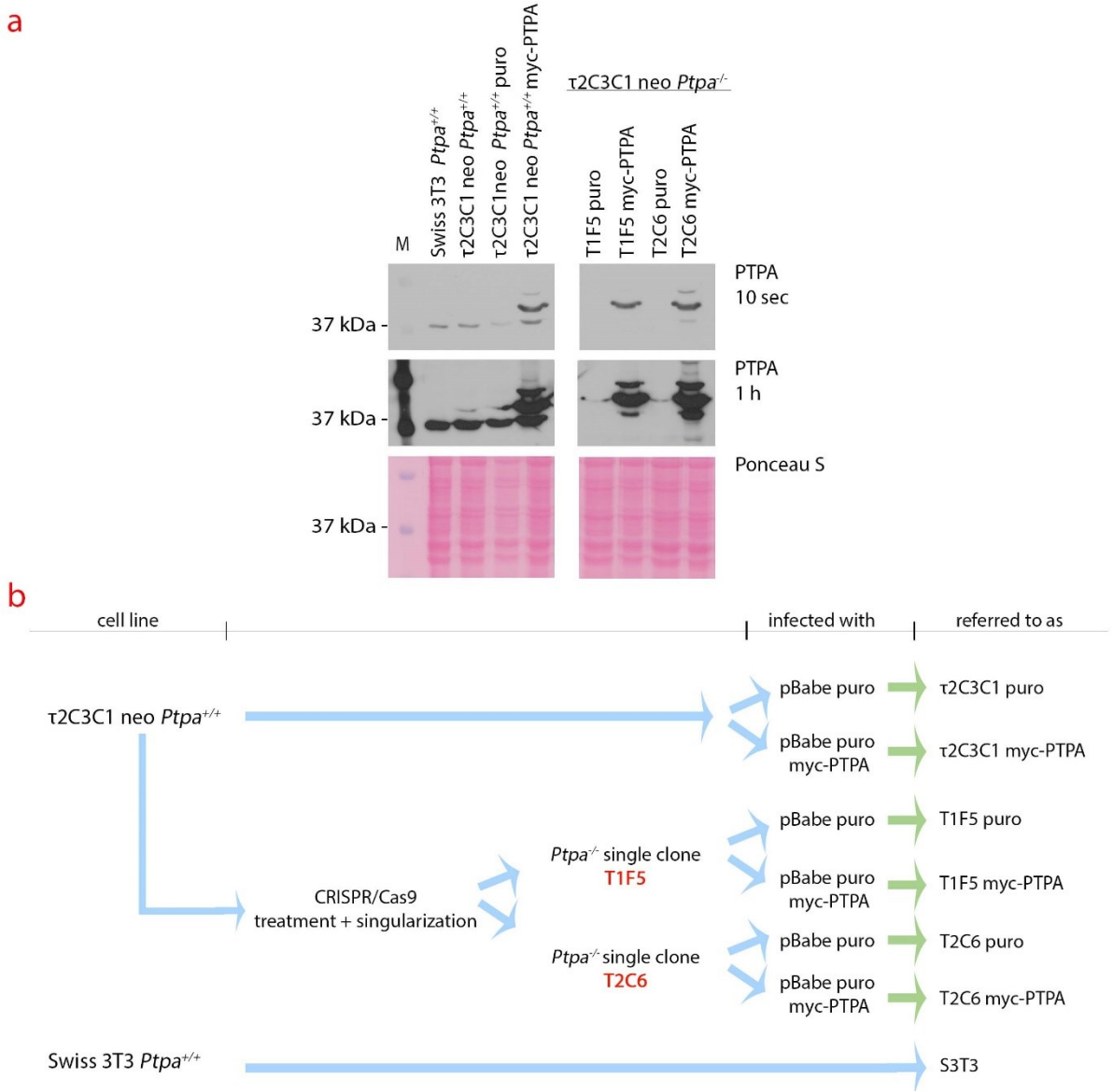

Figure 22 **Analysis of PTPA Expression in τ2C3C1 neo Cells Expressing PTPA and/or myc-PTPA and *Ptpa* Knock-Out Cells (a)** Western blot analysis of τ2C3C1 neo *Ptpa*$^{+/+}$ and τ2C3C1 neo *Ptpa*$^{-/-}$ single clones T1F5 and T2C6, all transfected with either pBabe puro or pBabe puro myc-PTPA. Swiss 3T3 *Ptpa*$^{+/+}$ and τ2C3C1 *Ptpa*$^{+/+}$ were used as controls. Whole cell lysates were separated on a 10% SDS-PAGE probed against PTPA (5G3). **(b)** Overview of cell lines and their labelling.

2.3.1.1. *Ptpa* Deletion Led to Enhanced Micronucleus Formation

As already showed with 326 # 7 MEFs and previously by Ingrid Frohner and colleagues of our lab, deletion of *Ptpa* leads to abnormal nucleus morphology, which manifests through the formation of micronuclei (Frohner et al. unpublished data). In our hands this phenotype was observed with Cre-Lox generated knock-out cells. Here we tested whether our new CRISPR/Cas9-generated *Ptpa* knock-out cells would show the same phenotype (Figure 23a).

In both *Ptpa* knock-out cell lines the percentage of cells with normal nuclei were reduced compared to wt cells. In the T1F5 puro cells only 75±4.6 % of counted cells showed normal nucleus morphology, in the T2C6 puro cells it were 77%±1.7%. The number of cells with one micronucleus (17%±2.8% T1F5, 13%±0.6% T2C6), two micronuclei (4%±1.2% T1F5, 5%±0.8%) and more than 2 micronuclei (only T2C6, 5%±0.8) was significantly higher than in wt cells. Expression of myc-PTPA almost restored normal nucleus morphology to wt levels (89%±1.2% T1F5 myc-PTPA, 93±1.9% T2C6 myc-PTPA). Hence, we deduced that the observed phenotype of abnormal nucleus formation was indeed caused by *Ptpa* deletion rather than a side effect from the CRISPR/Cas9 treatment. Overexpression of PTPA in PyMT *Ptpa*^{fl} cell lines did not affect nuclear morphology (Figure 23b).

a

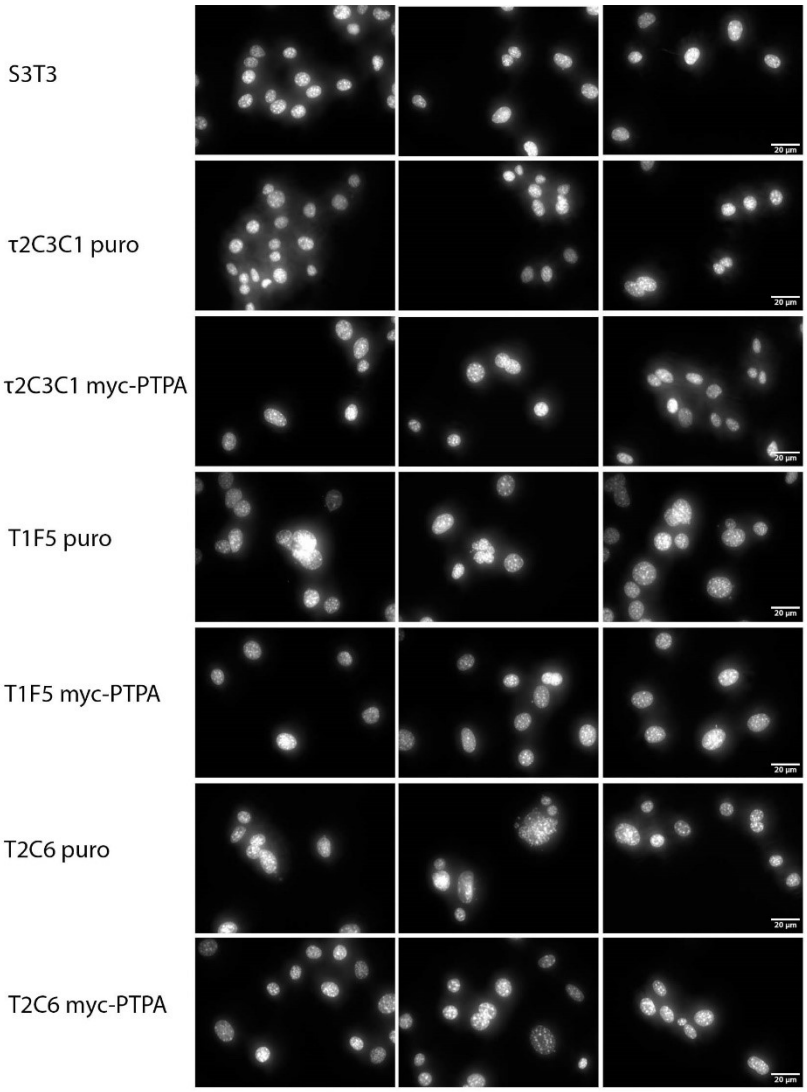

b

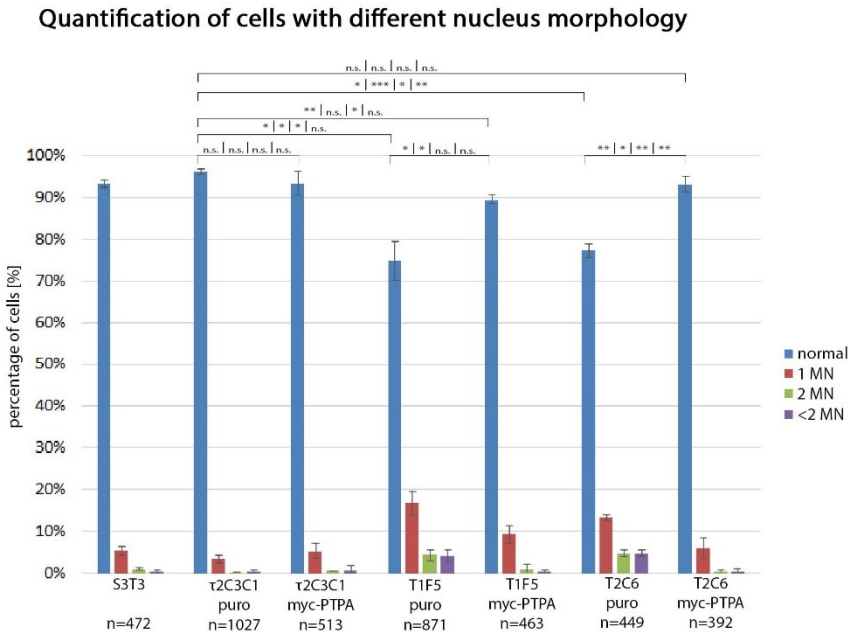

Figure 23 **Micronucleus Analysis of τ2C3C1 Cells Expressing PTPA and/or myc-PTPA and *Ptpa* Knock-Out Cells (a)** Representative pictures of DAPI staining of S3T3, τ2C3C1 puro, τ2C3C1 myc-PTPA, T1F5 puro, T1F5 myc-PTPA, T2C6 puro or T2C6 myc-PTPA. Pictures were recorded with Zeiss "ApoTome", 40x magnification. Only entirely visible cells were counted. Cells during mitosis were not taken into account. Scale bar = 20 µm **(b)** Quantification of counted cells. In blue cells with

normal nuclei, red showing the ones with one micronucleus (1 MN), green two (2 MN) and violet more than two (<2 MN). Standard deviation was calculated using the appropriate Excel function. Amount of counted cells is indicated below each cell line. Statistical significance was calculated using Student's T-Test (two tailed, unpaired, unequal variance). P values * < 0.05; ** < 0.01; *** < 0.001

2.3.1.2. Proliferation was Reduced in *Ptpa* Knock-Out Cells

Our lab showed that *Ptpa*$^{-/-}$ cells have a lower proliferation than wt cells (Hombauer et al. 2007; Frohner et al. unpublished data). Again, we wanted to show whether we could reproduce this phenotype in the new knock-out cells.

The proliferation of T1F5 and T2C6 PTPA knock-out cells was reduced compared to the τ2C3C1 wt cell lines (Figure 24a and b). Up to 96h the cell count of *Ptpa*$^{-/-}$ cells was even lower than the one of S3T3 cells, only superseding them after 168 hours. T2C6 puro cell count exceeded T1F5 cell count at 48 hours. Exogenous expression of myc-PTPA could increase the proliferation rate, but not restore it to wt levels. Interestingly, T2C6 myc-PTPA was the only cell line to clearly exceed the S3T3 negative control at the 96 hour time point and showed similar doubling times as the wt counterparts, at least at 48h and 72h. The observations from the cell count were supported by the calculated doubling times (Figure 24d). There was no remarkable difference between τ2C3C1 puro and myc-PTPA indicating that ectopic expression of PTPA did not affect the proliferation rate. Notably, the cell number of all PyMT-expressing cell lines further increased even after reaching confluency. In contrast, the non-transformed S3T3 cells stopped proliferating and cell numbers were even reduced at the 168h time point (Figure 24a).

Cell size of *Ptpa* knock-out cells was between 2µm and 5µm larger than the wt cells consistent with our previous observations. Clones expressing myc-PTPA showed a reduction in cell size compared to the knock-out, but did not reach the size of the wild type cells. Additionally we observed that the denser plates got, the compacter cells were, a phenomenon which we already had seen with the PyMT transformed 326 # 7 cells (Figure 24e).

a

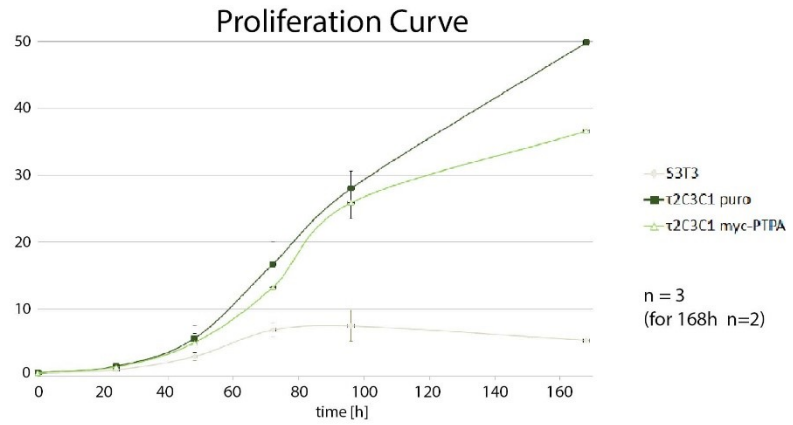

b

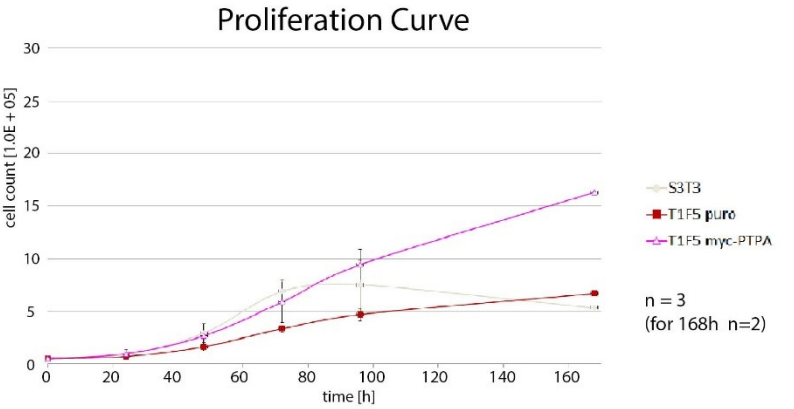

c

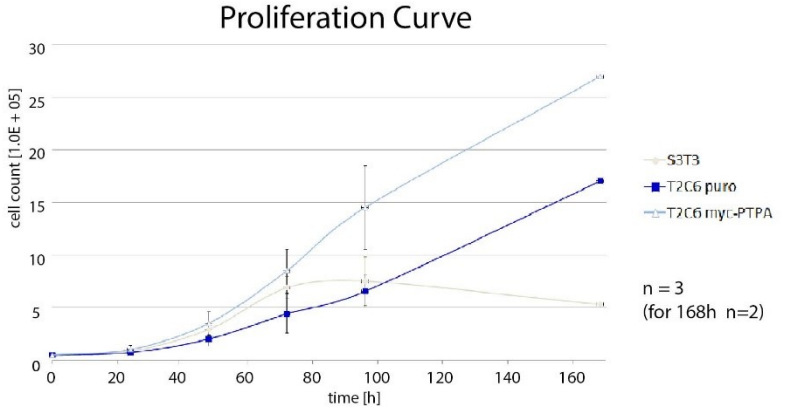

d

time point	24 hours	48 hours	72 hours	96 hours
S3T3	46.4 ± 36.7	14.2 ± 0.9	18.3 ± 1.1	42.8 ± 46.2
τ2C3C1 puro	17.1 ± 2.8	12.5 ± 0.1	14.4 ± 2.1	32.2 ± 9.2
τ2C3C1 myc-PTPA	18.5 ± 3.6	13.0 ± 1.1	16.0 ± 2.1	24.3 ± 5.2
T1F5 puro	152.9 ± 179.2	20.0 ± 3.0	22.6 ± 4.1	48.3 ± 8.2
T1F5 myc-PTPA	35.8 ± 15.2	16.6 ± 1.3	19.6 ± 1.1	36.1 ± 15.2
T2C6 puro	152.8 ± 191.2	17.0 ± 1.6	22.4 ± 5.1	211.2 ± 319.2
T2C6 myc-PTPA	32.3 ± 14.2	13.7 ± 1.3	17.7 ± 1.1	38.1 ± 23.2

e

after	24 hours [µm]	48 hours [µm]	76 hours [µm]	96 hours [µm]	168 hours [µm]
S3T3	19.7 ± 0.7	18.6 ± 0.3	18.4 ± 0.2	19.4 ± 2.0	20.1 ± 2.0
τ2C3C1 puro	19.4 ± 0.3	18.3 ± 0.4	17.2 ± 0.5	16.2 ± 0.8	18.5 ± 0.6
τ2C3C1 myc-PTPA	19.9 ± 0.3	18.6 ± 0.5	17.5 ± 0.6	16.3 ± 0.7	18.4 ± 0.5
T1F5 puro	25.0 ± 0.2	24.00 ± 0.4	23.4 ± 0.5	21.7 ± 2.8	22.6 ± 0.5
T1F5 myc-PTPA	23.6 ± 0.6	22.1 ± 0.4	22.0 ± 0.5	21.3 ± 0.7	22.6 ± 0.9
T2C6 puro	23.1 ± 0.4	21.5 ± 0.6	21.1 ± 0.7	20.2 ± 0.7	19.7 ± 1.1
T2C6 myc-PTPA	20.6 ± 0.5	19.4 ± 0.7	18.7 ± 0.8	17.5 ± 0.8	19.5 ± 1.0

Figure 24 **Analysis of Proliferation of τ2C3C1 Cells Expressing PTPA and/or myc-PTPA and *Ptpa* Knock-Out Cells** Proliferation over 7 days. 5 x 10^4 cells were plated each, cells were measured in duplicates. Swiss 3T3 cells were included as negative control. Results were split for easier display. For time points 24 hours to 96 hours n=3, for time point 168 hours n=2. **(a)** Curves from S3T3, τ2C3C1 puro and myc-PTPA cells. **(b)** Curves from S3T3, T1F5 puro and myc-PTPA cells. **(c)** Curves from S3T3, T2C6 puro and myc-PTPA cells. **(d)** Calculated doubling times of the five different cell lines after 24 hours each (see 4.6.1). **(e)** Average size of each cell line at each time point in µm.

The first 24 hours of the *Ptpa* knock-out puro cells had a very long doubling time. Hence, we performed a propidiumiodide staining 24 hours after plating to distinguish between living and dead cells (Figure 25). S3T3 cells showed the smallest portion of dead cells (1.7%), followed by τ2C3C1 puro (4.1%), τ2C3C1 myc-PTPA (3.7%), T1F5 myc-PTPA (4.8%) and T2C6 myc-PTPA (3.2%) cells. Both *Ptpa* knock-out clones showed a larger number of dead cells (T1F5 puro 8.9%, T2C6 puro 8.1%). Extrapolations of the dead cells and the doubling times, however, revealed that the amount of dead cells did not account for the differences observed in the proliferation curves (Material and Methods 4.6.1). Due to time reasons the propidiumiodide staining was performed once, hence the conclusion here is limited.

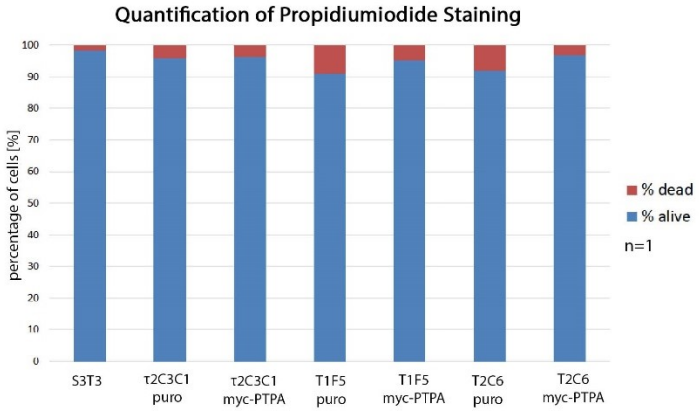

Figure 25 Propidiumiodide staining of cells after 24 hours. Blue part of the bar represents percentage of alive cells, red of dead ones. Cells were sorted using FACS Calibur, n=1.

2.3.2. Focus Formation was Reduced in *Ptpa* Knock-Out Cells, but not Restored by myc-PTPA

Up to this point we had investigated more general features of PTPA deletion with our new model system, but is there a difference in terms of focus formation ability? Therefore, we plated 500, 250 and 125 cells each on a layer of S3T3 cells.

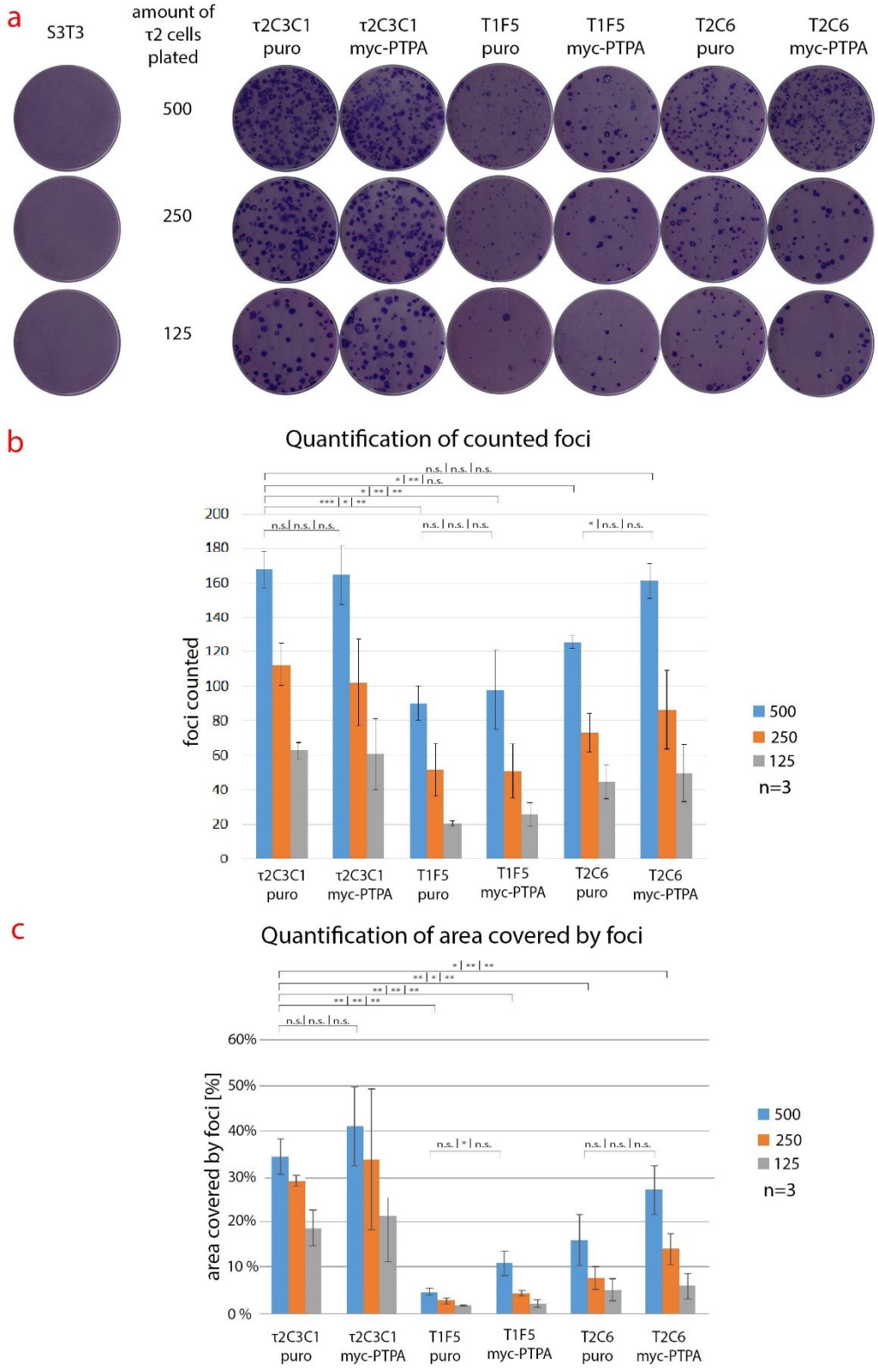

Figure 26 **Analysis of the Transformation Ability of PyMT in τ2C3C1 Cells Expressing PTPA and/or myc-PTPA and *Ptpa* Knock-Out Cells (a)** Representative scans of focus formation assays. S3T3 cells were plated together with 500, 250 or 125 cells of PyMT cells: τ2C3C1 puro, τ2C3C1 myc-PTPA, T1F5 puro, T1F5 myc-PTPA, T2C6 puro or T2C6 myc-PTPA. Foci were stained after 14 days. Graphical representation of the **(b)** counted foci and **(c)** of the measured area. Data in (b) and (c) are representative of three independent assays. Standard deviation and statistical significance are indicated. Statistical significance was calculated using Student's T-Test (two tailed, unpaired, unequal variance) with P values * < 0.05; ** < 0.01; *** < 0.001

Wild-type cells showed a focus formation efficiency between 35% and 50% (Figure 26a and b). In T1F5 puro cells focus formation efficiency was reduced to 16-21%, in T2C6 puro cells to 25-36%. Complementation with myc-PTPA hardly restored focus formation ability. Similary, the area covered by foci was significantly reduced from 35%/30%/20% (500/250/125 cells plated) in wt puro cells to 5%/3%/3% in T1F5 and 16%/8%/5% in T2C6 puro cells (Figure 26c). Re-expression of myc-PTPA did not lead to an overall significant increase in area coverage (11%/5%/2% T1F5 myc-PTPA, 27%/14%/6% T2C6 myc-PTPA). The criterion, for a combination of all values (F < F crit), in an ANOVA was not met.

2.3.3. Summary

In total we could show, that a *Ptpa* knock-out in τ2C3C1 cells led to reduced proliferation as well as enhanced micronucleus formation compared to τ2C3C1 wt cells. Although we found a reduction in focus formation in cells lacking PTPA, we could not find out whether this resulted from the *Ptpa* deletion, because cells expressing myc-PTPA could only partially rescue the phenotype, which was always more severe in T1F5 than in T2C6 cells.

3. Discussion

This thesis comprises the generation of stable knock-out cells of the protein phosphatase 2A Activator Protein PTPA in MEFs and PyMT-expressing MEFs. Subsequently, I tested the effect of *Ptpa* knock-out on the transformation potential of the viral oncogene PyMT. Preliminary studies in our lab, have suggested that PTPA might be needed for the proper transformation efficiency of PyMT and a correct assembly of the transformation complex (Stadtmann et al. 2019; Zrelski et al. unpublished data).

In this study we wanted to further substantiate these findings. We started the experiments with the the PyMT-expressing MEF 112 # 4 clone B6, a clone with which we had already obtained results that pointed to a reduced transformation efficiency in the absence of PTPA.

However, during the work with this clone we observed two major problems: (i) *Ptpa* was not deleted in all cells, which most probably masked the phenotype and (ii) in earlier passages we did not observe a transformation phenotype. Only upon longer culture, PyMT seemed to have transforming effects, interestingly correlating with the increased abundance of the 40 kDa fragment. In terms of the *Ptpa* deletion the mutation or loss of the *loxP* sites or loss of Cre expression were most probably responsible for the incomplete *Ptpa* knock-out, supported by the observation that the PTPA protein levels seemed to be increased when the cells were cultivated over a longer time period after Cre induction. Potentially, cells that had not been deleted were overgrowing the *Ptpa* knock-out cells, leading to the increased PTPA detection. However, we did not further investigate this.

The strength of the PyMT-related phenotypes and abundance of the 40 kDa fragment of PyMT was previously shown to be dependent on the time after infection with the PyMT retroviral vector (Stadtmann et al. 2019; Zrelski et al. unpublished data). The question of the origin of this phenotype

could not be answered in this study. One hypothesis may be that PyMT needs several cell cycles to induce a form of background mutations, in order to work its transformation abilities. For example it was found in an *in vivo* mammary mouse model that PyMT alone was insufficient to induce tumors and needed additional events, such as the accumulation of mutations, for tumorigenesis and further malignancy (Maglione et al. 2001). As we could not provide an explanation, we excluded the B6 clone from future experiments and tried two different ways to establish PTPA deficient PyMT expressing cells.

First we transfected *Ptpa*$^{fl/fl}$ MEFs with a new vector expressing high levels of CreER^{T} coupled to an antibiotic resistance gene. The overexpression of Cre resulted in chromosome instability, reflected in enhanced micronucleus formation and slower proliferation rates even in wt PTPA cells (Schwab et al. unpublished data), an issue which has been previously reported (Loonstra et al. 2001). MEFs without PyMT expression did not survive the tamoxifen treatment, while we were able to establish a stable *Ptpa* knock-out cell in PyMT expressing 326 # 7 cells (PyMT *Ptpa*$^{\Delta}$ puro). In the second approach we used CRISPR/Cas9 to delete *Ptpa* in NIH 3T3 (Tom Roberts) and the PyMT expressing τ2C3C1 neo cells. We obtained four knock-out clones, but with a low efficiency of only 2% of transfected cells. In the NIH 3T3 (Tom Roberts) cells we did not obtain any *Ptpa* knock-out clones.

The analysis of both cellular systems, 326 # 7 and τ2C3C1 neo clones, resulted in the confirmation of the phenotype of *Ptpa* deletion previously described in our lab (Frohner et al. unpublished data). We found that in *Ptpa* knock-out cells the formation of micronuclei was enhanced, the proliferation speed reduced and the cells enlarged in terms of size. Statistical significance was not reached in all cases, but from the combination of the results of both cell lines we are confident about the observed phenotype. In the proliferation experiments of 326 # 7 the inclusion of a 326 # 7 pBabe neo *Ptpa*$^{\Delta}$ would have been especially interesting but as indicated these cells did not survive deletion of PTPA.

Investigation of the PyMT induced transformation and the formation of the transformation complex revealed a clear picture in the 326 # 7 cell line. The complete loss of focus formation however stood in contrast to the results from the proliferation experiments, where we could not find a significant decrease in proliferation speed and cells did not stop proliferating even after reaching confluency. We hypothesized that in the absence of PTPA the PyMT expressing cells had a problem to overcome contact inhibition and form foci or that the absence of other PyMT expressing cells impaired their adhesion or growth. Further investigation of the transformation abilities in those cells, such as soft agar assays, could add further information to the picture.

In the τ2C3C1 neo clones we observed a reduction in focus formation upon *Ptpa* deletion. In contrast to the 326 # 7 cells, which regained their transforming abilities upon re-expression of PTPA, we found no significant rescue effect through the exogenous expression of myc-PTPA. The reduction and not complete abolishment of the transformation abilities was not surprising here, as the cancerous

properties of the τ2C3C1 neo cells are rather established. Due to probably large number of background mutations, also backed by the abnormal chromosome numbers, it is likely that those cells would be transformed even in the case of the loss of PyMT expression. Further, CRISPR/Cas9 is known to have off-target effects, which might have contributed here (Le Cong et al. 2013; Wang and Qi 2016).

The more relevant question is why myc-PTPA re-expression could not restore the number of foci formed to the level of their wildtype counterparts. When combined with the results from the proliferation experiments, it is possible that the reduced number of foci originated from the slower proliferation rate rather than an impaired transformation ability, explaining why the myc-PTPA expressing cells formed slightly more foci but did not restore to wt levels. Additional experiments with an extended incubation period of the focus formation assays could help answer the question: Does the loss of focus formation result from the direct effect of *Ptpa* deletion on PyMT or rather from the in general slower proliferation?

For the **immunoprecipitations** we could only perform experiments with the stable clones from the MEF 326 # 7. Here we found the enhanced association of PP2A A and C subunit as well as src kinase to PyMT in the PyMT $Ptpa^{\Delta}$ puro cells, which was a surprising outcome, especially since the preliminary results from the previous analysis of the B6 cells had suggested the opposite (Zrelski et al. unpublished data). The predominant question pending here is whether the functional impairment of PyMT induced transformation is due to an event at the PyMT protein or further downstream in the signalling cascade initiated by PyMT.

Our hypothesis that src kinase is not activated in the *Ptpa* knock-out cells proved to be incorrect, as not only the phosphorylation of tyrosine 527 (pY527) was lost but also detection of phosphorylated Y416 (pY416) was stronger in the PyMT $Ptpa^{\Delta}$ puro cells. This should have resulted in the enhanced or at least equally strong tyrosine phosphorylation of PyMT. Surprisingly PyMT tyrosine phosphorylation was reduced in these cells. The further decrease of PyMT tyrosine phosphorylation in the PyMT $Ptpa^{\Delta}$ myc-PTPA cells was puzzling because these cells regain transformation abilities and thus PyMT must form an active transformation complex in those cells. Evidently, PyMT only needs a small proportion of phosphorylated tyrosine residues to transform cells or only a small number of PyMT molecules were completely active. In the PyMT $Ptpa^{\Delta}$ puro cells, however, no such active PyMT must be present because these cells do not form foci. We could not probe for further associated proteins such as Shc, PI3K and PLC-γ1 or ask if only special tyrosine residues of PyMT were not phosphorylated. In addition, we only analysed the binding and activation of src kinase, but not of yes and fyn, the two other Src family kinases that associate to PyMT (Kornbluth et al. 1987; Horak et al. 1989). A more detailed prediction however here is not possible, as the antibodies used to detect src may cross-react with yes and fyn, which are essentially the same size as src. The differences in the tyrosine phosphorylations could be an indication for a differential regulation in PyMT $Ptpa^{fl}$ and $Ptpa^{\Delta}$ directly on PyMT; however

the origin of this remains elusive. PP2A *in vitro* has been reported to show phosphotyrosyl activity in the absence of PTPA, an observation which was so far not confirmed *in vivo* (Cayla et al. 1994; Frohner et al. unpublished data), an unlikely explanation for the differences we observed in tyrosine phosphorylation. To generate a better understanding of these findings, further investigation of the complex formation and the involved phosphorylations are required. For the regulation further downstream a line of arguments came to our minds. First of all, we asked whether the enhanced association of dimeric PP2A and src kinase is a kind of overcompensation for non-functional PyMT and if this hinders the signalling cascade. Previous reports have identified that only 10% of cellular src kinase is in complex with PyMT (DeSeau et al. 1987). Based on this finding and in combination with the calculations from the immunoprecipitations, approximately 15% of cellular src kinase would be in complex with PyMT. Since src plays a major role in the regulation of cellular processes, such as proliferation, survival, migration, adhesion, angiogenesis, differentiation, invasion and immune function (Lieu and Kopetz 2010), it is possible that the change in cellular stoichiometry results in a lack of this protein at the crucial point. A similar statement applies for PP2A (Ulug et al. 1992). Since PyMT predominantly displaces (or prevents the binding of) B and B' family subunits (Jackson and Pallas 2012), alternatively formed PP2A holoenzymes in the absence of PTPA could be another aspect important in this enigma. It was previously shown that effectors of the Hippo pathway YAP and TAZ were needed for proper transformation and that a loss of binding of those factors to PyMT did not interfere with the formation of the transformation complex. It further was shown that YAP was phosphorylated (most likely by a Src kinase) as well as dephosphorylated in the process. It was suggested that PP2A performs the dephosphorylation of YAP upon localization at PyMT (Rouleau et al. 2016). Although highly speculative, this could resemble one of the targets of PTPA-dependent PP2A, a consideration which does not stand in contrast to the information that catalytically inactive PP2A C subunit can assemble the transformation complex, as the association of YAP was not investigated in the paper (Ogris et al. 1999). Interestingly, this possibility would be a combination of a downstream signalling issue and a direct event at the PyMT protein, a prospect that would be worth examining. In this context activity measurements of co-immunoprecipitated PP2A C subunit could provide important evidence.

We suggest here a number of follow-up experiments, such as the performance of PyMT localization studies. The association to membranes has been shown to be necessary for the transformation ability of PyMT (Carmichael et al. 1982) and it has been shown that depending on the experimental set-up PyMT can associate to both, intracellular and cytoplasmic membranes. There have also been several hints regarding the complex formation, however the details of insertion into the membranes and where the PyMT-signalling exactly takes place remain elusive so far (reviewed in Schaffhausen and Roberts 2009). Hence not only the cellular localization of the PyMT protein itself, but also the location of the complex formation is of interest. We tried to localize the PyMT protein in our two cellular

models, an investigation using immunofluorescence and confocal microscopy which was unsuccessful in our hands so far (data not included). In addition, we did also not incorporate the needed control, a membrane staining. An approach with a fluorescently labelled PyMT, if possible, and expression of fluorescently labelled proteins in the different membranes could provide valuable information on the location. A second possibility to monitor the localization is to perform assays using membrane fractioning, thereby separating the different membrane systems. To gather information on the complex formation and whether it is different depending on the respective membrane, an immunoprecipitation in the following is advisable.

Further investigation of the 40 kDa fragment of PyMT in 326 # 7 MEFs would be necessary to enlighten whether this has a functional role or is simply an artefact of PyMT expression. Thereby identification of the included amino acid sequences would be the first step. From calculations the fragment should be approximately 300 amino acids in size. PyMT itself has 230 unique amino acids. Since this fragment is recognized by the PyST antibody, it must contain parts of the overlapping region. If we could determine whether also a stretch of the universally shared 79 amino acids at the N terminus is part of the fragment, for example through the incubation with an anti-Polyoma early antigen antibody (available from Abcam, Santa Cruz or one of our own antibodies), we would have a very strong hint that the MBD is not present. Alternatively, an analysis of the smaller PyMT protein with mass spectrometry is possible. Felici et al. showed in their study a highly tumorigenic C-terminally truncated 40 kDa fragment of PyMT. Contrasting to our data, in this study the fragment did not arise spontaneously and the authors fused a liphophilic omain to a PyMT mutant lacking the C terminal MBD, enabling membrane localization (Felici et al. 1999). Interestingly, we observed an increase in the percentage of the fragment in PyMT *Ptpa*$^{\Delta}$ puro and myc-PTPA 326 # 7 cells and also with higher passage number in B6 cells and this correlated with an increased ability of focus formation.

In addition to our already proposed assays, such as the performance in other transformation assays or activity measurements of the PP2A C subunit, we are interested whether a difference in the Ser/Thr phosphorylation on PyMT between PTPA wild-type (and floxed) and delta cells can be found. The analysis of the association of the Hippo pathway effector protein TAZ but especially YAP by PyMT mediated immunoprecipitation as well as monitoring the PP2A holoenzyme assembly and activity, with special regards to the B and B' family proteins by immunoprecipitation via the HA-tagged C subunit is in our prospect for further studies. Expression studies by RNA-seq regarding differential expression of downstream targets of src regulation could be able to unveil whether the variation between transforming and non-transforming PyMT lies here. Mass spectrometry analysis of precipitates of full-length PyMT and the 40 kDa protein regarding their tyrosine phosphorylation sites as well as the stoichiometry and manner of the complex formation are another angle to further elucidate the phenotype.

However, before all these experiments can be conducted, the establishment of valid cellular model systems is necessary, as we have to acknowledge that the convincing findings originate from one cell line, which on its own has a limited scientific value. In both cellular systems we lacked the control for a *Ptpa* knock-out cell line without PyMT expression, which would have been interesting in terms of rescue effect of PyMT in *Ptpa* knock-out cells, a hypothesis which arose from the survival of tamoxifen-treated 326 # 7 PyMT cells and was further supported by the CRISPR/Cas9 experiment. Therefore we concluded that in the whole study we were not able to produce a fully reliable cell line, a problem which we propose to solve with two different approaches, as the reproduction of our data in other reliable cellular systems is a prerequisite for further studies. The first one includes the multiplex CRISPR/Cas9 concept, in which a number of 2 – 7 gRNAs are provided from an all-in one vector. Thereby targeting of multiple loci, also within the same gene, is possible and the probability of generating knock-outs is enhanced (Le Cong et al. 2013; Sakuma et al. 2014). Eventually, a cellline without PyMT would survive this treatment, as we were also able in the past to generate *Ptpa* knock-out cells without first expressing PyMT, using the Cre-Lox system (Frohner et al, unpublished data). The alternative route is to target the protein PTPA using the novel application of the cereblon system, which can be activated and directed by the addition of phthalimide (Winter et al. 2015; Koduri et al. 2019), where our lab could already show that the targeting and subsequent degradation of exogenously expressed PTPA was successful. Eventually a combined application of those two systems will prove to be useful in similar studies in the future.

In summary, in this master thesis we could recapitulate the known phenotype of *Ptpa* deletion in mouse embryonic fibroblasts in two cellular models, provide evidence for the dependency of PyMT mediated cell transformation on PTPA in one of the two models and open up a collection of continuative questions.

4. Materials and Methods

4.1. Working with Bacteria

4.1.1. Solutions and Media

LB-medium

- 10 g Tryptone (AppliChem #A1553)
- 5 g Yeast Extract (AppliChem #A1552)
- 5 g NaCl
- dissolved in 1l dH_2O, autoclaved and stored at room temperature

Ampicillin-stock (100x) (Gerbu #1046)

Stock solution [10 mg/ml] dissolved in dH_2O; filer sterilized using 0.2 µm filter, stored at -20°C

LB-medium with Ampicillin

10 ml of 100x stock solution of Ampicillin added to 1l of LB medium

LB-agar plates with Ampicillin

- 10 g Tryptone
- 5 g Yeast Extract
- 5 g NaCl
- 15 g Agar (AppliChem #A0949)
- dissolved in 1l dH_2O, autoclaved, cooled to 50°C, Ampicillin added (final concentration 100µg/ml) and plates poured at room temperature, stored at 4°C

4.1.2. Bacterial strain

XL-1 Blue Escherichia Coli recA1 endA1 gyrA96 hsdR17 supE44 relA1 lac [F′ proAB lacIqZΔM15 Tn10 (TetR)]. (Tetracycline resistant)

4.1.3. Transformation of competent XL-1 Blue Escherichia Coli

Competent XL-1 Blue Escherichia Coli were thawed on ice. 10 µl of ligation product was added to an amount of 90 µl bacteria and incubated for 20 minutes on ice. Heat shock was performed at 42°C for 1 minute; bacteria were subsequently cooled down for 5 minutes on ice. Bacterial suspension was streaked out on LB-agar plates with Ampicillin and grown at 37°C overnight.

4.2. Methods for Generation of *Ptpa* Knock-Out Cells

4.2.1. Cre-Lox System

Ingrid Frohner established embryonic stem cells with the *loxP* sites between Exon 1 – 2 and 3 – 4 of the *Ptpa* locus (Figure 27), thereby creating floxed (flanked loxP) exons (Janbandhu et al. 2014). Tamoxifen induced, nuclear translocation of the Cre-ER^T fusion protein leads to the loss of Exons 2 and

3 via Cre-dependent recombination. Translation of the resulting mRNA will lead to a premature termination after 19 amino acids.

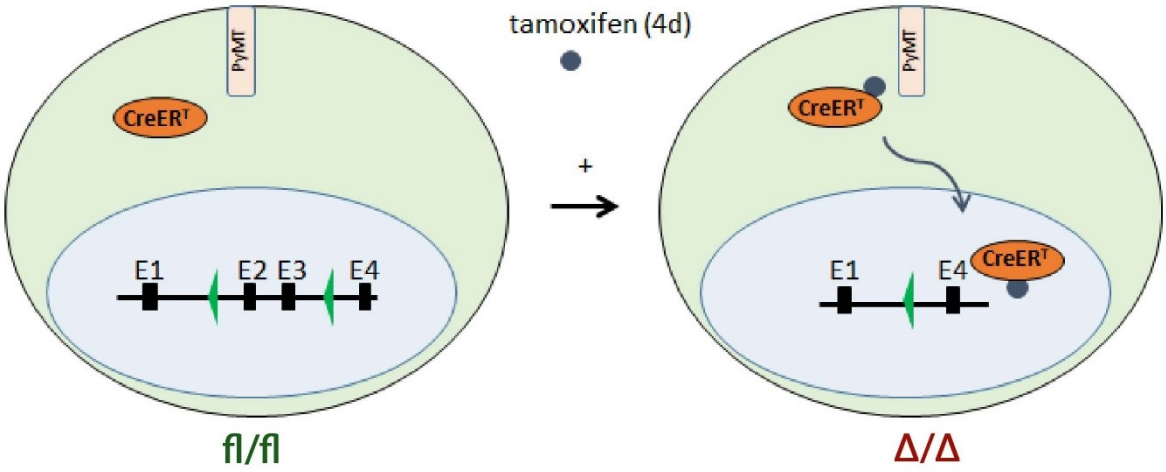

Figure 27 Strategy of *Ptpa* deletion by a Cre recombinase coupled to a tamoxifen-responsive estrogen receptor domain. Upon the administration of tamoxifen the Cre-ER^T fusion protein is recruited to the nucleus and excises Exons 2 and 3 of PTPA. Figure was adapted from Ingrid Frohner.

4.2.2. CRISPR/Cas9 System

For CRISPR/Cas9 mediated targeting of the PPP2R4 locus on murine chromosome 2, we used a combinatorial approach of two different gRNAs, c1 and c2 (Figure 28), exploiting the cells NHEJ repair mechanism to achieve *Ptpa* knock-out. Two expression vectors, both containing the genetic information for Cas9 expression, and one of the two gRNAs and a puromycin resistance were co-transfected into in NIH 3T3 or τ2C3C1 neo. The first gRNA (c1) bound within Exon 1, directly over the ATG of the Ptpa mRNA, the second (c2) within Exon 2 (Figure 28). Ingrid Frohner designed both similar to the ones that were used by Haplogen to generate the HAP *Ptpa* knock-out cell line. We chose the combinatorial approach because it has been reported that multiple gRNAs raise the efficiency in CRISPR/Cas9 mediated targeting (Le Cong et al. 2013; Xiangyang Chen et al. 2014; Xie et al. 2015).

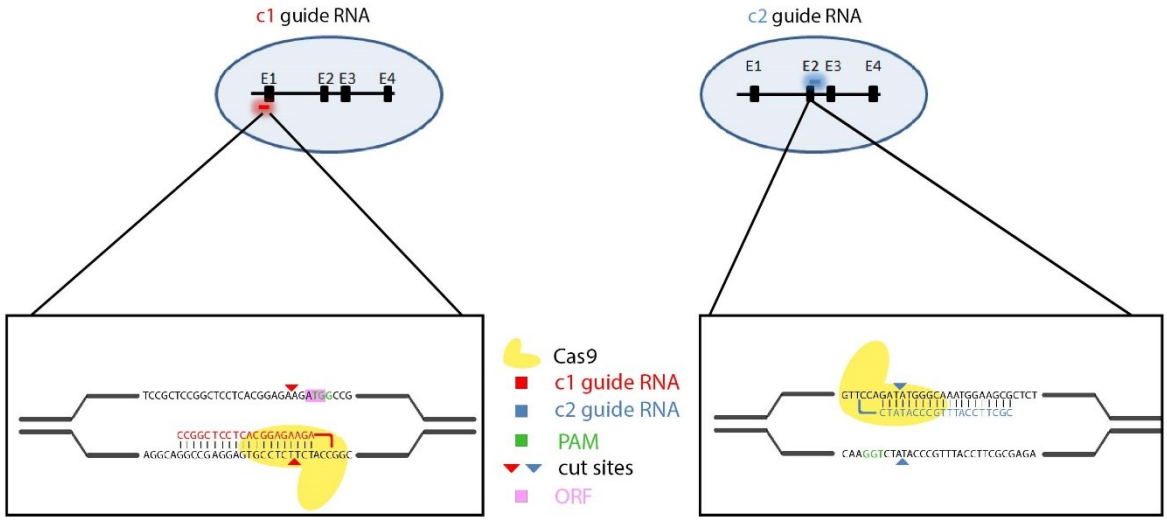

Figure 28 Strategy of *Ptpa* deletion by CRISPR/Cas9. Visualization of binding sites of the two used guide RNAs, c1 and c2, including a zoom-in.

4.3. Working with Nucleic Acids

4.3.1. Solutions and Media

Tail Lysis Buffer

- 100 mM Tris pH 8.0
- 5 mM EDTA pH 8.0
- 200 mM NaCl
- 0.1% SDS

Proteinase K (stock 20 mg/ml), final concentration 0.5 mg/ml

50 x TAE

- 2 M Tris
- 5.7% Acetic Acid
- 50 mM EDTA pH 8.0
- for usage dilute 1:50 in dH_20

Agarose (Sigma A9539)

GeneRuler 1kb plus DNA ladder, Ready-To-Use (75 to 20 000 bp) (Thermo Scientific # SM0311)

6x DNA loading dye (Fermentas #R0611)

- 4M Urea
- 50% (w/v) Sucrose
- 50mM EDTA pH 7.0

- 1% w/v Bromphenol blue

Ethidium bromide (AppliChem #A1151)

- 100 mg ethidium bromide
- 10 ml dH_20
- add to achieve a final concentration of 0.5 µg/ml

4.3.2. Preparation of Mammalian DNA for a PCR reaction

Tissue culture cells were washed 1x with warm PBS, trypsinised and washed off the plates with DMEM (+FCS, P/S, QMax). Harvested cells were pelleted by centrifugation for 5 minutes, 1400 rpm at room temperature. Supernatant was discarded and pellet was resuspended in tail lysis buffer including Proteinase K [0.5 mg/ml]. To the cell pellet approximately three times the volume of tail lysis buffer was applied. Lysis was performed at 55°C overnight on the shaker. Lysates were shortly centrifuged at 14 000 rpm and stored at 4°C.

4.3.3. PCR

4.3.3.1. Genotyping (wt/fl/delta or +/fl/Δ)

PCR was performed according to established protocol by IF. GoTaq PCR buffer and GoTag polymerase (Promega) were used in a mix of 30 µl (Table 2). Biometra T3000 Thermocycler was used for cycling (for programme see Table 3).

Due to the genotype three PCR products were possible: *Ptpa* wild-type (+) (270 bp), *Ptpa* floxed (fl) (366 bp) and *Ptpa* delta (Δ) (509 bp) (Figure 29).

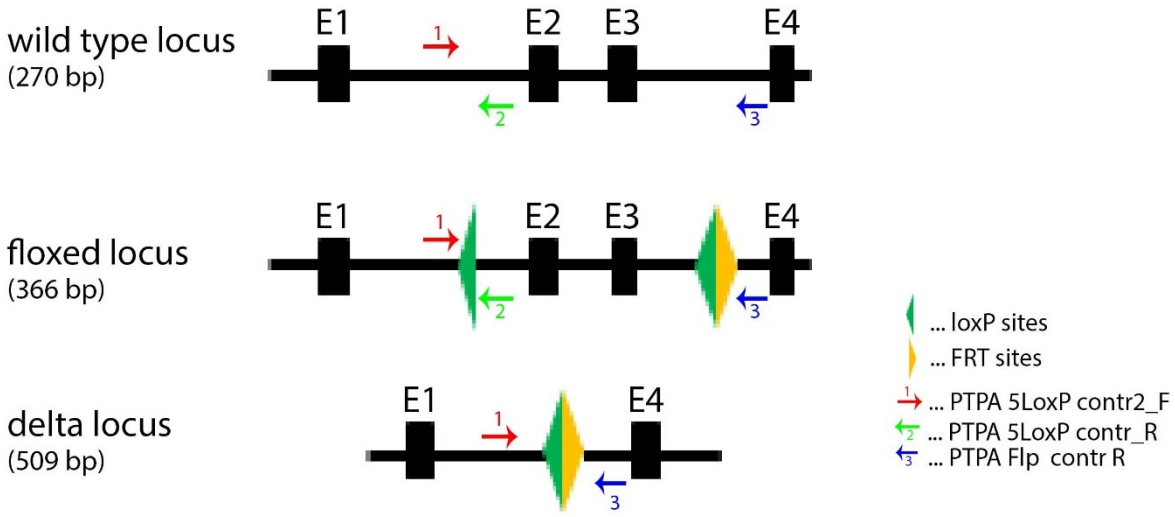

Figure 29 Schematic depiction of PPP2R4 locus with different configurations (wt/fl/Δ). Primer binding sites and size of resulting PCR fragments are indicated.

Table 2 Recipe for Genotyping PCR (creLox)

30 µl PCR Mix	
6 µl	5x GoTaq Buffer
0.3 µl	dNTPs [10 mM]
0.9 µl	Primer Mix (No: 1546, 1495, 1558, 3.3 µM each)
22 µl	dH_2O
0.3 µl	GoTag Polymerase
0.7 µl	Mouse DNA

Table 3 PCR programme for Amplification of the *Ptpa* locus

PCR Programme	**Temperature [°C]**	**Time**	**Repeats**
Initial Denaturation	95°C	5 min	1x
Denaturation	95°C	30 sec	32 x
Annealing	52°C	30 sec	
Elongation	72°C	45 sec	
Terminal Elongation	72°C	10 min	1x

4.3.3.2. Genotyping (CRISPR/Cas9 clones)

PCR was performed similar to established creLox-genotyping protocol by IF. GoTaq PCR buffer and GoTag polymerase (Promega) were used in a mix of 20 µl (Table 4). PCR programme was slightly adapted (Table 5). Biometra T3000 Thermocycler was used for cycling.

Three different PCR set-ups were performed:

- c1 (Primer No.: 2341 + 2343); calculated *Ptpa* wild-type size: 250 bp
- c2 (Primer No.: 2344 + 2346); calculated *Ptpa* wild-type size: 210 bp
- $c1_f$ + $c2_r$ (Primer No.: 2341 + 2346); no product in *Ptpa* wild-type.

Primers for the c1 PCR bond 119 bp up and 103 bp downstream the c1 guide RNA binding site, primers for the c2 PCR bound 119 bp up- and 72 bp downstream of c2 guide RNA binding site.

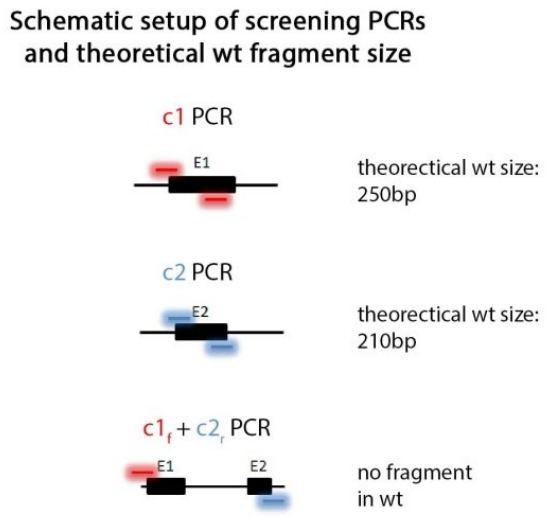

Figure 30 **Set-up for genotyping PCR in CRISPR/Cas9 screening** Primer pair of c1 was used to detect effects of CRISPR/Cas9 targeting the c1 guide RNA binding site, primer pair of c2 for the c2 guide RNA. The third PCR approach was a combination of c1 (forward primer) and c2 (reverse primer). Here the theoretical size would be over 10 000 bp.

Table 4 Recipe for Genotyping PCR (CRISPR/Cas9)

20 µl PCR Mix	
4 µl	5x GoTaq Buffer
0.2 µl	dNTPs [10 mM]
0.4 µl	forward Primer [3.3 µM]
0.4 µl	reverse Primer [3.3 µM]
0.2 µl	GoTag Polymerase
13.1 µl	dH_2O
0.7 µl	Mouse DNA

Table 5 PCR programme for Amplification of the *Ptpa* locus in the CRISPR/Cas9 screening

PCR Programme	**Temperature [°C]**	**Time**	**Repeats**
Initial Denaturation	95°C	5 min	1x
Denaturation	95°C	30 sec	35 x
Annealing	55°C	30 sec	
Elongation	72°C	30 sec	
Terminal Elongation	72°C	10 min	1x

4.3.3.3. Colony PCR (pJet1.2 Ligations)

Up to 5 colonies per LB-Amp plate of transformed XL1-*Blue E. Coli* from chapter 4.3.6 were picked off the plate for the colony PCR. PCR programme and reaction mix was adapted from PA (recipe see Table

6; programme Table 7). Gel fragments were eluted (chapter 4.3.5) and used for sequencing (chapter 4.3.12).

Table 6 Recipe for the PCR of pJet1.2 Ligations out of Bacterial Cultures

20 µl PCR Mix	
10 µl	2x Mastermix (prepared by PA)
0.4 µl	forward Primer (No: 2159, 3.3 µM)
0.4 µl	reverse Primer (No: 2160, 3.3 µM)
0.1 µl	GoTag Polymerase
9.1 µl	dH_2O
tip of bacterial culture	

Table 7 PCR programme for pJet1.2 Amplification out of Bacterial Cultures

PCR Programme	**Temperature [°C]**	**Time**	**Repeats**
Initial Denaturation	95°C	3 min	1x
Denaturation	94°C	30 sec	25 x
Annealing	60°C	30 sec	
Elongation	72°C	45 sec	
Terminal Elongation	72°C	3 min	1x

4.3.3.4. Q5 PCR for cDNA sequencing

For cDNA sequencing the Q5 Polymerase was used for DNA amplification. Q5 polymerase possesses proofreading activity which was crucial in the investigation of the *Ptpa* mRNA. As DNA template the cDNA from the reverse transcription was used (chapter 4.3.11). Recipe can be found in Table 8, programme in Table 9.

Three different PCR set-ups were performed:

- 170 aa *Ptpa* fragment (Primer No.: 2341 + 1356)
- 323 aa *Ptpa* fragment (Primer No.: 2341 + 1357)
- GAPDH (control)

Before loading onto an agarose gel 6x Loading Dye was supplemented to PCR. PCR products were eluted (chapter 4.3.5), ligated into pJet1.2 (chapter 4.3.6) and transformed into XL-1Blue *E.*Coli. Plasmids were isolated by Minipreparation (4.3.7) and used for sequencing (chapter 4.3.12).

Table 8 PCR recipe for Q5 PCR

50 µl PCR Mix	
10 µl	5x Q5 Buffer
0.5 µl	dNTPS [10mM]
2 µl	forward primer [3.3 µM]
2 µl	reverse primer [3.3 µM]
0.5 µl	Q5 Polymerase
35 µl	dH_2O
2 µl	cDNA

Table 9 PCR programme for Q5 PCR

PCR Programme	**Temperature [°C]**	**Time**	**Repeats**
Initial Denaturation	98°C	30 sec	1x
Denaturation	98°C	10 sec	35 x
Annealing	56°C	10 sec	
Elongation	72°C	30 sec	
Terminal Elongation	72°C	2 min	1x

4.3.3.5. Separation and Detection of PCR products

All PCR products were separated on a 1% - 2% agarose gel with TAE as running buffer. Ethidium bromide was supplemented in the agarose gel for DNA detection [0.5 µg/ml]. Herolab Transilluminator was used for visualization. Thermo Scientific GeneRuler 1kb plus DNA ladder was included in all detections.

4.3.4. Primer List

Table 10 Primer List for performed PCRs

PCR primer	Nr.	Sequence (5‘ – 3‘)
Genotyping PCR creLox		
PTPA 5LoxP contr2_F (forward)	1546	gttttttttaacctgaagtcatag
PTPA 5LoxP contr_R (reverse)	1495	cgcacatctagcagttctc
PTPA flp contr R (reverse)	1558	ctacagccctaaatcccatc
CRISPR PCR		
PTPA C1 contr1_s (forward)	2341	cgcgcgagtgactgtaattct
PTPA C1 contr1_as (reverse)	2343	tcctcagactcgggagac
PTPA C2 contr_s (forward)	2344	ggagggaagaattatttacctg
PTPA C2 contr2_as (reverse)	2346	gccactgactgataagcc
Ligation Amplification		
pJet1.2 forward	2159	cgactcactatagggagagcggc
pJet1.2 reverse	2160	aagaacatcgattttcatggcag
Reverse Transcription		
GAPDH forward	-	Primers provided by Seiser Lab, exact sequence not known
GAPDH reverse	-	Primers provided by Seiser Lab, exact sequence not known
PTPA C1 contr1_s (forward)	2341	cgcgcgagtgactgtaattct
PTPA 170aa SphI_R (reverse)	1356	cgACATgcatgcACCAATCTTGCAGAGACAAC
PTPA 323aa SphI_R (reverse)	1357	cgACATgcatgcGCCTGATGTGACGGGATG

4.3.5. Gel Elution (Promega Wizard SV Gel and PCR Clean-Up System (A9282))

PCR products were separated by agarose gel electrophoresis (percentage of agarose gel was selected in accordance to the size of the PCR products, between 1% and 2%). Each DNA fragment was cut out and taken up in an appropriate amount of Membrane binding solution and heated at 55°C until the mixture was viscous. In the following DNA solution was transferred onto a DNA binding membrane. Gel elution was performed according to the manufacturer’s protocol. DNA was eluted in nuclease-free water. DNA concentration was determined by Nanodrop 2000c measurement. Eluted products were stored at -20°C until further usage.

4.3.6. Ligation (Thermo Scientific CloneJET PCR cloning kit)

For ligation of the eluted DNA fragments the Thermo Scientific CloneJET PCR cloning kit (#K1231) was used. The manufacturer's protocol for sticky-end cloning was followed (blunting reaction). The ligation mixture can be found in Table 11. Ligation product was transformed into competent XL-1 Blue Escherichia Coli (chapter 4.1.3).

Table 11 Recipe for Ligation Mix

Ligation Mix	
5 µl	Buffer
2 µl	dH_2O
0.5 µl	blunting enzyme
75 ng	eluted PCR product
0.5 µl	vector (pJet1.2)
0.5 µl	ligase

4.3.7. Minipreparation (Monarch Plasmid Miniprep Kit, NEB)

For preparation of plasmids out of XL-1 Blue Escherichia Coli the Monarch Plasmid Miniprep Kit (New England Biolabs, #T1010) was used. 5 ml liquid LB Amp was inoculated with one bacterial colony each, centrifuged 30 minutes at 1600 rpm and 4°C (Megafuge 1.0 Heraeus - Sepatech). Subsequently Miniprep Kit protocol was followed. DNA was eluted by the addition of 30 µl nuclease-free water and concentration determined by Nanodrop 2000c measurements. Purified plasmids were stored at -20°C.

4.3.8. Midipreparation (Pure Yield Plasmid Midiprep System Kit, Promega)

To purify plasmids later on used in cell culture (e.g. generation of retroviral supernatants) DNA preparation via the Pure Yield Plasmid Midiprep System Kit (Promega #252219) was used. Bacterial colonies were inoculated in a 100 ml culture and centrifuged for 40 minutes at 3000 rpm and 4°C (RC5C - Sorvall Instruments). The manufacturer's protocol was followed. DNA was eluted by addition of nuclease-free dH2O and concentration was determined by Nanodrop 2000c measurements. Purified plasmids were stored at -20°C.

4.3.9. Plasmids

Table 12 List of Expression Vectors used in this Masterthesis

Mammalian Expression Vectors		**cloned by**
pBabe neo		J. P. Morgenstern, H. Land, Advanced mammalian gene transfer: high titre retroviral vectors with multiple drug selection markers and a complementary helper-free packaging cell line.
pBabe neo [PyMTUS]	murine Polyomavirus Middle Tumor Antigen, US variant	Lucas Stadtmann
pBabe neo [PyMTAU]	murine Polyomavirus Middle Tumor Antigen, AU variant	Lucas Stadtmann
pBabe puro		J. P. Morgenstern
pBabe puro [myc-PTPA]	myc-tagged mouse PTPA	Ingrid Frohner
pBabe hygro		J. P. Morgenstern
pBabe hygro [PyMT]	murine Polyomavirus Middle Tumor Antigen	Egon Ogris
px459 puro [c1 # 1]	Cas9 plus c1 gRNA	Ingrid Frohner
px459 puro [c2 # 1]	Cas9 plus c2 gRNA	Ingrid Frohner
pRetro super[p19Arfsh]	p19Arfsh plus green fluorescent protein-tagged creERT	Jamie James
pRetro [p19Arfsh CreERT]	p19Arfsh PGK creERT T2A bleomycin	Ingrid Frohner
Bacterial Expression Vectors		
pJet1.2 blunt	Ampicillin resistance, cloning vector	Thermo Scientific
pB'HJPyST #1	Expression vector of PyST - Antigen	Ingrid Mudrak

Respective Vector maps can be found in the appendix (chapter 6.8).

4.3.10. RNA Isolation (RNeasy Mini Kit, Qiagen 74106)

For RNA isolation cells were detached with trypsin and washed off cell culture with pre-warmed PBS. Cell count was determined using LUNA cell counter (chapter 4.4.8.1). Between $5x10^5$ and $1x10^7$ cells were used as input and centrifuged for 5 minutes at 1200 rpm. PBS was removed and cell pellet taken up in 300 µl Buffer RLT. The centrifugation step after cell lysis was skipped, as this is not necessesary when purifying RNA from animal cells. For the isolation the whole cell lysate was further used and the manufacturer's protocol was followed. The optional step (DNase digestion) was not performed. Isolated RNA was eluted in 30 µl RNase free dH_2O.

Bench and pipettes were thoroughly cleaned before working with RNA.

4.3.11. Reverse Transcription (Revert Aid)

For cDNA synthesis Thermo Scientific RevertAid First Strand cDNA Synthesis Kit (#K1621) were performed according to manufacturer's protocol. The optional step (65°C for 5 minutes) was included to open up secondary structures. The reverse transcription recipe can be found in Table 13. For reverse transcription isolated RNA was used. Reverse transcription mix was gently mixed and briefly centrifuged. Reverse transcription was performed at 42°C for 60 minutes and terminated at 72°C for 5 minutes. Obtained cDNA was stored at -20°C and further used as input in PCR (chapter 4.3.3.4).

Table 13 Recipe for Reverse Transcription

Reverse Transcription Mix	
100 pmol	$Oligo(dT)_{18}$ primer
150 ng	isolated RNA
to 12 µl	dH_2O (nuclease free)
65°C for 5 minutes	
4 µl	5x Reaction Buffer
1 µl	Ribolock RNase Inhibitor
2 µl	dNTPs [10mM]
1 µl	RevertAid M-MuLV RT

4.3.12. DNA Sequencing

DNA sequencing was performed by LGC genomics. DNA with a final concentration of 100 ng/µl was submitted. Either primer to a final concentration of 1.4 µM were supplied or the primers were added by LGC genomics. For sequencing the forward and reverse primer of the pJet1.2 amplification were used (Table 10). For analysation ApE programme was used. Sequences can be found in the appendix 6.6 and 6.7.

4.4. Working in Tissue Culture

4.4.1. Solutions and Media

Growth Medium: DMEM + 10% Fetal Calf Serum + Glutamine + P/S

- Dulbecco's Modified Eagle's Medium (DMEM) – high glucose; (Sigma #D5671)
- Fetal Calf Serum (FCS) (Gibco #4023696J), stored at -20°C
- Glucose (QMax)
- Penicillin & Streptomycin
    - 0.6 g Penicillin-G
    - 1 g Steptomycin-sulfate
    - 10 ml 10x PBS
    - fill up to 100 ml with dH_2O
    - filter sterilized (0.2µm) and stored at -20°C

Freezing Medium

- 90% FCS
- 10% Dimethylsulfoxide (DMSO, Applichem #A3672.0250)
- stored at -20°C

Geneticin [12mg/ml] (Gibco #11811-098)

- 1.2g Geneticin
- 100 ml DMEM+P/S
- filter sterilized and stored at -20°C

Hygromycin B [50mg/ml]

- aliquoted and stored at -20°C

Puromycin [10mg/ml] (Sigma #P-7255)

- 100 mg Puromycin
- 10 ml dH_2O
- filter sterilized (0.2µm), aliquoted and stored at -20°C

Blasticidine [2.5 mg/ml]

- 50 mg Blasticidin S (Invitrogen #R210-01)
- 20 ml dH_2O
- filter sterilized (0.2µm) and stored at -20°C

Zeocin [100 mg/ml]

- Invitrogen #R25001
- stored at -20°C

Trypsin (Serva #37296)

- 250 mg trypsin
- 25 ml 10x PBS
- 220 ml dH_2O
- 5 ml 1% Na-EDTA (pH 7.4)
- filter sterilized (0.2µm) and stored at -20°C

4.4.2. Cultivation of Mammalian Cells

Cells were cultured in Dulbecco's Modified Eagle's Medium (DMEM) supplemented with 10% fetal calf serum (FCS), Penicillin (100 units/ml) and Streptomycin (100 µg/ml) (P/S) and Qmax at 37°C at either 5% or 7.5% (NIH T.R. 3T3, τ2C3C1 neo, Swiss 3T3) CO_2. If necessary antibiotics (puromycin [2.5 µg/ml], hygromycin B [100µg/ml], neomycin (G418 geneticin) [250µg/ml], zeocin [100 µg/ml]) were added to the medium (Table 14 – cell types). DMEM and PBS were pre-warmed to 37°C, trypsin to room temperature.

For splitting, plates were washed once with PBS, then detached by adding trypsin and incubation for 5 minutes at 37°C. Cells were resuspended in an appropriate amount of DMEM (+FCS, P/S, Qmax) and a fractional amount (between 50% (1:2) and 2% (1:50) of cells) was transferred to a new tissue culture dish. For freezing cells were centrifuged 5 minutes at 1200 rpm, resuspended in an appropriate volume of FCS + 10% DMSO and subsequently transferred to cryo-tubes. After 10 minutes cooling down on ice, cells were first stored at -80°C for two days and then transferred to either liquid nitrogen or a -150°C freezer. For thawing cryo-tubes were warmed in the 37°C water-bath until the suspension was liquid. Cells were then immediately taken up in 9 ml DMEM (+FCS, P/S, Qmax). After centrifugation (5 minutes, 1200 rpm) supernatant was sucked off, pellet taken up in fresh DMEM (+FCS, P/S, Qmax) and plated on a tissue culture dish. Appropriate amounts of selection antibiotics were added 24 hours after thawing.

Upon infection with bacteria Gentamycin (1:1000) was added until two days post clearance of infection. Bacterial infection occurred during the testing of the new primary MEFs described in 2.2, except for the 326 # 7 cells (577 MEF # 4 *Ptpa*$^{fl/fl}$, 578 MEF #1 *Ptpa*$^{fl/fl}$, 624 MEF # 1 *Ptpa*$^{fl/fl}$, 624 MEF # 4 *Ptpa*$^{fl/+}$) .

Ptpa deletion was induced by addition of Tamoxifen [1 µM], dissolved in Ethanol, to the culture medium twice, two days apart. An equal amount of Ethanol was added to control cells (MOCK).

Table 14 **List of Cell Lines used in this Masterthesis**. Passage for certain cell lines undisclosed (ud).

Mammalian Cell Lines	**passage**	**immortalized with**	**additional vectors**	**created by**
112 MEF # 4 *Ptpa*$^{fl/fl}$ single clone B6	ud	pBabe puro p19Arfsh GFPcreERT	pBabe hygro; pBabe hygro PyMT	Ingrid Frohner
326 MEF # 7 *Ptpa*$^{fl/fl}$	ud	pRetro p19Arfsh PGK creERT T2A bleomycin	pBabe neo; pBabe neo $PyMT_{US}$ (+ pBabe puro or pBabe puro myc-PTPA)	Ingrid Frohner / Michaela Zrelski
577 MEF # 4 *Ptpa*$^{fl/fl}$	P0 (14.12.16)	pRetro p19Arfsh PGK creERT T2A bleomycin	pBabe neo; pBabe neo $PyMT_{AU}$; pBabe neo $PyMT_{US}$	Ingrid Frohner / Michaela Zrelski
578 MEF # 1 *Ptpa*$^{fl/fl}$	P0 (14.12.16)	pRetro p19Arfsh PGK creERT T2A bleomycin		Ingrid Frohner / Michaela Zrelski
624 MEF # 1 *Ptpa*$^{fl/fl}$	P1 (28.11.16)	pRetro p19Arfsh PGK creERT T2A bleomycin	pBabe neo; pBabe neo $PyMT_{US}$	Ingrid Frohner / Michaela Zrelski
624 MEF # 4 *Ptpa*$^{fl/+}$	P1 (28.11.16)	pRetro p19Arfsh PGK creERT T2A bleomycin	pBabe neo; pBabe neo $PyMT_{US}$	Ingrid Frohner / Michaela Zrelski
NIH Tom Roberts *Ptpa*$^{+/+}$	ud	3T3 protocol	px459 puro c1 + px459 puro c2 (transiently)	lab stock Michaela Zrelski
τ2 *Ptpa*$^{+/+}$	ud	3T3 protocol	puro PyMT	lab stock
τ2 *Ptpa*$^{+/+}$ single clone C3C1	ud	3T3 protocol	neo PyMT; px459 puro c1 + px459 puro c2 (transiently)	lab stock / Michaela Zrelski
Swiss *Ptpa*$^{+/+}$	ud	3T3 protocol		lab stock
Platinum E packaging cells	ud			purchased (BioLabs)

4.4.3. Transfection Agents

2x HBS

- 280 mM NaCl
- 50 mM Hepes pH 7.12 (AppliChem #A1069)
- 1.5 mM Na_2HPO_4
- accurate pH (7.12) is important, filter sterilized (0.2µm) and stored at 4°C

2.5 M $CaCl_2$

- 36.8 g $CaCl_2.2H_2O$
- 100 ml H_2O
- autoclave and stored at 4°C

Chloroquine (1000x)

- 25 mM in PBS
- 0.129 g Chloroquine (Sigma #C-6628)
- 10 ml dH_2O
- filter sterilized (0.2µm) and stored at -20°C

Polybrene (1000x)

- 4 mg/ml in PBS
- 40 mg Polybrene (Hexadimethrine bromide, Sigma #52495)
- 10 ml dH_2O
- filter sterilized (0.2µm) and stored at -20°C

Turbofectin 8.0 (Origene)

4.4.4. Calcium Phosphate Transfection (Platinum E cells)

Platinum E Retroviral Packaging cells (BioLabs) were thawed, selected with 10 µg/ml blasticidine and a number of $2x10^6$ cells were plated per p60 culture dish. Culture medium was taken off, cells were washed with pre-warmed PBS and incubated with the transfection mix (Table 15). The DNA mix was prepared beforehand. HBS was aerated while adding the DNA mix, which led to the formation of calcium-phosphate-DNA-precipitates. Per p60 plate in total 5 ml (1 ml transfection mix, 4 ml DMEM (+FCS, P/S, Qmax) plus chloroquine (25µM final conc.) were added and incubated for 24 hours. After incubation, transfection mix was taken off, discarded and transfected cells were cultured in 3 ml of DMEM (+ FCS, P/S, Qmax) for another 24 hours. Supernatant was taken off, centrifuged at 1600 rpm for 5 minutes (at room temperature), aliquoted and stored at -80°C. Procedure was repeated for the p60 plates (addition of DMEM, incubation and harvesting of retroviral supernatant).

All dishes and liquids in contact with retroviral supernatant were cleaned through incubation with Hypochlorite.

Table 15 Recipe for DNA transfection mix

DNA transfection mix	
500 µl	HBS
500 µl	DNA mix: 450 µl (H_2O + 10 µg DNA) + 50 µl $CaCl_2$

Retroviral supernatant was generated for the pBabe and pRetro vectors (Table 12).

4.4.5. Infection with Retroviral Supernatant

Mouse embryonic fibroblasts were plated on a p60 dish to reach a confluency of 80%. Growth medium was taken off and cells were incubated with 1.5 ml retroviral supernatant + Polybrene (8µg/ml final conc.) for three hours. In the following, for overnight incubation, 3 ml DMEM (+ FCS, P/S, Qmax) was added to the plates. Medium was changed on the next day, appropriate selection antibiotics supplemented 24-48 hours after infection. Success of infection was additionally tested by immunoblotting for the expression of the recombinant protein.

4.4.6. Transfection with Turbofectin 8.0 (Origene)

NIH 3T3 Tom Roberts and τ2C3C1 neo cells were plated to a confluency of approximately 90%. Since the cells otherwise would have been too confluent, reverse transfection protocol was applied. Therefore, the cells seeded on a tissue culture dish shortly after the Turbofectin/plasmid mix was added. 700 µl Optimem was mixed with 5.0 µg plasmid and vortexed gently. 15 µl Turbofectin was added, again gently mixed and incubated for 15 minutes at room temperature. Either 4.2 x 10^5 (NIH 3T3 Tom Roberts) or 3.5 x 10^5 (τ2C3C1 neo) were seeded and incubated with the transfection mix for 24 hours. Afterwards medium was changed and supplemented with 5 µg/ml puromycin. To kill untransfected cells, selection with puromycin was performed for 16 hours.

The px459 vectors were transfected with Turbofectin 8.0 (Table 12).

4.4.7. Screening of CRISPR/Cas9 treated cells

To plate one cell per well cells were minimally diluted to a concentration of 1 cell per 100 µl (10 cells/ml) and distributed in two 96-well plates each. The other half of the mixed clones were frozen and stored at -80°C. A small sample was taken for genotyping PCR (chapter 4.3.2 and 4.3.3.2).

Minimal dilutions in 96-well plates were monitored through the light microscope (Olympus CKX41). Cells were grown until confluency in the 96-well plate, then transferred to a 24-well plate and in the following to a 6-well plate. Remaining cells in the 96 well plate were further grown to confluency and

then directly lysed in the well by the addition of Tail Lysis Buffer + Proteinase K and incubation overnight at 37°C for genotyping PCR (chapter 4.3.2 and 4.3.3.2). Half of the cells from the 6-well plate were frozen, the other half further expanded to p100 plates. Protein lysates were prepared of the cells from the p100 plates and analysed by immunoblotting. Promising clones were analysed by DNA sequencing of cloned fragments of the genotyping PCR. The cDNA of the isolated mRNA of still promising clones was additionally sequenced.

4.4.8. Cell Concentration Determination

4.4.8.1. CASY Counter TCC (Innovatis)

To determine the concentration of a cell suspension for plating 50µl were diluted in 5 ml of CASYton buffer. For the measurement of the proliferation curve either 100 µl, 50µl or 25 µl of the cell suspension were diluted in 5 ml of CASYton buffer, depending on the number of cells.

4.4.8.2. Luna Automated Cell Counter (Logos Biosystems)

To determine the concentration of a cell suspension for plating 10 µl of cell suspension was diluted with 10 µl trypan blue (supplied by Logos Biosystems). 10µl was embedded in the slot of Luna Cell Counting Slides and measured according to the manufacturer's protocol.

4.4.9. Assays

4.4.9.1. Focus Formation Assay

Phosphate Buffer pH 6.0

- 74 mM NaH_2PO_4
- 9 mM Na_2HPO_4
- dissolved in dH_2O

Giemsa's azure eosin methylene blue solution (Merck 1.09204)

- 0.4% w/v in buffered methanol
- pH 6.9
- working solution diluted 1:10 with phosphate buffer

CASY counter TTC (Innovatis) was used to measure cell number. Cells were diluted to a concentration of 1000 cells/ml. Non-oncogenic cells were plated for monolayer formation (B6 *Ptpa*^{fl} hygro 2x10^4 cells, 326#7 *Ptpa*^{fl} neo 5x10^4, S3T3 *Ptpa*$^{+/+}$ 8x10^4) and an appropriate amount of potential tumor cells were added. The seeding numbers for all cells were chosen according to previous experience with the respective cell line, including the observation of their proliferation speed. 500, 200 and 100 PyMT-expressing cells were seeded for less transformed young B6 cells, 200, 100 and 50 for old B6 cells (see chapter 2.1). For 326#7 and τ2C3C1 neo cells 500, 250 and 125 PyMT cells were plated. Cells were

grown in the incubator at the respective conditions. B6 cells were incubated for different durations (see Table 1a and b). 326#7 and τ2C3C1 cells were incubated for 14 days, medium was changed after 7 days.

Before fixation, plates were washed 2 times with cold PBS and then fixed 7 minutes with methanol. After air-drying plates were stained for 30 minutes with Giemsa's solution. Assays were destained with dH_2O. Air-dried plates were scanned, foci counted blindfolded. Quantification of the area covered by foci was performed as previously described (Guzmán et al. 2014).

4.4.9.2. Proliferation Curve

$5x10^4$ cells of each cell line were seeded in duplicates in 6-well plates and incubated over the course of either five or seven days. Each day one time point (desirably with a 24 hour difference to the last one) was measured by harvesting and counting the cells with the CASY counter TTC (Innovatis). Amount of trypsin to detach cells and amount of DMEM (+ FCS, P/S, Qmax) was selected appropriate to cell numbers. Either 100 µl, 50µl or 25 µl of cell suspension were used for measurement. Absolute cell count as well as doubling times were calculated, cell size monitored.

4.4.9.3. Cell Death Assay

$5x10^4$ cells of each cell line were seeded in 6-well plates and grown for 24 hours. Cells were harvested, centrifuged 5 minutes at 1200 rpm, 4°C and taken up in 1 ml PBS. Cells were measured with FACSCalibur first, then 1 µl propidiumiodide was added, slightly vortexed and measured again. Measurement and gating was performed by Ingrid Frohner.

4.4.9.4. Micronucleus Formation

An appropriate amount of cells was seeded on a cloverslip (NA #1.0). Cells were grown to confluency, fixed with 3.7 % Paraformaldehyde in PBS for 10 minutes/RT, afterwards permeabilized 0.2% Triton-X/PBS for 10 min/RT. After blocking with 2 % BSA/PBS for 1h/RT coverslips were incubated with Hoechst 33342 (0.75 µg/ml) for 10 minutes, room temperature and in the dark. Slides were washed 3x with PBS and 1x with dH_2O. Slides were mounted with VectaShield on a superfrost + object carrier. For detection Zeiss Axiovert 200M "ApoTome" 40x magnification was used. Four categories were determined: normal nucleus, one micronucleus, two micronuclei or more than two micronuclei, quantification was performed blindfolded.

4.4.9.5. Metaphase Spreads

- Colcemide: Karyomax in HBS (10 µg/ml), Thermo
- 0.56 % KCl w/v in dH_2O (0.28 g in 50 ml), stored at RT
- MAA fixate: 3 parts Methanol, 1 part Acetic acid (stored at -20°C)

$2x10^5$ (τ2C3C1 neo) or $1x10^6$ (NIH 3T3 Tom Roberts) cells were plated on a p100. DMEM was replaced with 10 ml DMEM + 100 µg Karyomax for 1h at 37°C. Medium was collected in a 50 ml falcon. p100 dish was incubated with trypsin (3 ml, 5 min, 37°C), cells were washed off plates and taken up in 4 ml DMEM to achieve a single cell suspension. Cell suspension was pooled with first medium and cells were pelleted 200g, 5 min at RT. Supernatant was kept, pellet resuspended in 15 ml warm KCl and incubated for 12 minutes at 37°C. 0.5 ml ice cold MAA was added and inverted. Another centrifugation round (200 g, 5 min, RT) was performed. Supernatant was decanted and pellet taken up in 2 ml of MAA fixative. 12 ml of MAA was added and cell suspension incubated for 20 minutes at -20°C. Three times washing (centrifugation (200g, 5 min, RT) plus resuspension) was performed. Pellet was resuspended in 2 ml MAA fixative and stored at -20°C.

For slide preparation in total 30 µl of cell suspension was dropped from a height of 20 – 30 cm onto a superfrost+ object carriers. Slides were air dried for two days. Chromosomes were stained by incubation for 10 minutes with 1:1000 diluted Hoechst 33342 Staining. Slides were mounted with VectaShield onto coverslips with NA#1.5. Metaphase spreads were recorded using Zeiss LSM 700 confocal microscope (63x magnification).

4.5. Working with Proteins

4.5.1. Solutions and Media

4.5.1.1. General Reagents & Materials

20 x PBS

- 2.8 M NaCl
- 54 mM KCl
- 30 mM $KH2PO_4$
- 160 mM $Na_2HPO_4.2H_2O$
- dissolved in dH_2O, stored at RT
- for usage 1:20 diluted in dH_20

IP Wash

- 10% Glycerol
- 20 mM Tris pH 8.0
- 135 mM NaCl
- dissolved in dH_20, stored at 4°C

IP Lyse

- IP Wash
- 1% NP-10 (Nonidet P-40 Amresco #E109, dissolved in dH_20)
- 0.1% SDS
- 150 mM NaCl
- 10 mM Sodium Phosphate pH 7.2
- dissolved in dH_20, stored at 4°C

Protease Inhibitors

- Phenylmethylsulfonyl fluoride (PMSF) (Roche # 10 837 091 001); 0.2 M (0.697 g) in 20 ml Isopropanol, 200x stock solution, stored in dark at RT
- Aprotinin (Simga #A-6279); 200x stock solution, stored at 4°C
- Complete (25x) (Roche # 11 836 145 001); 1 tablet dissolved in 2 ml IP Lyse, stored at 4°C

Phosphatase Inhibitors

- 50 mM Sodium Fluoride (Merck #6449); dissolved in IP Lyse, stored at 4°C
- 20 mM Sodium Pyrophosphate (Merck #1.06591); dissolved in IP Lyse, stored at 4°C
- Sodium orthovanadate (Sigma #S-6508); 200x stock solution, stored at -20°C
- β-Glycerophosphate (Sigma #G-6251); 100x stock solution (activated), pH 10.0, stored at -20°C

Tris-Buffered Saline (TBS, pH 7.5)

- 137 mM NaCl
- 2.7 mM KCl
- 25 mM Tris
- dissolved in dH_20, pH adjusted with HCl, stored at RT

4.5.1.2. Reagents for Antibody Coupling

Sodium Borate (di-sodium tetraborate) (Merck 1.06306), 0.2 M, pH 9

Dimethylpimelimidate dihydrochloride (Sigma D8388); 20 mM; 52 g dissolved in 10 Sodium Borate

Ethanolamine (2-Aminoethanol) (Sigma Aldrich 39,813-6); 0.2 M pH 8, 6.25 ml Ethanolamin in 500 ml dH_2O, pH adjusted with HCl

Glycine; 100 mM, pH 3

Protein A Sepharose Beads (GE Healthcare #17-0780-01)

4.5.1.3. SDS-PAGE Reagents & Materials

30% Acrylamide

- 29.2% Acrylamide (Serva #10675)
- 0.8% N,N'-Methylene-bisacrylamide (Serva #29195)
- dissolved in dH_20, stored at 4°C
- for storage Mixed-bed ion-exchange AG 501-X8(d) Resin (Biorad #142-6425) added

1M Tris pH 8.8 (for separation gel); 242.3 g Tris in dH_2O dissolved, pH adjusted with HCl, filled up to 500 ml with dH_2O, autoclaved and stored at 4°C

1M Tris pH 6.8 (for stacking gel); 60.5 g Tris in 1l dH_2O dissolved, pH adjusted with HCl, filled up to 2l with dH_2O, autoclaved and stored at 4°C adjust pH with HCl, stored at 4°C

20% SDS (Sodiumdodecylsulfate) (Amresco #0227), 40g SDS dissolved in dH_2O, slightly heated and then filled up to 200 ml with dH_2O, stored at RT

10% APS (Ammoniumperoxodisulfate) (Merck #1201); 1g APS dissolved in 10 ml dH_2O, stored at 4°C

TEMED (N,N,N',N'-Tetramethylenediamine) (Fluke #87689)

10x Running Buffer

- 250 mM Tris
- 2 M Glycine
- 0.1% SDS
- dissolved in dH_2O, stored at RT
- for usage 1:10 diluted with dH_2O

GSD (3x)

- 335 mM DTT (Gerbu #1008)
- 20 ml dH_20
- 230 mM SDS
- 4.5 M Glycerol (Merck #1.04092)
- a bit of Bromphenol Blue (Serva #15375) and a few drops 1M Tris pH 6.8, stored at -20°C

Precision Plus Protein™ All Blue Standards, diluted 1:10 with GSD

Instant Blue (Coomassie) Staining Solution (Expedeon, reused, stored at 4°C)

4.5.1.4. Western Blot Reagents & Materials

3 mm Whatman chromatography paper (3030-6461)

Protran nitrocellulose membrane (Whatman 10402493)

Transfer Buffer

- 25 mM Tris
- 190 mM Glycine
- dissolved in dH_2O
- then 20% (v/v) Methanol added, stored at 4°C

Ponceau S stock solution

- 2% (w/v) Ponceau S (Serva #33429)
- 30% (w/v) Trichloroacetic acid (AppliChem #A1431)
- 30% (w/v) Sulfosalicylic acid (Merck #1.00691)
- dissolved in dH_2O, stored at RT
- for usage 1:10 diluted with dH_2O

4.5.1.5. Immunoblotting reagents

20% Sodium Azide (Merck #67188); 2g Sodium Azide in 10 ml dH_20, stored in dark at 4°C

1% Thimerosal (Sigma #T-5125); 0.5g Thimerosal in 50 ml dH_20, stored in dark at RT

PBS-Tween; dilute PBS stock 1:20, add 0.05% Tween-20), stored at RT

TBS-Tween; dilute TBS stock 1:10, add 0.05% Tween-20), stored at RT

3% Non-Fat Dry Milk (Merck #1.15363); 30 g NFDM, 1000 ml PBS-Tween, 0.02% Sodium Azide, stored at 4°C

0.5% Non-Fat Dry Milk; 5 g NFDM, 1000 ml PBS-Tween, 0.1% Thimerosal, stored at 4°C

3% Bovine Serum Albumin; 15 g BSA (Sigma #A-9647) dissolved in 500 ml TBS-Tween, filter sterilized and stored at 4°C

1% Bovine Serum Albumin; 5 g BSA dissolved in 500 ml TBS-Tween, filter sterilized and stored at 4°C

ECL Western Blotting Detection Reagent (GE Healthcare Amersham RPN2108)

ECL Select Western Blotting Detection Reagent (GE Healthcare Amersham RPN2235)

4.5.1.6. Immunofluorescence Reagents

3.7% Paraformaldehyde (in PBS), stored at -20°C

0.2% Triton X-100 (w/v) (Merck #1.12298)

- Stock solution 10% (10 g Triton X-100 in dH_2O)
- 1:500 diluted in PBS, stored at RT

Hoechst 33342 Staining [750 µg/ml]

- 1000 µg Hoechst 33342
- dissolved in 1.3 ml dH_2O
- stored at -20°C (in the dark)

4.5.2. Affinity Purification of Polyclonal Antibodies

PyST 8th bleed antibody was purified according to the routine protocol for the affinity purification of polyclonal antibodies in our lab. The antigen pΔ'His PyST [1.5 µg/µl], against which the PyST antibody was raised, was tested whether the PyMT and/or the PyST recognize it and subsequently 200 µg of the antigen pΔ'His PyST were run on a large 12.5% SDS-PAGE and transferred to a nitrocellulose membrane. The membrane was stained with PonceauS, the protein band cut out and blocked with 3% NFDM in PBS-T, washed 5x with PBS-T and incubated with 1 ml antiserum for 2-3 days on the rotator at 4°C. Membrane was washed two times (10mM Tris pH 8.0, 1x + 0.5M NaCl). Antibodies were eluted by acidic elution (4x 100mM Glycin, pH 2.5, incubation for 2 minutes). Acid was neutralized by addition of 1M Tris pH 8.0. Purified antibodies were stored at 4°C (+Sodium Azide).

Purified antibodies were tested for efficiency and specificity in immunoblotting, immunofluorescence and immunoprecipitation.

4.5.3. Crosslinking of Antibodies to Protein A Sepharose beads

Protocol of for the coupling of HA-antibody 12CA5 to protein A sepharose beads was followed (Harlow and Lane 1999). 0.5 ml solid protein A beads, already coated with BSA, were mixed with 1.5 purified PyST 8th bleed antibody and rotated at room temperature for 2 hours. Beads were spun down 1 minute at 1000 rpm, transferred to 10 ml sodium borate, spun and washed again with 10 ml sodium borate. 5 µl of beads were removed at stored for later testing. Beads were coupled by resuspending in 10 ml dimethylpimelimidate in sodium borate and rotated for 1 hour at room temperature. Again 5 µl of beads were removed and stored.

Reaction was stopped by washing them once in 10 ml ethanolamine and incubation at room temperature for 2 hours on rotator. After incubation with ethanolamine, beads were spun again, washed twice with 10 ml glycine (pH 3.0) and immediately 6 times with 10 ml TBS. To the last wash 0.02% Sodium Azide was added. Beads were stored in a 1:1 slurry at 4°C.

4.5.4. Isolation of Mammalian Proteins

Tissue culture plates were washed 3 times with cold PBS and 1x with IP Wash. Cells were scraped off plates with a rubber sponge and pelleted by centrifugation (10 minutes, 1200 rpm, 4°C). Whole cell lysates were prepared by adding an appropriate amount of IP lyse supplied with protease (2mM PMSF, Aprotinin, Complete) and phosphatase (50 mM Sodiumfluoride, 20mM Sodium pyrophosphate, 1mM Sodium-orthovanadate, 10mM β-Glycerophosphate) inhibitors, resuspending and incubation for 10 minutes on ice. Lysates were centrifuged for 10 minutes with 14 000 rpm at 4°C. Supernatant was transferred to new tubes, pellets either discarded or stored at -20°C (if needed for genotyping PCRs).

4.5.5. BioRad Bradford Assay / Protein Concentration Measurement

Bio-Rad protein assay dye reagent (Bradford) was diluted 1:5 in dH_2O to achieve a total volume of 2.5 ml (500 µl Bio-Rad + 2 ml dH_2O) in a plastic cuvette. In the standard procedure 2 µl of protein extract were added to the cuvette, inverted and incubated for 5 minutes. Afterwards the cuvette was inverted again and optical density (OD) at λ = 595 nm was measured using a photometer. If the protein concentration was higher than the linearity limit of the assay (> OD 0.9), a dilution series of the protein extract in the cuvette was prepared to ensure a reliable result. According to the resulting optical density protein concentrations were equilibrated using IP lyse. If the total protein concentration was necessary, calculation with a pre-measured BSA standard (by Ingrid Frohner) was performed.

4.5.6. Immunoprecipitation

For IP of B6 cells lysates with adjusted concentrations were supplied with 2µl (old B6 cells) or 4 µl (young B6 cells) PyST antiserum from 3rd bleed or preimmune serum (PreB) and incubated 1 hour/4°C, then transferred onto protein A sepharose beads (100 µl or 50 µl slurry) and incubated for another hour. In case of the PyMT IPs of 326#7 MEFs, antibody (PyST 8th bleed) and beads were crosslinked, therefore protein solution was directly incubated with 50 µl (slurry) PyST antibody crosslinked beads for 1h/4°C. For the test IP for the crosslinked antibodies, 2 µl of PyST 8th bleed antibody and 50 µl (1:1 bead/volume suspension) of coupled PyST 8th bleed antibodies/Protein A sepharose beads were used. Non-crosslinked IP was in total incubated for 2 hours, coupled antibodies for 1 hour, IP was therefore started later and lysates were kept at 4°C in the meantime.

10% of the input and the supernatant were kept and supplied with 3xGSD. Beads were washed 1x with IP lyse (+ Inhibitors) and 3x with TBS (in-between centrifuged 1 minute, 1000 rpm, 4°C), then taken up in 100 µl 1xGSD.

4.5.7. Sodium dodecyl sulfate polyacrylamide gel electrophoresis (SDS-PAGE)

The running gel was prepared according to the recipe in the correct percentage of acrylamide (Table 16). Acrylamide, Tris pH 8.8, dH_2O and SDS were mixed and subsequently degassed for five minutes.

Polymerisation was induced by the addition of APS and TEMED. Gels were quickly poured, depending on the need either in large (~ 15x25 cm) or small (~ 10x7 cm) gel casters and overlaid with 96% Ethanol. After polymerisation, gel was washed with dH_2O and stacking gel prepared according to recipe (Table 17). Marker was diluted 1:10 in 1x GSD, protein samples either with 3x GSD (lysates) or 1x GSD (IPs) (boiled for 5 minutes at 95°C) and loaded onto gels. Electrophoresis was run at either ~ 100 mA per gel (approximately 2 hours) or ~ 8 mA per gel overnight in 1x Running Buffer.

Table 16 Recipe for 1 large or 8 small separating gels in different Acrylamide percentages

Reagent	**7.5 %**	**10 %**	**12.5 %**	**15 %**
30 % Acrylamide	10.1 ml	13.4 ml	16.7 ml	20.0 ml
1M Tris pH 8.8	15.0 ml	15.0 ml	15.0 ml	15.0 ml
20 % SDS	200 µl	200 µl	200 µl	200 µl
dH_2O	15.0 ml	11.7 ml	8.3 ml	5.0 ml
10 % APS	134 µl	134 µl	134 µl	134 µl
TEMED	26 µl	26 µl	26 µl	26 µl

Table 17 Recipe for 1 large or 8 small stacking gels

Reagent	**Amount**
30 % Acrylamide	1.7 ml
1M Tris pH 6.8	1.25 ml
20 % SDS	50 µl
dH_2O	7.1 ml
10 % APS	50 µl
TEMED	10 µl

4.5.8. Western Blot

For Western blotting a sandwich was assembled in the following order: “sponge, two slices of whatmann paper, nitrocellulose membrane, separating gel, two slices of whatmann paper, sponge”, all soaked in transfer buffer with Methanol (20% v/v). Proteins were transferred by wet blotting onto nitrocellulose membranes at 4°C either 3.5 hours (0.5 A) or overnight (0.1 A). Transfer buffer with Methanol (20% v/v) was used for blotting. Membranes were stained with PonceauS, destained with dH_2O and blocked with either 3% NFDM in PBS-Tween or 3% BSA in TBS-Tween (Phosphoantibodies) for 1 hour at room temperature. Primary antibodies were diluted in 0.5% NFDM in PBS-Tween (including 1% Thimerosal, 1:1000 diluted) or 2% BSA in TBS-Tween, incubated overnight/4°C (Table 18). 0.02% Sodiumazide was added to reduce microbial growth. Western blots were washed three

times with PBS-T or TBS-T, incubated with the appropriate secondary antibody (HRP-conjugated, IPs only with light chain antibodies, Table 19) 1 hour at room temperature, again washed three times with PBS-T/TBS-T and developed using ECL Visualization Solution, if necessary with up to 20% ECL Select. Fuji photographic films were exposed to detect protein signals. Photographic films were scanned. Quantification was performed using ImageJ (chapter 4.6.2).

Table 18 List of Primary Antibodies used in this Masterthesis in Western Blot Analysis. Where disclosed, antigens are indicated.

Antibody	**host animal**	**clonality**	**antigen**	**source/ producer**	**dilution**	**in**
PyST/PyMT						
PyST 3rd bleed (serum)	rabbit	poly	HisPyST full length 195 aa + 7aa n-terminal His tag	Ogris lab	1:10 000	0.5 % NFDM/PBS-T
PyST 8th bleed (serum)[1]	rabbit	poly	HisPyST full length 195 aa + 7aa n-terminal His tag	Ogris lab	1:10 000	0.5 % NFDM/PBS-T
PyMT 6th bleed (serum)	rabbit	poly	deltaN200 deltaC105 total length 127aa+19aa	Ogris lab	1:10 000	0.5 % NFDM/PBS-T
PTPA						
5G3	mouse	mono	Full length mouse PTPA	Ogris lab	1:100	0.5 % NFDM/PBS-T
1D2-6A7[2]	mouse	mono		Ogris lab	1:50	0.5 % NFDM/PBS-T
R171 4th bleed (serum)	rabbit	poly		Ogris lab	1:10 000	0.5 % NFDM/PBS-T
PPP2R4 (C-10)[3]	mouse	mono	PPP2R4	SantaCruz (sc-398242)	1:500	0.5 % NFDM/PBS-T
src (α327)	mouse	mono	full length native protein	Joan Brugge, Harvard Medical School, Boston, MA	1:100	0.5 % NFDM/PBS-T

Cas9 (7A9)	mouse	mono	recombinant protein specific to the amino terminus of Cas9 from Streptococcus pyogenes	Ogris lab	1:100	0.5 % NFDM/PBS-T
Cre Recombinase (D7L7L)	rabbit	mono	synthetic peptide corresponding to residues near the amino terminus of bacteriophage-P1 Cre recombinase protein	cell signaling (#15036)	1:2000	0.5 % NFDM/PBS-T
PP2A antibodies						
PP2A A subunit (4C10)	mouse	mono	aa 1-168 of recombinant human PP2A (subunit A)	Ogris lab	1:100	0.5 % NFDM/PBS-T
PP2A A subunit (p63) [1]	rabbit	poly	MAAADGDSLY	Ogris lab	1:10 000	0.5 % NFDM/PBS-T
PP2A C subunit (4B1-3B2-H8)	mouse	mono	1-144aa of human PP2A catalytic subunit, α isoform	Ogris lab	1:100	0.5 % NFDM/PBS-T
PP2A C subunit (11H12)[4]	mouse	mono	DTLKYSFLQFDPAPR	Ogris lab	1:100	0.5 % NFDM/PBS-T
PP2A C subunit (Sat20 3rd bleed)	rabbit	poly	288-303aa of human PP2A catalytic subunit α isoform	Europentec (#20)	1:10 000	0.5 % NFDM/PBS-T
PP4 C subunit (7B5-G47B5-G4)	mouse	mono	EHLQKDFIIFEAAPQET	Ogris lab	1:100	0.5 % NFDM/PBS-T
Phosphotyrosine Antibodies						
pTyr 100	mouse	mono	phospho-tyrosine containing peptides	cell signalling (#9411)	1:5000	2 % BSA/TBS-T
src pY416	rabbit	mono	synthetic phosphopeptide corresponding to residues surrounding	cell signaling (#2101)	1:2000	2 % BSA/TBS-T

			Tyr419 of human Src.			
src pY527	rabbit	mono	synthetic phosphopeptide corresponding to residues surrounding Tyr530 of human Src	cell signaling (#2105)	1:2000	2 % BSA/TBS-T
tags						
HA (16B12)	mouse	mono	CYPYDVPDYASL	Covance (#MMS-101R)	1:10 000	0.5 % NFDM/PBS-T
myc (4A6)	mouse	mono	MEQKLISEEDL	Millipore (05-724)	1:2000	0.5 % NFDM/PBS-T
loading controls						
GAPDH	mouse	mono	Rabbit muscle GAPDH	Abcam (ab8245)	1:10 000	0.5 % NFDM/PBS-T
β Actin (2A3-6A5-G2)	mouse	mono		Ogris lab	1:500	0.5 % NFDM/PBS-T
α/β - Tubulin	mouse	mono		Ogris lab	1:20 000	0.5 % NFDM/PBS-T

[1] purified antibody; [2] C terminal; [3] not specific; [4] C terminal (possibly phosphorylation sensitive)

Table 19: List of Secondary Antibodies used in the thesis. Blots incubated with anti-mouse secondary antibody were supplemented with the normal anti blue marker, those with anti-rabbit secondary antibodies with the HRP-coupled anti blue marker.

Secondary Antibody	**Host Animal**	**Company**	**Dilution**	**Remarks**
anti-mouse HRP coupled	goat	Jackson (#115-035- 008)	1:10 000	IgG, Fcγ fragment specific
anti-rabbit HRP coupled	goat	Jackson (#111-035- 008)	1:10 000	IgG, Fcγ fragment specific
anti-mouse HRP coupled	goat	Jackson (115-035-174)	1:5000	Light chain
anti-rabbit HRP coupled	goat	Jackson (#211-032-171)	1:5000	Light chain
α-anti BLUE marker 2D2-F11X63	mouse	Ogris lab	1:10 000	monoclonal
α-anti BLUE marker 2D2-F11X63	mouse	Ogris lab	1: 10 000	monoclonal, HRP coupled

4.5.9. Coomassie Staining of Gels

For Coomassie staining SDS-PA gels were disassembled and directly incubated in the Instant Blue staining solution for 2 hours on the shaker at room temperature. Coomassie Staining solution was reused and stored at 4°C; gel was destained in dH_2O overnight.

4.5.10. Immunofluorescence

For immunofluorescence either an appropriate number of cells were seeded onto a coverslip (NA #1 or NA#1.5 (confocal)). Cells were grown to confluency, fixed with 3.7 % Paraformaldehyde in PBS for 10 minutes/RT, afterwards permeabilized 0.2% Triton-X/PBS for 10 min/RT. After blocking with 2 % BSA/PBS for 1h/RT, slides were incubated with antibodies in 1%BSA/PBS overnight at 4°C, then 1h at RT with appropriate secondary antibody (Table 20). For nucleus staining Hoechst 33342 (Stock 750µg/ml), diluted 1:1000 (0.75 µg/ml) in PBS was used (10 minutes, RT, dark). Slides were washed 1x with dH_20 and mounted with VectaShield. Several PBS washings were between every step. For detection Zeiss Axiovert 200M "ApoTome" (63x magnification) and Zeiss LSM 700 (confocal, 63x magnification) were used.

Table 20 List of Antibody and secondary Antibody used in Immunofluorescence Stainings

Antibody	**source animal**	**clonality**	**company**	**dilution**	**in**
PyST 8th bleed (purified)	rabbit	polyclonal	Ogris lab	1:100	1 % BSA/PBS
Secondary Antibodies					
Alexa Fluor 488 (anti-rabbit)	goat	polyclonal	Life Technologies A11034	1:1000	1 % BSA/PBS

4.6. Quantification Methods

4.6.1. Calculation Doubling Times and Extrapolations

Doubling times of cells were calculated according to the equation:

$$DT = \frac{0.301}{K}$$

The proliferation constant K is calculated as indicated below:

$$K = \frac{\log(N2) - log(N1)}{t2 - t1}$$

N is the cell concentration and t the time.

Calculation of the extrapolations whether the number of dead cells could compensate for the differences in cell count were based on upper equation.

$$extrapolation = \frac{0.301}{DT} * 10^{K*(t2-t1)+log^{rN}}$$

The relative cell concentration rN is calculated as indicated below:

$$rN = \frac{N1}{N2(alive)} * 100$$

4.6.2. Western Blot and Immunoprecipitation

Fiji ImageJ Windows 64-bit version was used for quantification of signal intensity of western blots. In western blots of lysates signals were normalized to a loading control (table 11).

For quantification of immunoprecipitations a dilution series of either the τ2 puro (1:2 to 1:16 or the *Ptpa*$^{\Delta}$ myc-PTPA (1 to 1: 4) cells was included (

Supplementary Figure *3*). A logarithmic curve was calculated using the appropriate Excel function and the parameters (A, B) red-out. Those parameters were used to calculate amounts of other signals using the equation:

$$\mathrm{x} = \mathrm{e}^{\frac{\mathrm{y}-\mathrm{B}}{\mathrm{A}}}$$

With y being the absolute value obtained from the measurement of ImageJ and A and B the parameters of the respective logarithmic curve. X was then normalized to the values of the respective PyMT signal from the PyMT *Ptpa*^{fl} puro cells.

5. References

Ahmed, Samrein B. M.; Prigent, Sally A. (2017): Insights into the Shc Family of Adaptor Proteins. In: *Journal of molecular signaling* 12, S. 2. DOI: 10.5334/1750-2187-12-2.

Allison, A. C.; Black, P. H. (1967): Lysosomal changes in lytic and nonlytic infections with the simian vacuolating virus (SV40). In: *Journal of the National Cancer Institute* 39 (4), 775-780, 782-7.

Alvarez, Angel; Barisone, Gustavo A.; Diaz, Elva (2014): Focus formation: a cell-based assay to determine the oncogenic potential of a gene. In: *Journal of visualized experiments : JoVE* (94). DOI: 10.3791/51742.

Barouch, D. H.; Harrison, S. C. (1994): Interactions among the major and minor coat proteins of polyomavirus. In: *Journal of virology* 68 (6), S. 3982–3989.

Barrangou, Rodolphe; Fremaux, Christophe; Deveau, Hélène; Richards, Melissa; Boyaval, Patrick; Moineau, Sylvain et al. (2007): CRISPR provides acquired resistance against viruses in prokaryotes. In: *Science (New York, N.Y.)* 315 (5819), S. 1709–1712. DOI: 10.1126/science.1138140.

Berger, H.; Wintersberger, E. (1986): Polyomavirus small T antigen enhances replication of viral genomes in 3T6 mouse fibroblasts. In: *Journal of virology* 60 (2), S. 768–770.

Boggon, Titus J.; Eck, Michael J. (2004): Structure and regulation of Src family kinases. In: *Oncogene* 23 (48), S. 7918–7927. DOI: 10.1038/sj.onc.1208081.

Bolotin, Alexander; Quinquis, Benoit; Sorokin, Alexei; Ehrlich, S. Dusko (2005): Clustered regularly interspaced short palindrome repeats (CRISPRs) have spacers of extrachromosomal origin. In: *Microbiology (Reading, England)* 151 (Pt 8), S. 2551–2561. DOI: 10.1099/mic.0.28048-0.

Brouns, Stan J. J.; Jore, Matthijs M.; Lundgren, Magnus; Westra, Edze R.; Slijkhuis, Rik J. H.; Snijders, Ambrosius P. L. et al. (2008): Small CRISPR RNAs guide antiviral defense in prokaryotes. In: *Science (New York, N.Y.)* 321 (5891), S. 960–964. DOI: 10.1126/science.1159689.

Brown, M. T.; Cooper, J. A. (1996): Regulation, substrates and functions of src. In: *Biochimica et biophysica acta* 1287 (2-3), S. 121–149. DOI: 10.1016/0304-419x(96)00003-0.

Buchowiecka, A. K. (2014): Puzzling over protein cysteine phosphorylation—assessment of proteomic tools for S-phosphorylation profiling. In: *The Analyst* 139 (17), S. 4118–4123. DOI: 10.1039/c4an00724g.

Burchell, A.; Cohen, P. (1978): Is phosphorylase phosphatase a manganese metalloenzyme? proceedings. In: *Biochemical Society transactions* 6 (1), S. 220–222.

Burnett, G.; Kennedy, E. P. (1954): The enzymatic phosphorylation of proteins. In: *The Journal of biological chemistry* 211 (2), S. 969–980.

Campbell, K. S.; Auger, K. R.; Hemmings, B. A.; Roberts, T. M.; Pallas, D. C. (1995): Identification of regions in polyomavirus middle T and small t antigens important for association with protein phosphatase 2A. In: *Journal of virology* 69 (6), S. 3721–3728.

Campbell, K. S.; Ogris, E.; Burke, B.; Su, W.; Auger, K. R.; Druker, B. J. et al. (1994): Polyoma middle tumor antigen interacts with SHC protein via the NPTY (Asn-Pro-Thr-Tyr) motif in middle tumor antigen. In: *Proceedings of the National Academy of Sciences of the United States of America* 91 (14), S. 6344–6348.

Carmichael, G. G.; Schaffhausen, B. S.; Dorsky, D. I.; Oliver, D. B.; Benjamin, T. L. (1982): Carboxy terminus of polyoma middle-sized tumor antigen is required for attachment to membranes, associated protein kinase activities, and cell transformation. In: *Proceedings of the National Academy of Sciences of the United States of America* 79 (11), S. 3579–3583.

Cayla, X.; Goris, J.; Hermann, J.; Hendrix, P.; Ozon, R.; Merlevede, W. (1990): Isolation and characterization of a tyrosyl phosphatase activator from rabbit skeletal muscle and Xenopus laevis oocytes. In: *Biochemistry* 29 (3), S. 658–667.

Cayla, X.; van Hoof, C.; Bosch, M.; Waelkens, E.; Vandekerckhove, J.; Peeters, B. et al. (1994): Molecular cloning, expression, and characterization of PTPA, a protein that activates the tyrosyl phosphatase activity of protein phosphatase 2A. In: *The Journal of biological chemistry* 269 (22), S. 15668–15675.

Chang, Yuan; Moore, Patrick S. (2012): Merkel cell carcinoma: a virus-induced human cancer. In: *Annual review of pathology* 7, S. 123–144. DOI: 10.1146/annurev-pathol-011110-130227.

Chen, J.; Martin, B.; Brautigan, D. (1992a): Regulation of protein serine-threonine phosphatase type-2A by tyrosine phosphorylation. In: *Science* 257 (5074), S. 1261–1264. DOI: 10.1126/science.1325671.

Chen, J.; Tobin, G. J.; Pipas, J. M.; van Dyke, T. (1992b): T-antigen mutant activities in vivo: roles of p53 and pRB binding in tumorigenesis of the choroid plexus. In: *Oncogene* 7 (6), S. 1167–1175.

Chen, Xiangyang; Xu, Fei; Zhu, Chengming; Ji, Jiaojiao; Zhou, Xufei; Feng, Xuezhu; Guang, Shouhong (2014): Dual sgRNA-directed gene knockout using CRISPR/Cas9 technology in Caenorhabditis elegans. In: *Scientific reports* 4, S. 7581. DOI: 10.1038/srep07581.

Choi, Peter S.; Meyerson, Matthew (2014): Targeted genomic rearrangements using CRISPR/Cas technology. In: *Nature communications* 5, S. 3728. DOI: 10.1038/ncomms4728.

Cieśla, Joanna; Frączyk, Tomasz; Rode, Wojciech (2011): Phosphorylation of basic amino acid residues in proteins: important but easily missed. In: *Acta biochimica Polonica* 58 (2), S. 137–148.

Courtneidge, S. A.; Smith, A. E. (1983): Polyoma virus transforming protein associates with the product of the c-src cellular gene. In: *Nature* 303 (5916), S. 435–439.

Culleré, X.; Rose, P.; Thathamangalam, U.; Chatterjee, A.; Mullane, K. P.; Pallas, D. C. et al. (1998): Serine 257 phosphorylation regulates association of polyomavirus middle T antigen with 14-3-3 proteins. In: *Journal of virology* 72 (1), S. 558–563.

DeCaprio, James A.; Garcea, Robert L. (2013): A cornucopia of human polyomaviruses. In: *Nature reviews. Microbiology* 11 (4), S. 264–276. DOI: 10.1038/nrmicro2992.

Delbue, Serena; Ferrante, Pasquale; Provenzano, Maurizio (2014): Polyomavirus BK and prostate cancer: an unworthy scientific effort? In: *Oncoscience* 1 (4), S. 296–303.

Deltcheva, Elitza; Chylinski, Krzysztof; Sharma, Cynthia M.; Gonzales, Karine; Chao, Yanjie; Pirzada, Zaid A. et al. (2011): CRISPR RNA maturation by trans-encoded small RNA and host factor RNase III. In: *Nature* 471 (7340), S. 602–607. DOI: 10.1038/nature09886.

Denis, Deborah; Rouleau, Cecile; Schaffhausen, Brian S. (2017): A Transformation-Defective Polyomavirus Middle T Antigen with a Novel Defect in PI3 Kinase Signaling. In: *Journal of virology* 91 (2). DOI: 10.1128/JVI.01774-16.

DeSeau, V.; Rosen, N.; Bolen, J. B. (1987): Analysis of pp60c-src tyrosine kinase activity and phosphotyrosyl phosphatase activity in human colon carcinoma and normal human colon mucosal cells. In: *Journal of cellular biochemistry* 35 (2), S. 113–128. DOI: 10.1002/jcb.240350205.

Doherty, J.; Freund, R. (1997): Polyomavirus large T antigen overcomes p53 dependent growth arrest. In: *Oncogene* 14 (16), S. 1923–1931. DOI: 10.1038/sj.onc.1201025.

Dunant, N.; Ballmer-Hofer, K. (1997): Signalling by Src family kinases: lessons learnt from DNA tumour viruses. In: *Cellular signalling* 9 (6), S. 385–393.

Eichhorn, Pieter J. A.; Creyghton, Menno P.; Bernards, René (2009): Protein phosphatase 2A regulatory subunits and cancer. In: *Biochimica et biophysica acta* 1795 (1), S. 1–15. DOI: 10.1016/j.bbcan.2008.05.005.

Erickson, Kimberly D.; Bouchet-Marquis, Cedric; Heiser, Katie; Szomolanyi-Tsuda, Eva; Mishra, Rabinarayan; Lamothe, Benjamin et al. (2012): Virion assembly factories in the nucleus of polyomavirus-infected cells. In: *PLoS pathogens* 8 (4), e1002630. DOI: 10.1371/journal.ppat.1002630.

Evans, Gareth L.; Caller, Laura G.; Foster, Victoria; Crump, Colin M. (2015): Anion homeostasis is important for non-lytic release of BK polyomavirus from infected cells. In: *Open biology* 5 (8). DOI: 10.1098/rsob.150041.

Felici, A.; Giorgio, M.; Krauzewicz, N.; Della Rocca, C.; Santoro, M.; Rovere, P. et al. (1999): Medullary thyroid carcinomas in transgenic mice expressing a Polyoma carboxyl-terminal truncated middle-T and wild type small-T antigens. In: *Oncogene* 18 (14), S. 2387–2395. DOI: 10.1038/sj.onc.1202578.

Fellner, Thomas; Lackner, Daniel H.; Hombauer, Hans; Piribauer, Patrick; Mudrak, Ingrid; Zaragoza, Katrin et al. (2003): A novel and essential mechanism determining specificity and activity of protein phosphatase 2A (PP2A) in vivo. In: *Genes & development* 17 (17), S. 2138–2150. DOI: 10.1101/gad.259903.

Fluck, Michele M.; Schaffhausen, Brian S. (2009): Lessons in signaling and tumorigenesis from polyomavirus middle T antigen. In: *Microbiology and molecular biology reviews : MMBR* 73 (3), S. 542. DOI: 10.1128/MMBR.00009-09.

Frohner et al. (unpublished data).

Fujiwara, Nobuyuki; Usui, Tatsuya; Ohama, Takashi; Sato, Koichi (2016): Regulation of Beclin 1 Protein Phosphorylation and Autophagy by Protein Phosphatase 2A (PP2A) and Death-associated Protein Kinase 3 (DAPK3). In: *The Journal of biological chemistry* 291 (20), S. 10858–10866. DOI: 10.1074/jbc.M115.704908.

Garnett, Mathew J.; Marais, Richard (2004): Guilty as charged. B-RAF is a human oncogene. In: *Cancer cell* 6 (4), S. 313–319. DOI: 10.1016/j.ccr.2004.09.022.

Good, P. J.; Welch, R. C.; Barkan, A.; Somasekhar, M. B.; Mertz, J. E. (1988): Both VP2 and VP3 are synthesized from each of the alternative spliced late 19S RNA species of simian virus 40. In: *Journal of virology* 62 (3), S. 944–953.

Götz, J.; Probst, A.; Ehler, E.; Hemmings, B.; Kues, W. (1998): Delayed embryonic lethality in mice lacking protein phosphatase 2A catalytic subunit Calpha. In: *Proceedings of the National Academy of Sciences of the United States of America* 95 (21), S. 12370–12375.

Gross, Ludwik (1953): A filterable agent, recovered from Ak leukemic extracts, causing salivary gland carcinomas in C3H mice. In: *Proceedings of the Society for Experimental Biology and Medicine.*

Society for Experimental Biology and Medicine (New York, N.Y.) 83 (2), S. 414–421. DOI: 10.3181/00379727-83-20376.

Gu, Pengyu; Qi, Xin; Zhou, Yue; Wang, Yun; Gao, Xiang (2012): Generation of Ppp2Ca and Ppp2Cb conditional null alleles in mouse. In: *Genesis (New York, N.Y. : 2000)* 50 (5), S. 429–436. DOI: 10.1002/dvg.20815.

Guan, K. L.; Dixon, J. E. (1991): Evidence for protein-tyrosine-phosphatase catalysis proceeding via a cysteine-phosphate intermediate. In: *The Journal of biological chemistry* 266 (26), S. 17026–17030.

Guo, Feng; Stanevich, Vitali; Wlodarchak, Nathan; Sengupta, Rituparna; Jiang, Li; Satyshur, Kenneth A.; Xing, Yongna (2014): Structural basis of PP2A activation by PTPA, an ATP-dependent activation chaperone. In: *Cell Research* 24 (2), S. 190–203. DOI: 10.1038/cr.2013.138.

Guo, H.; Damuni, Z. (1993): Autophosphorylation-activated protein kinase phosphorylates and inactivates protein phosphatase 2A. In: *Proceedings of the National Academy of Sciences of the United States of America* 90 (6), S. 2500–2504. DOI: 10.1073/pnas.90.6.2500.

Guzmán, Camilo; Bagga, Manish; Kaur, Amanpreet; Westermarck, Jukka; Abankwa, Daniel (2014): ColonyArea: an ImageJ plugin to automatically quantify colony formation in clonogenic assays. In: *PloS one* 9 (3), e92444. DOI: 10.1371/journal.pone.0092444.

Harlow, Edward; Lane, David (1999): Using antibodies. A laboratory manual. Cold Spring Harbor, NY: Cold Spring Harbor Laboratory Press.

Hemmings, B. A.; Adams-Pearson, C.; Maurer, F.; Müller, P.; Goris, J.; Merlevede, W. et al. (1990): alpha- and beta-forms of the 65-kDa subunit of protein phosphatase 2A have a similar 39 amino acid repeating structure. In: *Biochemistry* 29 (13), S. 3166–3173.

Hombauer, Hans; Weismann, David; Mudrak, Ingrid; Stanzel, Claudia; Fellner, Thomas; Lackner, Daniel H.; Ogris, Egon (2007): Generation of active protein phosphatase 2A is coupled to holoenzyme assembly. In: *PLoS Biology* 5 (6), e155. DOI: 10.1371/journal.pbio.0050155.

Horak, I. D.; Kawakami, T.; Gregory, F.; Robbins, K. C.; Bolen, J. B. (1989): Association of p60fyn with middle tumor antigen in murine polyomavirus-transformed rat cells. In: *Journal of virology* 63 (5), S. 2343–2347.

Hunter, Tony (2014): The genesis of tyrosine phosphorylation. In: *Cold Spring Harbor perspectives in biology* 6 (5), a020644. DOI: 10.1101/cshperspect.a020644.

Hwang, Justin H.; Pores Fernando, Arun T.; Faure, Nathalie; Andrabi, Shaida; Adelmant, Guillaume; Hahn, William C. et al. (2014): Polyomavirus small T antigen interacts with yes-associated protein to regulate cell survival and differentiation. In: *Journal of virology* 88 (20), S. 12055–12064. DOI: 10.1128/JVI.01399-14.

Ichaso, Natalia; Dilworth, Stephen (2001): Cell transformation by the middle T-antigen of polyoma virus. In: *Oncogene* (20).

Indra, A. K.; Warot, X.; Brocard, J.; Bornert, J. M.; Xiao, J. H.; Chambon, P.; Metzger, D. (1999): Temporally-controlled site-specific mutagenesis in the basal layer of the epidermis. Comparison of the recombinase activity of the tamoxifen-inducible Cre-ER(T) and Cre-ER(T2) recombinases. In: *Nucleic acids research* 27 (22), S. 4324–4327.

Ishino, Y.; Shinagawa, H.; Makino, K.; Amemura, M.; Nakata, A. (1987): Nucleotide sequence of the iap gene, responsible for alkaline phosphatase isozyme conversion in Escherichia coli, and identification of the gene product. In: *Journal of Bacteriology* 169 (12), S. 5429–5433.

Jackson, Jennifer B.; Pallas, David C. (2012): Circumventing cellular control of PP2A by methylation promotes transformation in an Akt-dependent manner. In: *Neoplasia (New York, N.Y.)* 14 (7), S. 585–599.

Janbandhu, Vaibhao C.; Moik, Daniel; Fässler, Reinhard (2014): Cre recombinase induces DNA damage and tetraploidy in the absence of loxP sites. In: *Cell cycle (Georgetown, Tex.)* 13 (3), S. 462–470. DOI: 10.4161/cc.27271.

Jang, Hyun-Jun; Suh, Pann-Ghill; Lee, Yu Jin; Shin, Kyeong Jin; Cocco, Lucio; Chae, Young Chan (2018): PLCγ1: Potential arbitrator of cancer progression. In: *Advances in biological regulation* 67, S. 179–189. DOI: 10.1016/j.jbior.2017.11.003.

Janssens, Veerle; Longin, Sari; Goris, Jozef (2008): PP2A holoenzyme assembly: in cauda venenum (the sting is in the tail). In: *Trends in biochemical sciences* 33 (3), S. 113–121. DOI: 10.1016/j.tibs.2007.12.004.

Jinek, Martin; Chylinski, Krzysztof; Fonfara, Ines; Hauer, Michael; Doudna, Jennifer A.; Charpentier, Emmanuelle (2012): A programmable dual-RNA-guided DNA endonuclease in adaptive bacterial immunity. In: *Science (New York, N.Y.)* 337 (6096), S. 816–821. DOI: 10.1126/science.1225829.

Jordens, Jan; Janssens, Veerle; Longin, Sari; Stevens, Ilse; Martens, Ellen; Bultynck, Geert et al. (2006): The protein phosphatase 2A phosphatase activator is a novel peptidyl-prolyl cis/trans-isomerase. In: *The Journal of biological chemistry* 281 (10), S. 6349–6357. DOI: 10.1074/jbc.M507760200.

Juan, Wen Chun; Ong, S. Tiong (2012): The role of protein phosphorylation in therapy resistance and disease progression in chronic myelogenous leukemia. In: *Progress in molecular biology and translational science* 106, S. 107–142. DOI: 10.1016/B978-0-12-396456-4.00007-9.

Kaplan, D. R.; Whitman, M.; Schaffhausen, B.; Pallas, D. C.; White, M.; Cantley, L.; Roberts, T. M. (1987): Common elements in growth factor stimulation and oncogenic transformation. 85 kd phosphoprotein and phosphatidylinositol kinase activity. In: *Cell* 50 (7), S. 1021–1029.

Katakura, Y.; Alam, S.; Shirahata, S. (1998): Immortalization by gene transfection. In: *Methods in cell biology* 57, S. 69–91.

Kiely, Maeve; Kiely, Patrick A. (2015): PP2A: The Wolf in Sheep's Clothing? In: *Cancers* 7 (2), S. 648–669. DOI: 10.3390/cancers7020648.

Koduri, Vidyasagar; McBrayer, Samuel K.; Liberzon, Ella; Wang, Adam C.; Briggs, Kimberly J.; Cho, Hyejin; Kaelin, William G. (2019): Peptidic degron for IMiD-induced degradation of heterologous proteins. In: *Proceedings of the National Academy of Sciences of the United States of America* 116 (7), S. 2539–2544. DOI: 10.1073/pnas.1818109116.

Kornbluth, S.; Sudol, M.; Hanafusa, H. (1987): Association of the polyomavirus middle-T antigen with c-yes protein. In: *Nature* 325 (7000), S. 171–173. DOI: 10.1038/325171a0.

Kremmer, E.; Ohst, K.; Kiefer, J.; Brewis, N.; Walter, G. (1997): Separation of PP2A core enzyme and holoenzyme with monoclonal antibodies against the regulatory A subunit: abundant expression of both forms in cells. In: *Molecular and Cellular Biology* 17 (3), S. 1692–1701.

Lange, Anika; Gegg, Moritz; Burtscher, Ingo; Bengel, Doris; Kremmer, Elisabeth; Lickert, Heiko (2012): Fltp(T2AiCre): a new knock-in mouse line for conditional gene targeting in distinct mono- and multiciliated tissues. In: *Differentiation; research in biological diversity* 83 (2), S105-13. DOI: 10.1016/j.diff.2011.11.003.

Lapek, John D.; Tombline, Gregory; Kellersberger, Katherine A.; Friedman, Michelle R.; Friedman, Alan E. (2015): Evidence of histidine and aspartic acid phosphorylation in human prostate cancer cells. In: *Naunyn-Schmiedeberg's archives of pharmacology* 388 (2), S. 161–173. DOI: 10.1007/s00210-014-1063-4.

Le Cong; Ran, F. Ann; Cox, David; Lin, Shuailiang; Barretto, Robert; Habib, Naomi et al. (2013): Multiplex genome engineering using CRISPR/Cas systems. In: *Science (New York, N.Y.)* 339 (6121), S. 819–823. DOI: 10.1126/science.1231143.

Lieu, Christopher; Kopetz, Scott (2010): The SRC family of protein tyrosine kinases: a new and promising target for colorectal cancer therapy. In: *Clinical colorectal cancer* 9 (2), S. 89–94. DOI: 10.3816/CCC.2010.n.012.

Lin, Jiecong; Wong, Ka-Chun (2018): Off-target predictions in CRISPR-Cas9 gene editing using deep learning. In: *Bioinformatics (Oxford, England)* 34 (17), i656-i663. DOI: 10.1093/bioinformatics/bty554.

Lipmann, F. A.; Levene, P. A. (1932): Serinephosphoric acid obtained on hydrolysis of vitellinic acid. In: *Journal of biological chemistry* (98), S. 109–114.

Listgarten, Jennifer; Weinstein, Michael; Kleinstiver, Benjamin P.; Sousa, Alexander A.; Joung, J. Keith; Crawford, Jake et al. (2018): Prediction of off-target activities for the end-to-end design of CRISPR guide RNAs. In: *Nature biomedical engineering* 2 (1), S. 38–47. DOI: 10.1038/s41551-017-0178-6.

Liu, Wei; Krump, Nathan A.; Buck, Christopher B.; You, Jianxin (2019): Merkel Cell Polyomavirus Infection and Detection. In: *Journal of visualized experiments : JoVE* (144). DOI: 10.3791/58950.

Longin, Sari; Zwaenepoel, Karen; Louis, Justin V.; Dilworth, Stephen; Goris, Jozef; Janssens, Veerle (2007): Selection of protein phosphatase 2A regulatory subunits is mediated by the C terminus of the catalytic Subunit. In: *The Journal of biological chemistry* 282 (37), S. 26971–26980. DOI: 10.1074/jbc.M704059200.

Loonstra, A.; Vooijs, M.; Beverloo, H. B.; Allak, B. A.; van Drunen, E.; Kanaar, R. et al. (2001): Growth inhibition and DNA damage induced by Cre recombinase in mammalian cells. In: *Proceedings of the National Academy of Sciences of the United States of America* 98 (16), S. 9209–9214. DOI: 10.1073/pnas.161269798.

Ludlow, J. W.; DeCaprio, J. A.; Huang, C. M.; Lee, W. H.; Paucha, E.; Livingston, D. M. (1989): SV40 large T antigen binds preferentially to an underphosphorylated member of the retinoblastoma susceptibility gene product family. In: *Cell* 56 (1), S. 57–65.

Maglione, J. E.; Moghanaki, D.; Young, L. J.; Manner, C. K.; Ellies, L. G.; Joseph, S. O. et al. (2001): Transgenic Polyoma middle-T mice model premalignant mammary disease. In: *Cancer Research* 61 (22), S. 8298–8305.

Magnusdottir, Audur; Stenmark, Pål; Flodin, Susanne; Nyman, Tomas; Hammarström, Martin; Ehn, Maria et al. (2006): The crystal structure of a human PP2A phosphatase activator reveals a novel fold and highly conserved cleft implicated in protein-protein interactions. In: *The Journal of biological chemistry* 281 (32), S. 22434–22438. DOI: 10.1074/jbc.C600100200.

Makarova, Kira S.; Grishin, Nick V.; Shabalina, Svetlana A.; Wolf, Yuri I.; Koonin, Eugene V. (2006): A putative RNA-interference-based immune system in prokaryotes: computational analysis of the predicted enzymatic machinery, functional analogies with eukaryotic RNAi, and hypothetical mechanisms of action. In: *Biology direct* 1, S. 7. DOI: 10.1186/1745-6150-1-7.

Makarova, Kira S.; Koonin, Eugene V. (2015): Annotation and Classification of CRISPR-Cas Systems. In: *Methods in molecular biology (Clifton, N.J.)* 1311, S. 47–75. DOI: 10.1007/978-1-4939-2687-9_4.

Makarova, Kira S.; Wolf, Yuri I.; Alkhnbashi, Omer S.; Costa, Fabrizio; Shah, Shiraz A.; Saunders, Sita J. et al. (2015): An updated evolutionary classification of CRISPR-Cas systems. In: *Nature reviews. Microbiology* 13 (11), S. 722–736. DOI: 10.1038/nrmicro3569.

Maqsood, Muhammad Irfan; Matin, Maryam M.; Bahrami, Ahmad Reza; Ghasroldasht, Mohammad M. (2013): Immortality of cell lines: challenges and advantages of establishment. In: *Cell biology international* 37 (10), S. 1038–1045. DOI: 10.1002/cbin.10137.

Matthews, Harry R. (1995): Protein kinases and phosphatases that act on histidine, lysine, or arginine residues in eukaryotic proteins: A possible regulator of the mitogen-activated protein kinase cascade. In: *Pharmacology & Therapeutics* 67 (3), S. 323–350. DOI: 10.1016/0163-7258(95)00020-8.

Meili, R.; Cron, P.; Hemmings, B. A.; Ballmer-Hofer, K. (1998): Protein kinase B/Akt is activated by polyomavirus middle-T antigen via a phosphatidylinositol 3-kinase-dependent mechanism. In: *Oncogene* 16 (7), S. 903–907. DOI: 10.1038/sj.onc.1201605.

Moens, U.; Seternes, O. M.; Johansen, B.; Rekvig, O. P. (1997): Mechanisms of transcriptional regulation of cellular genes by SV40 large T- and small T-antigens. In: *Virus genes* 15 (2), S. 135–154.

Moens, Ugo; Krumbholz, Andi; Ehlers, Bernhard; Zell, Roland; Johne, Reimar; Calvignac-Spencer, Sébastien; Lauber, Chris (2017): Biology, evolution, and medical importance of polyomaviruses. An update. In: *Infection, genetics and evolution : journal of molecular epidemiology and evolutionary genetics in infectious diseases* 54, S. 18–38. DOI: 10.1016/j.meegid.2017.06.011.

Moorhead, Greg B. G.; Trinkle-Mulcahy, Laura; Ulke-Lemée, Annegret (2007): Emerging roles of nuclear protein phosphatases. In: *Nature reviews. Molecular cell biology* 8 (3), S. 234–244. DOI: 10.1038/nrm2126.

Morgan, Gregory J. (2014): Ludwik Gross, Sarah Stewart, and the 1950s discoveries of Gross murine leukemia virus and polyoma virus. In: *Studies in history and philosophy of biological and biomedical sciences* 48 Pt B, S. 200–209. DOI: 10.1016/j.shpsc.2014.07.013.

Nagy, A. (2000): Cre recombinase. The universal reagent for genome tailoring. In: *Genesis (New York, N.Y. : 2000)* 26 (2), S. 99–109.

Ogris, E.; Gibson, D. M.; Pallas, D. C. (1997): Protein phosphatase 2A subunit assembly. The catalytic subunit carboxy terminus is important for binding cellular B subunit but not polyomavirus middle tumor antigen. In: *Oncogene* 15 (8), S. 911–917. DOI: 10.1038/sj.onc.1201259.

Ogris, E.; Mudrak, I.; Mak, E.; Gibson, D.; Pallas, D. C. (1999): Catalytically inactive protein phosphatase 2A can bind to polyomavirus middle tumor antigen and support complex formation with pp60(c-src). In: *Journal of virology* 73 (9), S. 7390–7398.

Ogris, E.; Mudrak, I.; Wintersberger, E. (1992): Polyomavirus large and small T antigens cooperate in induction of the S phase in serum-starved 3T3 mouse fibroblasts. In: *Journal of virology* 66 (1), S. 53–61.

Ogris, E.; Rotheneder, H.; Mudrak, I.; Pichler, A.; Wintersberger, E. (1993): A binding site for transcription factor E2F is a target for trans activation of murine thymidine kinase by polyomavirus large T antigen and plays an important role in growth regulation of the gene. In: *Journal of virology* 67 (4), S. 1765–1771.

Olsen, Jesper V.; Blagoev, Blagoy; Gnad, Florian; Macek, Boris; Kumar, Chanchal; Mortensen, Peter; Mann, Matthias (2006): Global, in vivo, and site-specific phosphorylation dynamics in signaling networks. In: *Cell* 127 (3), S. 635–648. DOI: 10.1016/j.cell.2006.09.026.

Orgad, S.; Brewis, N. D.; Alphey, L.; Axton, J. M.; Dudai, Y.; Cohen, P. T. (1990): The structure of protein phosphatase 2A is as highly conserved as that of protein phosphatase 1. In: *FEBS letters* 275 (1-2), S. 44–48.

Pallas, D. C.; Fu, H.; Haehnel, L. C.; Weller, W.; Collier, R. J.; Roberts, T. M. (1994): Association of polyomavirus middle tumor antigen with 14-3-3 proteins. In: *Science (New York, N.Y.)* 265 (5171), S. 535–537.

Pallas, D. C.; Morgan, W.; Roberts, T. M. (1989): The cellular proteins which can associate specifically with polyomavirus middle T antigen in human 293 cells include the major human 70-kilodalton heat shock proteins. In: *Journal of virology* 63 (11), S. 4533–4539.

Pallas, D. C.; Shahrik, L. K.; Martin, B. L.; Jaspers, S.; Miller, T. B.; Brautigan, D. L.; Roberts, T. M. (1990): Polyoma small and middle T antigens and SV40 small t antigen form stable complexes with protein phosphatase 2A. In: *Cell* 60 (1), S. 167–176.

Paoli, Paolo de; Carbone, Antonino (2013): Carcinogenic viruses and solid cancers without sufficient evidence of causal association. In: *International journal of cancer* 133 (7), S. 1517–1529. DOI: 10.1002/ijc.27995.

Pawson, T.; Schlessinger, J. (1993): SH2 and SH3 domains. In: *Current biology : CB* 3 (7), S. 434–442.

Pelletier, Stephane; Gingras, Sebastien; Green, Douglas R. (2015): Mouse genome engineering via CRISPR-Cas9 for study of immune function. In: *Immunity* 42 (1), S. 18–27. DOI: 10.1016/j.immuni.2015.01.004.

Porrás, A.; Gaillard, S.; Rundell, K. (1999): The simian virus 40 small-t and large-T antigens jointly regulate cell cycle reentry in human fibroblasts. In: *Journal of virology* 73 (4), S. 3102–3107.

Price, N. E.; Mumby, M. C. (2000): Effects of regulatory subunits on the kinetics of protein phosphatase 2A. In: *Biochemistry* 39 (37), S. 11312–11318. DOI: 10.1021/bi0008478.

Ran, F. Ann; Hsu, Patrick D.; Lin, Chie-Yu; Gootenberg, Jonathan S.; Konermann, Silvana; Trevino, Alexandro E. et al. (2013a): Double nicking by RNA-guided CRISPR Cas9 for enhanced genome editing specificity. In: *Cell* 154 (6), S. 1380–1389. DOI: 10.1016/j.cell.2013.08.021.

Ran, F. Ann; Hsu, Patrick D.; Wright, Jason; Agarwala, Vineeta; Scott, David A.; Zhang, Feng (2013b): Genome engineering using the CRISPR-Cas9 system. In: *Nature protocols* 8 (11), S. 2281–2308. DOI: 10.1038/nprot.2013.143.

Rayment, I.; Baker, T. S.; Caspar, D. L.; Murakami, W. T. (1982): Polyoma virus capsid structure at 22.5 A resolution. In: *Nature* 295 (5845), S. 110–115.

Roskoski, Robert (2015): Src protein-tyrosine kinase structure, mechanism, and small molecule inhibitors. In: *Pharmacological research* 94, S. 9–25. DOI: 10.1016/j.phrs.2015.01.003.

Rouleau, Cecile; Pores Fernando, Arun T.; Hwang, Justin H.; Faure, Nathalie; Jiang, Tao; White, Elizabeth A. et al. (2016): Transformation by Polyomavirus Middle T Antigen Involves a Unique Bimodal Interaction with the Hippo Effector YAP. In: *Journal of virology* 90 (16), S. 7032–7045. DOI: 10.1128/JVI.00417-16.

Ruvolo, Peter P. (2016): The broken "Off" switch in cancer signaling: PP2A as a regulator of tumorigenesis, drug resistance, and immune surveillance. In: *BBA clinical* 6, S. 87–99. DOI: 10.1016/j.bbacli.2016.08.002.

Sablina, Anna A.; Hector, Melissa; Colpaert, Nathalie; Hahn, William C. (2010): Identification of PP2A complexes and pathways involved in cell transformation. In: *Cancer Research* 70 (24), S. 10474–10484. DOI: 10.1158/0008-5472.CAN-10-2855.

Sakuma, Tetsushi; Nishikawa, Ayami; Kume, Satoshi; Chayama, Kazuaki; Yamamoto, Takashi (2014): Multiplex genome engineering in human cells using all-in-one CRISPR/Cas9 vector system. In: *Scientific reports* 4, S. 5400. DOI: 10.1038/srep05400.

Schaffhausen, Brian S.; Roberts, Thomas M. (2009): Lessons from polyoma middle T antigen on signaling and transformation: A DNA tumor virus contribution to the war on cancer. In: *Virology* 384 (2), S. 304–316. DOI: 10.1016/j.virol.2008.09.042.

Scheidtmann, K. H.; Mumby, M. C.; Rundell, K.; Walter, G. (1991): Dephosphorylation of simian virus 40 large-T antigen and p53 protein by protein phosphatase 2A: inhibition by small-t antigen. In: *Molecular and Cellular Biology* 11 (4), S. 1996–2003. DOI: 10.1128/mcb.11.4.1996.

Schmitz, Michael H. A.; Held, Michael; Janssens, Veerle; Hutchins, James R. A.; Hudecz, Otto; Ivanova, Elitsa et al. (2010): Live-cell imaging RNAi screen identifies PP2A–B55α and importin-β1 as key mitotic exit regulators in human cells. In: *Nature cell biology* 12 (9). DOI: 10.1038/ncb2092.

Schwab et al. (unpublished data).

Sents, Ward; Ivanova, Elitsa; Lambrecht, Caroline; Haesen, Dorien; Janssens, Veerle (2013): The biogenesis of active protein phosphatase 2A holoenzymes: a tightly regulated process creating phosphatase specificity. In: *The FEBS journal* 280 (2), S. 644–661. DOI: 10.1111/j.1742-4658.2012.08579.x.

Sents, Ward; Meeusen, Bob; Kalev, Petar; Radaelli, Enrico; Sagaert, Xavier; Miermans, Eline et al. (2017): PP2A Inactivation Mediated by PPP2R4 Haploinsufficiency Promotes Cancer Development. In: *Cancer Research* 77 (24), S. 6825–6837. DOI: 10.1158/0008-5472.CAN-16-2911.

Shenk, T. E.; Carbon, J.; Berg, P. (1976): Construction and analysis of viable deletion mutants of simian virus 40. In: *Journal of virology* 18 (2), S. 664–671.

Sheridan, Clare; Downward, Julian (2013): Inhibiting the RAS-PI3K pathway in cancer therapy. In: *The Enzymes* 34 Pt. B, S. 107–136. DOI: 10.1016/B978-0-12-420146-0.00005-6.

Shi, Yigong (2009): Serine/threonine phosphatases: mechanism through structure. In: *Cell* 139 (3), S. 468–484. DOI: 10.1016/j.cell.2009.10.006.

Shmakov, Sergey; Savitskaya, Ekaterina; Semenova, Ekaterina; Logacheva, Maria D.; Datsenko, Kirill A.; Severinov, Konstantin (2014): Pervasive generation of oppositely oriented spacers during CRISPR adaptation. In: *Nucleic acids research* 42 (9), S. 5907–5916. DOI: 10.1093/nar/gku226.

Singh, Priti; Schimenti, John C.; Bolcun-Filas, Ewelina (2015): A mouse geneticist's practical guide to CRISPR applications. In: *Genetics* 199 (1), S. 1–15. DOI: 10.1534/genetics.114.169771.

Smart, J. E.; Oppermann, H.; Czernilofsky, A. P.; Purchio, A. F.; Erikson, R. L.; Bishop, J. M. (1981): Characterization of sites for tyrosine phosphorylation in the transforming protein of Rous sarcoma virus (pp60v-src) and its normal cellular homologue (pp60c-src). In: *Proceedings of the National Academy of Sciences of the United States of America* 78 (10), S. 6013–6017. DOI: 10.1073/pnas.78.10.6013.

Smith, A. E.; Kamen, R.; Mangel, W. F.; Shure, H.; Wheeler, T. (1976): Location of the sequences coding for capsid proteins VP1 and VP2 on polyoma virus DNA. In: *Cell* 9 (3), S. 481–487.

Soeda, E.; Arrand, J. R.; Smolar, N.; Griffin, B. E. (1979): Sequence from early region of polyoma virus DNA containing viral replication origin and encoding small, middle and (part of) large T antigens. In: *Cell* 17 (2), S. 357–370.

Sontag, Estelle; Fedorov, Sergei; Kamibayashi, Craig; Robbins, David; Cobb, Melanie; Mumby, Marc (1993): The interaction of SV40 small tumor antigen with protein phosphatase 2A stimulates the map kinase pathway and induces cell proliferation. In: *Cell* 75 (5), S. 887–897. DOI: 10.1016/0092-8674(93)90533-V.

Sontag, Jean-Marie; Sontag, Estelle (2014): Protein phosphatase 2A dysfunction in Alzheimer's disease. In: *Frontiers in molecular neuroscience* 7, S. 16. DOI: 10.3389/fnmol.2014.00016.

Stadtmann et al. (2019): diploma thesis.

Stehelin, D.; Varmus, H. E.; Bishop, J. M.; Vogt, P. K. (1976): DNA related to the transforming gene(s) of avian sarcoma viruses is present in normal avian DNA. In: *Nature* 260 (5547), S. 170–173.

Sternberg, N.; Hamilton, D. (1981): Bacteriophage P1 site-specific recombination. I. Recombination between loxP sites. In: *Journal of molecular biology* 150 (4), S. 467–486.

Stone, S. R.; Hofsteenge, J.; Hemmings, B. A. (1987): Molecular cloning of cDNAs encoding two isoforms of the catalytic subunit of protein phosphatase 2A. In: *Biochemistry* 26 (23), S. 7215–7220.

Su, W.; Liu, W.; Schaffhausen, B. S.; Roberts, T. M. (1995): Association of Polyomavirus middle tumor antigen with phospholipase C-gamma 1. In: *The Journal of biological chemistry* 270 (21), S. 12331–12334.

Thomas, S. M.; Brugge, J. S. (1997): Cellular functions regulated by Src family kinases. In: *Annual review of cell and developmental biology* 13, S. 513–609. DOI: 10.1146/annurev.cellbio.13.1.513.

Tian, Yu; Li, Dawei; Dahl, Jean; You, John; Benjamin, Thomas (2004): Identification of TAZ as a binding partner of the polyomavirus T antigens. In: *Journal of virology* 78 (22), S. 12657–12664. DOI: 10.1128/JVI.78.22.12657-12664.2004.

Treisman, R.; Kamen, R. (1981): Structure of polyoma virus late nuclear RNA. In: *Journal of molecular biology* 148 (3), S. 273–301.

Treisman, R.; Novak, U.; Favaloro, J.; Kamen, R. (1981): Transformation of rat cells by an altered polyoma virus genome expressing only the middle-T protein. In: *Nature* 292 (5824), S. 595–600.

Ulug, E. T.; Cartwright, A. J.; Courtneidge, S. A. (1992): Characterization of the interaction of polyomavirus middle T antigen with type 2A protein phosphatase. In: *Journal of virology* 66 (3), S. 1458–1467.

Valle, Mikel; Chen, Xiaojiang S.; Donate, Luis Enrique; Fanning, Ellen; Carazo, José María (2006): Structural basis for the cooperative assembly of large T antigen on the origin of replication. In: *Journal of molecular biology* 357 (4), S. 1295–1305. DOI: 10.1016/j.jmb.2006.01.021.

van Duyne, Gregory D. (2015): Cre Recombinase. In: *Microbiology spectrum* 3 (1), S. 14. DOI: 10.1128/microbiolspec.MDNA3-0014-2014.

Vanhaesebroeck, Bart; Guillermet-Guibert, Julie; Graupera, Mariona; Bilanges, Benoit (2010): The emerging mechanisms of isoform-specific PI3K signalling. In: *Nature reviews. Molecular cell biology* 11 (5), S. 329–341. DOI: 10.1038/nrm2882.

Virshup, D. M. (2000): Protein phosphatase 2A: a panoply of enzymes. In: *Current opinion in cell biology* 12 (2), S. 180–185.

Wagner, Paul D.; Vu, Ngoc-Diep (2000): Histidine to aspartate phosphotransferase activity of nm23 proteins: phosphorylation of aldolase C on Asp-319. In: *The Biochemical journal* 346 (3), S. 623–630. DOI: 10.1042/bj3460623.

Wallace, Julie A.; Pitarresi, Jason R.; Sharma, Nandini; Palettas, Marilly; Cuitiño, Maria C.; Sizemore, Steven T. et al. (2014): Protein kinase C Beta in the tumor microenvironment promotes mammary tumorigenesis. In: *Frontiers in oncology* 4, S. 87. DOI: 10.3389/fonc.2014.00087.

Wang, Fangyuan; Qi, Lei S. (2016): Applications of CRISPR Genome Engineering in Cell Biology. In: *Trends in cell biology* 26 (11), S. 875–888. DOI: 10.1016/j.tcb.2016.08.004.

Winter, Georg E.; Buckley, Dennis L.; Paulk, Joshiawa; Roberts, Justin M.; Souza, Amanda; Dhe-Paganon, Sirano; Bradner, James E. (2015): DRUG DEVELOPMENT. Phthalimide conjugation as a strategy for in vivo target protein degradation. In: *Science (New York, N.Y.)* 348 (6241), S. 1376–1381. DOI: 10.1126/science.aab1433.

Wright, Addison V.; Nuñez, James K.; Doudna, Jennifer A. (2016): Biology and Applications of CRISPR Systems: Harnessing Nature's Toolbox for Genome Engineering. In: *Cell* 164 (1-2), S. 29–44. DOI: 10.1016/j.cell.2015.12.035.

Xie, Kabin; Minkenberg, Bastian; Yang, Yinong (2015): Boosting CRISPR/Cas9 multiplex editing capability with the endogenous tRNA-processing system. In: *Proceedings of the National Academy of Sciences of the United States of America* 112 (11), S. 3570–3575. DOI: 10.1073/pnas.1420294112.

Yu, X. X.; Du, X.; Moreno, C. S.; Green, R. E.; Ogris, E.; Feng, Q. et al. (2001): Methylation of the protein phosphatase 2A catalytic subunit is essential for association of Balpha regulatory subunit but not SG2NA, striatin, or polyomavirus middle tumor antigen. In: *Molecular biology of the cell* 12 (1), S. 185–199.

Zhao, Bin; Tumaneng, Karen; Guan, Kun-Liang (2011): The Hippo pathway in organ size control, tissue regeneration and stem cell self-renewal. In: *Nature cell biology* 13 (8), S. 877–883. DOI: 10.1038/ncb2303.

Zhou, Jin; Pham, Huong T.; Ruediger, Ralf; Walter, Gernot (2003): Characterization of the Aalpha and Abeta subunit isoforms of protein phosphatase 2A: differences in expression, subunit interaction, and evolution. In: *The Biochemical journal* 369 (Pt 2), S. 387–398. DOI: 10.1042/BJ20021244.

Zrelski et al. (unpublished data).

Ich habe mich bemüht, sämtliche Inhaber der Bildrechte ausfindig zu machen und ihre Zustimmung zur Verwendung der Bilder dieser Arbeit eingeholt. Sollte dennoch eine Urheberrechtsverletzung bekannt warden, ersuche ich um Meldung bei mir.

6. Appendix

6.1. Analysis of Variances for Focus Formation Assays of B6 MEFs

Single Factor ANOVA of Old B6 PyMT *Ptpa*^{fl} cells
Quantification of counted foci

Summary

groups	*count*	*sum*	*average*	*variance*
200 cells	4	1.065	0.266	0.001
100 cells	3	0.850	0.283	0.001
50 cells	4	1.240	0.310	0.001

ANOVA

source of variation	*degrees of freedom*	*F*	*p-value*	*F crit*
between groups	2	3.18	0.09	4.46
within groups	8			
total	10			

Single Factor ANOVA of Old B6 PyMT *Ptpa*$^{\Delta}$ cells
Quantification of counted foci

Summary

groups	*count*	*sum*	*average*	*variance*
200 cells	4	0.635	0.936	0.157
100 cells	3	0.700	0.233	0.830
50 cells	4	0.840	0.928	0.271

ANOVA

source of variation	*degrees of freedom*	*F*	*p-value*	*F crit*
between groups	2	0.69	0.53	4.46
within groups	8			
total	10			

Single Factor ANOVA of Old B6 PyMT *Ptpa*^{fl} cells
Quantification of area covered by foci

Summary

groups	*count*	*sum*	*average*	*variance*
200 cells	4	0.635	0.159	0.006
100 cells	3	0.700	0.233	0.004
50 cells	4	0.840	0.210	0.0039

ANOVA

source of variation	*degrees of freedom*	*F*	*p-value*	*F crit*
between groups	2	1.11	0.37	4.46
within groups	8			
total	10			

Single Factor ANOVA of Old B6 PyMT *Ptpa*$^{\Delta}$ cells
Quantification of area covered by foci

Summary

groups	*count*	*sum*	*average*	*variance*
200 cells	4	2.913	0.728	0.280
100 cells	3	3.417	1.139	0.003
50 cells	4	2.333	0.583	0.242

ANOVA

source of variation	*degrees of freedom*	*F*	*p-value*	*F crit*
between groups	2	1.40	0.30	4.46
within groups	8			
total	10			

Supplementary Figure 1 Results of the Single Factor Analysis of Variances (ANOVA) of Quantification of foci and Quantification of average area covered by foci in old B6 PyMT cells expressing PTPA or *Ptpa* knock-out cells.

Single Factor ANOVA of Young B6 PyMT *Ptpa*^{fl} cells
Quantification of counted foci

Summary

groups	*count*	*sum*	*average*	*variance*
500 cells	2	0.055	0.028	0.000
200 cells	2	0.150	0.075	0.000
100 cells	2	0.200	0.100	0.001

ANOVA

source of variation	*degrees of freedom*	*F*	*p-value*	*F crit*
between groups	2	9.43	0.05	9.55
within groups	3			
total	5			

Single Factor ANOVA of Young B6 PyMT *Ptpa*$^{\Delta}$ cells
Quantification of counted foci

Summary

groups	*count*	*sum*	*average*	*variance*
500 cells	2	0.065	0.031	0.001
200 cells	2	0.040	0.020	0.000
100 cells	2	0.080	0.040	0.003

ANOVA

source of variation	*degrees of freedom*	*F*	*p-value*	*F crit*
between groups	2	0.15	0.86	9.55
within groups	3			
total	5			

Single Factor ANOVA of Young B6 PyMT *Ptpa*^{fl} cells
Quantification of area covered by foci

Summary

groups	*count*	*sum*	*average*	*variance*
500 cells	2	0.330	0.165	0.054
200 cells	2	0.820	0.410	0.336
100 cells	2	0.010	0.005	0.000

ANOVA

source of variation	*degrees of freedom*	*F*	*p-value*	*F crit*
between groups	2	0.63	0.59	9.55
within groups	3			
total	5			

Single Factor ANOVA of Young B6 PyMT *Ptpa*$^{\Delta}$ cells
Quantification of area covered by foci

Summary

groups	*count*	*sum*	*average*	*variance*
500 cells	2	0.430	0.215	0.092
200 cells	2	0.130	0.065	0.008
100 cells	2	0.000	0.000	0.000

ANOVA

source of variation	*degrees of freedom*	*F*	*p-value*	*F crit*
between groups	2	0.72	0.55	9.55
within groups	3			
total	5			

Supplementary Figure 2 Results of the Single Factor Analysis of Variances (ANOVA) of Quantification of foci and Quantification of average area covered by foci in young B6 PyMT cells expressing PTPA or *Ptpa* knock-out cells.

6.2. Quantification of Immunoprecipitations

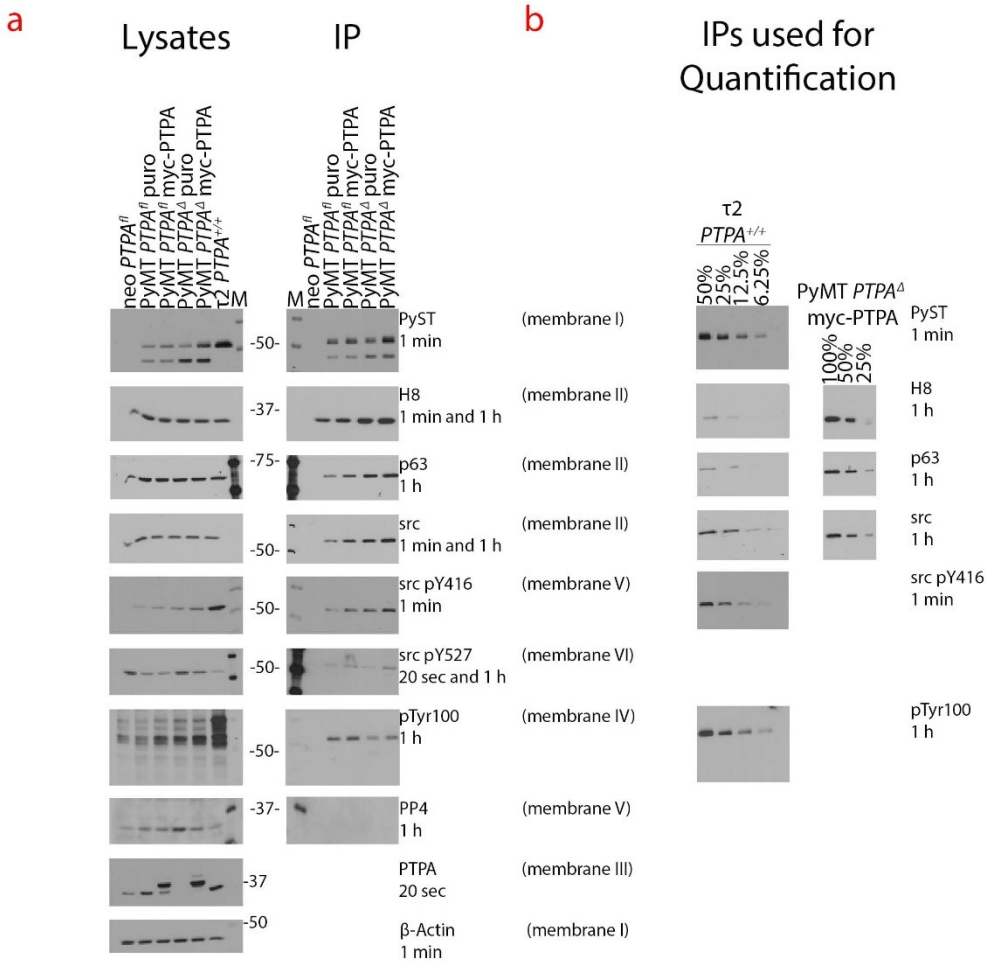

Supplementary Figure 3 **Interaction of PyMT and its Associated Proteins in 326 # 7 Cells Expressing PTPA and/or myc-PTPA and *Ptpa* Knock-Out Cells (extended)** Immunoprecipitation was performed via PyMT, using the rabbit polyclonal anti-PyST antibody. Empty vector (326 # 7 neo *Ptpa*^{fl}) was used as negative control. 326 # 7 cells expressing PyMT (*Ptpa*^{fl} puro, *Ptpa*^{fl} myc-PTPA, *Ptpa*$^{\Delta}$ puro and *Ptpa*$^{\Delta}$ myc-PTPA) were analysed. τ2 *Ptpa*$^{+/+}$ were included as positive control.10% of the protein amount of the IP were loaded for the lysates (left panel). 50%, 25%, 12.5% and 6.25% of τ2 *Ptpa*$^{+/+}$ IP and 100%, 50% and 25% of PyMT *Ptpa*$^{\Delta}$ myc-PTPA IP were loaded to enable a more exact quantification. τ2 *PTPA*$^{+/+}$ dilution series was used for the quantification of PyMT, src kinase (n=2), pY416 src kinase and PyMT (pTyr100), PyMT *Ptpa*$^{\Delta}$ myc-PTPA dilution series for PP2A A and C subunit (n=3) and src kinase (n=2). Logarithmic curves were calculated and used for quantification (Materials and Methods). Proteins were separated on a 10% SDS-PAGE and transferred to 6 nitrocellulose membranes. Membranes were incubated with antibodies in the following order: Membrane I: PyST (PyMT), β-Actin; Membrane II: H8 (PP2A C Subunit), src, p63 (PP2A A Subunit); Membrane III: PTPA; Membrane IV; pTyr100; Membrane V: pY416; PP4; Membrane VI: pY527. For the detection of pY416 src kinase 5% ECL Select was used, for the detection of the Co-IPs of PP2A A and C subunit, src kinase, pY527 src kinase and PP4 15% ECL Select were used. Blots are representative of 4 independent experiments.

6.3. Quantification of CRISPR/Cas9 Treated Cells

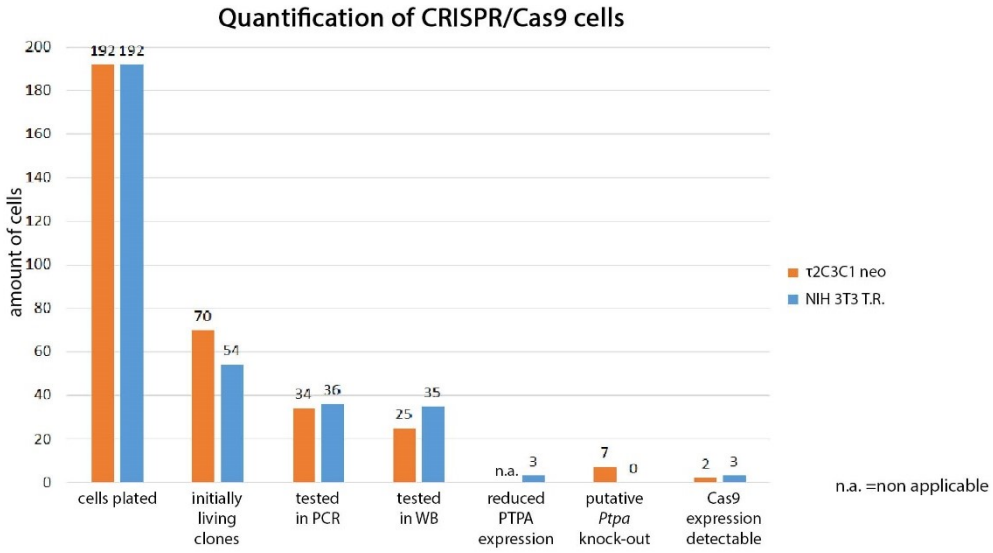

Supplementary Figure 4 Statistics and summary of CRISPR/Cas9 experiment of both cell lines, τ2C3C1 neo (orange) and NIH Tom Roberts (blue).

6.4. List of τ2C3C1 neo Clones after CRISPR/Cas9 PTPA c1 + c2 Transfections

plate	clone	96w	24w	6w	PCR	frozen	lysate	putative *Ptpa* KO	Cas9 expressing
1	T1A2	10.7.	10.7.	20.7.	25.7.	21./28.7.	2.8.		
1	T1A5	7.7.	7.7.	14.7.	19.7.	19./20.7.	26.7.		
1	T1A6	7.7.	7.7.	13.7.	19.7.	20./24.7.	28.7.		
1	T1A11	7.7.	7.7.	10.7.	11.7.	19./20.7.	21.7.		
1	T1B1	† 11.7.							
1	T1B4	† 13.7.							
1	T1B5								
1	T1B7	11.7.	11.7.						
1	T1B11	14.7.	14.7.		19.7.				
1	T1C6	10.7.	10.7.	20.7.	25.7.	28.7./3.8.	7.8.		
1	T1C8	†11.7.							
1	T1C9	† 17.7.							
1	T1C10	† 17.7.							
1	T1D3								
1	T1D10	7.7.	7.7.	13.7.	19.7.	21.7.	24.7.		
1	T1D12	7.7.	7.7.	24.7.	19.7.	4./8.8.	18.8.		
1	T1E1	† 17.7.							
1	T1E5	† 17.7.							
1	T1E6	† 17.7.							
1	T1E10								
1	T1F4	7.8.	7.8.	18.8.		2x 25.8.	28.8.	**YES**	
1	T1F5	17.7.	17.7.	28.7.	25.7.	7./16.8.	18.8.	**YES**	
1	T1F8	14.7.	14.7.	25.7.	25.7.	28./31.7.	4.8.		
1	T1F10								
1	T1G2	10.7.	10.7.	14.7.	19.7.	17./21.7.	24.7.		
1	T1G5	13.7.	13.7.	20.7.	25.7.	21./31.7.	4.8.		
1	T1G6								
1	T1G8	7.7.	7.7.	10.7.	11.7.	19./20.7.	21.7.		
1	T1G9								
1	T1G12	† 13.7.							
1	T1H1								
1	T1H2								
1	T1H3								
1	T1H10								
1	T1H12	11.7.	11.7.	24.7.	24.8.	28.7./4.8.	10.8.		
2	T2A2	14.7.	14.7.						
2	T2A6								
2	T2A7	17.7.	17.7.	19.7.	25.7.	20./28.7.	31.7.	**YES**	
2	T2A8	† 17.7.	† 17.7.						
2	T2A11	† 17.7.							
2	T2B1	† 17.7.	† 17.7.						
2	T2B6	† 11.7.							
2	T2B8	† 10.7.	11.7.						
2	T2B11	10.7.	10.7.	19.7.	25.7.	21./28.7.	2.8.		
2	T2B12	† 14.7.							

2	T2C1	7.7.	7.7.	17.7.	19.7.	28./31.7.	4.8.		
2	T2C2	† 11.7.							
2	T2C3								
2	T2C4								
2	T2C5*	7.7.	7.7.	10.7.	11.7.	13./17.7.	19.7.	**YES**	
2	T2C6	10.7.	10.7.	19.7.	25.7.	21./31.7.	4.8.	**YES**	
2	T2C7								
2	T2D4	7.7.	7.7.	3.8.	8.8.	11./18.8.	25.8.		**YES**
2	T2D6	24.7.	18.8.						
2	T2D11	7.7.	7.7.	14.7.	19.7.	17./21.7.	26.7.		
2	T2E1	7.7.	7.7.	13.7.	12.7.	21.7.	24.7.		
2	T2E2	† 11.7.							
2	T2E3								
2	T2E5	10.7.	17.7.						
2	T2E6	† 10.7.							
2	T2F9								
2	T2F10								
2	T2F11								
2	T2G5	18.8.	18.8.						
2	T2G6	24.7.	24.7.	23.8.		25.8./4.9.	13.9.		
2	T2G7	† 11.7.							
2	T2G9	7.7.	7.7.	20.7.	25.7.	28.7./4.8.	7.8.	**YES**	
2	T2H5								
2	T2H6	7.7.	7.7.	17.7.	19.7.	19./26.7.	28.7.	**YES**	**YES**
2	T2H8	10.7.	10.7.	11.7.	12.7.	17./21.7.	26.7.		
2	T2H9								

6.5. List of NIH 3T3 Tom Roberts Clones after CRISPR/Cas9 PTPA c1 + c2 Transfections

plate	clone	96w	24w	6w	PCR	frozen	lysate	reduced PTPA	Cas9 expressing
1	N1A5	† 13.7.	13.7.	11.8.		25./30.8.	4.9.		
1	N1A6	† 13.7.							
1	N1A7	7.7.	7.7.	21.7.	19.7.	2./16.8.	18.8.		
1	N1A11**	7.7.	7.7.	13.7.	19.7.	21./26.7.	31.7.		
1	N1B7	10.7.	10.7.	19.7.	25.7.	24./26.7.	31.7.		
1	N1B11	14.7.	14.7.	28.7.		4./11.8.	18.8.		
1	N1B12								
1	N1C4								
1	N1C7	20.7.	20.7.	26.7.	24.8.	2./4.8.	10.8.	**YES**	**YES**
1	N1D1	24.7.	24.7.						
1	N1D5	13.7.	13.7.	24.7.		28.7./3.8.	7.8.		
1	N1D7	7.7.	7.7.	14.7.		19./21.7.	28.7.		
1	N1E4	7.7.	7.7.	14.7.	1.8.	19./26.7.	31.7.		
1	N1E7	7.7.	7.7.	20.7.	24.8.	28.7./3.8.	18.8.		
1	N1E11	7.7.	7.7.	19.7.	1.8.	21./28.7.	2.8.		
1	N1E12	† 13.7.							
1	N1F3	10.7.	10.7.	14.7.	19.7.	19./21.7.	28.7.		
1	N1F9	† 17.7.	7.7.						

1	N1F10				19.7.				
1	N1F11	7.7.	7.7.	14.7.	19.7.	20./25.7.	28.7.		
1	N1F12	† 13.7.							
1	N1G4								
1	N1G8	24.7.	24.7.	16.8.		25./30.8.	4.9.	**YES**	
1	N1G10	13.7.	13.7.	19.7.	25.7.	25./28.7.	2.8.		
1	N1H12	17.7.	17.7.	28.7.		8./16.8.	24.8.		
2	N2A8	† 13.7.							
2	N2B4	14.7.	14.7.	24.7.	1.8.	28.7./4.8.	10.8.		
2	N2B9	14.7.	14.7.	2.8.	8.8.	11./25.8.	28.8.		
2	N2B10	17.7.	17.7.			31.7./7.8.	11.8.		**YES**
2	N2B11	† 13.7.							
2	N2B12	7.7.	7.7.	19.7.	19.7.	21./25.7.	31.7.		
2	N2C4	10.7.	10.7.						
2	N2C8	17.7.	17.7.						
2	N2C10	7.7.	7.7.	21.7.		28.7./3.8.	7.8.		
2	N2D2	13.7.	13.7.	2.8.	1.8.	11./25.8.	28.8.		
2	N2D10	7.7.	7.7.	20.7.	1.8.	28.7./4.8.	10.8.		
2	N2D12	† 13.7.							
2	N2E2	7.7.	7.7.	19.7.	19.7.	21./25.7.	28.7.		**YES**
2	N2E3	7.7.	18.8.	4.9.		2./6.10.			
2	N2F6	20.7.	20.7.	31.7.	24.8.	8./16.8.	18.8.		
2	N2F7								
2	N2F8								
2	N2F10	7.7.	7.7.	20.7.		25./28.7.	2.8.		
2	N2G2	7.7.	7.7.	14.7.	19.7.	19./21.7.	28.7.		
2	N2G4	13.7.	13.7.	14.7.	19.7.	19./24.7.	28.7.	**YES**	
2	N2G6	25.7.	25.7.	16.8.		25.8./4.9.	13.9.		
2	N2G8	13.7.	13.7.	19.7.	19.7.	21./28.7.	4.8.		
2	N2G9	7.7.	7.7.	19.7.	19.7.	21./26.7.	31.7.		
2	N2G10	10.7.	10.7.	14.7.	19.7.	21./28.7.	2.8.		
2	N2G12	13.7.	13.7	28.7.	1.8.	3./7.8.	18.8.		
2	N2H2	17.7.	17.7.	31.7.	1.8.	4./11.8.	18.8.		
2	N2H6	17.7.	17.7.	31.7.	8.8.	16.8.	24.8.		
2	N2H8	10.7.	10.7.	19.7.	19.7.	25./28.7.	2.8.		
2	N2H11	14.7.	14.7.	7.8.		18./25.8.	28.8.		

* singularized on 96-well plate
** 2 clones
† died on that day

6.6. T1F5 Sequence

Alignment was performed using Emboss Needle Alignment tool. Upper Sequence is *Ptpa* wild-type mRNA. *Ptpa* coding sequence in reference sequence is marked in orange. In T1F5 mRNA two base pairs (AT) are deleted at position 356-357, marked in red, resulting in a frameshift and premature stop after 45 amino acids. PCR was performed using PTPA C1 contr1_s (forward) and PTPA 170aa SphI_R (reverse) or PTPA 323aa SphI_R (reverse) primers. Wild-type amino acid sequence is indicated in green, amino acid sequence that arises from frameshift in **blue**.

```
EMBOSS_001    5'-    1 GGCGCCCCGCACCAAGATGGCCGCTGCCTCGGTCGGCGCGGCCGCCGCGA     50

EMBOSS_001    5'-    1 --------------------------------------------------       0

EMBOSS_001          51 GACGGCCGTTGGTGGGCATGCTCCCTGAGTGCCTCGCACCGGCATGGCTG    100

EMBOSS_001           1 --------------------------------------------------       0

EMBOSS_001         101 CCGCCTTCGCGCGAGTGACTGTAATTCTCGGCTTCCGGTCCTAGCCAGTC    150
                                 |||||||||||||||||||||||||||||||||||||
EMBOSS_001           1 ---------------TGACTGTAATTCTCGGCTTCCGGTCCTAGCCAGTC     35

EMBOSS_001         151 AGCGCTCATTTCCCTGCTGGAAGCTTGGCGGAGCCGGGGAGAGCTGCGGG    200
                       ||||||||||||||||||||||||||||||||||||||||||||||||||
EMBOSS_001          36 AGCGCTCATTTCCCTGCTGGAAGCTTGGCGGAGCCGGGGAGAGCTGCGGG     85

EMBOSS_001         201 GTGAACATTGAGAGGGACCGGCGAGCATCCGCTCCGGCTCCTCACGGAGA    250
                       |||||||||||||||||||||||||||||||||||||||||||||||||||
EMBOSS_001          86 GTGAACATTGAGAGGGACCGGCGAGCATCCGCTCCGGCTCCTCACGGAG-    134

                        1    M  A  E  G  E  R  Q  P  P  P  D  S  S  E  E  T     16
EMBOSS_001         251 AGATGGCCGAGGGCGAGCGGCAGCCGCCGCCAGATTCTTCAGAAGAGACC    300
                       ||||||||||||||||||||||||||||||||||||||||||||||||||||
EMBOSS_001         135 AGATGGCCGAGGGCGAGCGGCAGCCGCCGCCAGATTCTTCAGAAGAGACC    184
                        1    M  A  E  G  E  R  Q  P  P  P  D  S  S  E  E  T     16

                       17  P  P  T  T  Q  N  F  I  I  P  K  K  E  I  H  T  V     33
EMBOSS_001         301 CCTCCAACTACTCAGAACTTTATCATTCCAAAAAAGGAGATCCACACAGT    350
                       ||||||||||||||||||||||||||||||||||||||||||||||||||||
EMBOSS_001         185 CCTCCAACTACTCAGAACTTTATCATTCCAAAAAAGGAGATCCACACAGT    234
                       17  P  P  T  T  Q  N  F  I  I  P  K  K  E  I  H  T  V     33

                       34    P  D  M  G  K  W  K  R  S  Q  A  Y  A  D  Y  I  W     50
EMBOSS_001         351 TCCAGATATGGGCAAATGGAAGCGCTCTCAGGCATATGCTGACTACATTG    400
                       |||||  ||||||||||||||||||||||||||||||||||||||||||||
EMBOSS_001         235 TCCAG--ATGGGCAAATGGAAGCGCTCTCAGGCATATGCTGACTACATTG    282
                       34    P    D  G  Q  M  E  A  L  S  G  I  C STOP          45

EMBOSS_001         401 GCTTCATCCTTACCCTCAATGAAGGTGTGAAGGGGAAGAAGCTGACCTTC    450
                       ||||||||||||||||||||||||||||||||||||||||||||||||||||
EMBOSS_001         283 GCTTCATCCTTACCCTCAATGAAGGTGTGAAGGGGAAGAAGCTGACCTTC    332

EMBOSS_001         451 GACTACAAAGTCTCTGAGGCCATCGAGAAGCTGGTGGCACTTCTTGATAC    500
                       ||||||||||||||||||||||||||||||||||||||||||||||||||||
EMBOSS_001         333 GACTACAAAGTCTCTGAGGCCATCGAGAAGCTGGTGGCACTTCTTGATAC    382

EMBOSS_001         501 GCTGGATAGGTGGATTGATGAAACCCCGCCAGTGGACCAGCCTTCCCGGT    550
                       ||||||||||||||||||||||||||||||||||||||||||||||||||||
EMBOSS_001         383 GCTGGATAGGTGGATTGATGAAACCCCGCCAGTGGACCAGCCTTCCCGGT    432

EMBOSS_001         551 TTGGGAACAAAGCCTACAGAACCTGGTATGCCAAACTTGATCAGGAAGCA    600
                       ||||||||||||||||||||||||||||||||||||||||||||||||||||
EMBOSS_001         433 TTGGGAACAAAGCCTACAGAACCTGGTATGCCAAACTTGATCAGGAAGCA    482

EMBOSS_001         601 GAAAACTTGGTGGCCACAGTGGTCCCCACCCACCTGGCTGCTGCTGTGCC    650
                       ||||||||||||||||||||||||||||||||||||||||||||||||||||
EMBOSS_001         483 GAAAACTTGGTGGCCACAGTGGTCCCCACCCACCTGGCTGCTGCTGTGCC    532
```

```
EMBOSS_001       651 TGAAGTGGCAGTTTACCTGAAGGAGGCTGTGGGGAACTCCACACGAATTG    700
                     ||||||||||||||||||||||||||||||||||||||||||||||||||
EMBOSS_001       533 TGAAGTGGCAGTTTACCTGAAGGAGGCTGTGGGGAACTCCACACGAATTG    582

EMBOSS_001       701 ACTATGGCACAGGGCATGAGGCTGCCTTTGCTGCTTTCCTCTGTTGTCTC    750
                     ||||||||||||||||||||||||||||||||||||||||||||||||||
EMBOSS_001       583 ACTATGGCACAGGGCATGAGGCTGCCTTTGCTGCTTTCCTCTGTTGTCTC    632

EMBOSS_001       751 TGCAAGATTGGTGTACTCCGGGTG---GACGACCAGGTGGCTATTGTCTT    797
                     |||||||||||||.|       ||   |.|||.|.|
EMBOSS_001       633 TGCAAGATTGGTGCA-------TGCATGTCGATCTG--------------    661

EMBOSS_001       798 CAAGGTGTTTGATAGGTATCTTGAGGTTATGCGGAAGTTGCAGAAGACAT    847

EMBOSS_001       662 --------------------------------------------------    661

EMBOSS_001       848 ACAGGATGGAGCCTGCAGGCAGCCAGGGCGTATGGGGTCTGGATGACTTC    897

EMBOSS_001       662 --------------------------------------------------    661

EMBOSS_001       898 CAGTTCCTGCCCTTCATCTGGGGCAGCTCACAGCTCATAGACCACCCCCA    947

EMBOSS_001       662 --------------------------------------------------    661

EMBOSS_001       948 CCTGGAGCCCAGACATTTCGTGGATGAGAAGGCGGTGAGCGAGAACCACA    997

EMBOSS_001       662 --------------------------------------------------    661

EMBOSS_001       998 AGGACTACATGTTTCTCCAGTGCATCCTGTTCATCACTGAGATGAAGACT   1047

EMBOSS_001       662 --------------------------------------------------    661

EMBOSS_001      1048 GGCCCCTTTGCGGAACACTCCAACCAGCTGTGGAACATCAGTGCTGTCCC   1097

EMBOSS_001       662 --------------------------------------------------    661

EMBOSS_001      1098 CTCCTGGTCTAAAGTGAACCAGGGCCTCATTCGAATGTATAAGGCAGAGT   1147

EMBOSS_001       662 --------------------------------------------------    661

EMBOSS_001      1148 GCCTGGAGAAGTTCCCTGTGATCCAGCACTTCAAGTTCGGGAGCCTGCTG   1197

EMBOSS_001       662 --------------------------------------------------    661

EMBOSS_001      1198 CCCATCCATCCCGTCACATCAGGCTAGGAGAGGCTGAACTACCAGAGCCA   1247

EMBOSS_001       662 --------------------------------------------------    661

EMBOSS_001      1248 CCCTGGCCAGGTTCCTGTGCTCTCTGTGACCCAGCACCCCTCCCGCCCAC   1297 - 3′

EMBOSS_001       662 --------------------------------------------------    661 - 3′
```

6.7. T2C6 mRNA Sequences

6.7.1. Colony Number 1

Alignment was performed using Emboss Needle Alignment tool. Upper Sequence is *Ptpa* wild-type mRNA. *Ptpa* coding sequence in reference sequence is marked in orange. In T2C6 mRNA two base pairs (AT) are deleted at position 356-357, marked in red, resulting in a frameshift and premature stop after 45 amino acids. PCR was performed using PTPA C1 contr1_s (forward) and PTPA 323aa SphI_R (reverse) primers. Wild-type amino acid sequence is indicated in green, amino acid sequence that arises from frameshift in **blue**. One missense mutation in the coding sequence was found (violet colour). This mutation could also originate in an error made by the polymerase during PCR. The wild-type sequence is provided as long as necessary, to show the result of the frameshift. Full-length amino acid sequence is not provided here.

```
EMBOSS_001    5'-    1 GGCGCCCCGCACCAAGATGGCCGCTGCCTCGGTCGGCGCGGCCGCCGCGA     50

EMBOSS_001    5'-    1 --------------------------------------------------      0

EMBOSS_001          51 GACGGCCGTTGGTGGGCATGCTCCCTGAGTGCCTCGCACCGGCATGGCTG    100

EMBOSS_001           1 --------------------------------------------------      0

EMBOSS_001         101 CCGCCTTCGCGCGAGTGACTGTAATTCTCGGCTTCCGGTCCTAGCCAGTC    150

EMBOSS_001           1 --------------------------------------------------      0

EMBOSS_001         151 AGCGCTCATTTCCCTGCTGGAAGCTTGGCGGAGCCGGGGAGAGCTGCGGG    200
                                 ||||||||||||||||||||||||||||||||||||
EMBOSS_001           1 ----------------CTGGAAGCTTGGCGGAGCCGGGGAGAGCTGCGGG     34

EMBOSS_001         201 GTGAACATTGAGAGGGACCGGCGAGCATCCGCTCCGGC-TCCTCACGGAG    249
                       |||||||||||||||||||||||||||||||||||| ||.||||||||
EMBOSS_001          35 GTGAACATTGAGAGGGACCGGCGAGCATCCGCTCCGGCTTCTTCACGGAG     84

                     1     M  A  E  G  E  R  Q  P  P  P  D  S  S  E  E  T    16
EMBOSS_001         250 AAGATGGCCGAGGGCGAGCGGCAGCCGCCGCCAGATTCTTCAGAAGAGAC    299
                       ||||||||.||||||||||||||||||||||||||||||||||||||||||
EMBOSS_001          85 -AGATGGCCAAGGGCGAGCGGCAGCCGCCGCCAGATTCTTCAGAAGAGAC    133
                     1     M  A  K  G  E  R  Q  P  P  P  D  S  S  E  E  T    16

                    17   P  P  T  T  Q  N  F  I  I  P  K  K  E  I  H  T     32
EMBOSS_001         300 CCCTCCAACTACTCAGAACTTTATCATTCCAAAAAAGGAGATCCACACAG    349
                       ||||||||||||||||||||||||||||||||||||||||||||||||||||
EMBOSS_001         134 CCCTCCAACTACTCAGAACTTTATCATTCCAAAAAAGGAGATCCACACAG    183
                    17   P  P  T  T  Q  N  F  I  I  P  K  K  E  I  H  T     32

                    33 V  P  D  M  G  K  W  K  R  S  Q  A  Y  A  D  Y  I W   50
EMBOSS_001         350 TTCCAGATATGGGCAAATGGAAGCGCTCTCAGGCATATGCTGACTACATT    399
                       ||||||  ||||||||||||||||||||||||||||||||||||||||||||
EMBOSS_001         184 TTCCAG--ATGGGCAAATGGAAGCGCTCTCAGGCATATGCTGACTACATT    231
                    33 V  P     D  G  Q  M  E  A  L  S  G  I  C STOP        45


EMBOSS_001         400 GGCTTCATCCTTACCCTCAATGAAGGTGTGAAGGGGAAGAAGCTGACCTT    449
                       ||||||||||||||||||||||||||||||||||||||||||||||||||||
EMBOSS_001         232 GGCTTCATCCTTACCCTCAATGAAGGTGTGAAGGGGAAGAAGCTGACCTT    281

EMBOSS_001         450 CGACTACAAAGTCTCTGAGGCCATCGAGAAGCTGGTGGCACTTCTTGATA    499
                       ||||||||||||||||||||||||||||||||||||||||||||||||||||
EMBOSS_001         282 CGACTACAAAGTCTCTGAGGCCATCGAGAAGCTGGTGGCACTTCTTGATA    331

EMBOSS_001         500 CGCTGGATAGGTGGATTGATGAAACCCCGCCAGTGGACCAGCCTTCCCGG    549
                       ||||||||||||||||||||||||||||||||||||||||||||||||||||
EMBOSS_001         332 CGCTGGATAGGTGGATTGATGAAACCCCGCCAGTGGACCAGCCTTCCCGG    381
```

```
EMBOSS_001       550 TTTGGGAACAAAGCCTACAGAACCTGGTATGCCAAACTTGATCAGGAAGC    599
                     ||||||||||||||||||||||||||||||||||||||||||||||||||||
EMBOSS_001       382 TTTGGGAACAAAGCCTACAGAACCTGGTATGCCAAACTTGATCAGGAAGC    431

EMBOSS_001       600 AGAAAACTTGGTGGCCACAGTGGTCCCCACCCACCTGGCTGCTGCTGTGC    649
                     ||||||||||||||||||||||||||||||||||||||||||||||||||||
EMBOSS_001       432 AGAAAACTTGGTGGCCACAGTGGTCCCCACCCACCTGGCTGCTGCTGTGC    481

EMBOSS_001       650 CTGAAGTGGCAGTTTACCTGAAGGAGGCTGTGGGGAACTCCACACGAATT    699
                     ||||||||||||||||||||||||||||||||||||||||||||||||||||
EMBOSS_001       482 CTGAAGTGGCAGTTTACCTGAAGGAGGCTGTGGGGAACTCCACACGAATT    531

EMBOSS_001       700 GACTATGGCACAGGGCATGAGGCTGCCTTTGCTGCTTTCCTCTGTTGTCT    749
                     ||||||||||||||||||||||||||||||||||||||||||||||||||||
EMBOSS_001       532 GACTATGGCACAGGGCATGAGGCTGCCTTTGCTGCTTTCCTCTGTTGTCT    581

EMBOSS_001       750 CTGCAAGATTGGTGTACTCCGGGTGGACGACCAGGTGGCTATTGTCTTCA    799
                     ||||||||||||||||||||||||||||||||||||||||||||||||||||
EMBOSS_001       582 CTGCAAGATTGGTGTACTCCGGGTGGACGACCAGGTGGCTATTGTCTTCA    631

EMBOSS_001       800 AGGTGTTTGATAGGTATCTTGAGGTTATGCGGAAGTTGCAGAAGACATAC    849
                     ||||||||||||||||||||||||||||||||||||||||||||||||||||
EMBOSS_001       632 AGGTGTTTGATAGGTATCTTGAGGTTATGCGGAAGTTGCAGAAGACATAC    681

EMBOSS_001       850 AGGATGGAGCCTGCAGGCAGCCAGGGCGTATGGGGTCTGGATGACTTCCA    899
                     ||||||||||||||||||||||||||||||||||||||||||||||||||||
EMBOSS_001       682 AGGATGGAGCCTGCAGGCAGCCAGGGCGTATGGGGTCTGGATGACTTCCA    731

EMBOSS_001       900 GTTCCTGCCCTTCATCTGGGGCAGCTCACAGCTCATAGACCACCCCCACC    949
                     ||||||||||||||||||||||||||||||||||||||||||||||||||||
EMBOSS_001       732 GTTCCTGCCCTTCATCTGGGGCAGCTCACAGCTCATAGACCACCCCCACC    781

EMBOSS_001       950 TGGAGCCCAGACATTTCGTGGATGAGAAGGCGGTGAGCGAGAACCACAAG    999
                     ||||||||||||||||||||||||||||||||||||||||||||||||||||
EMBOSS_001       782 TGGAGCCCAGACATTTCGTGGATGAGAAGGCGGTGAGCGAGAACCACAAG    831

EMBOSS_001      1000 GACTACATGTTTCTCCAGTGCATCCTGTTCATCACTGAGATGAAGACTGG   1049
                     ||||||||||||||||||||||||||||||||||||||||||||||||||||
EMBOSS_001       832 GACTACATGTTTCTCCAGTGCATCCTGTTCATCACTGAGATGAAGACTGG    881

EMBOSS_001      1050 CCCCTTTGCGGAACACTCCAACCAGCTGTGGAACATCAGTGCTGTCCCCT   1099
                     ||||||||||||||||||||||||||||||||||||||||||||||||||||
EMBOSS_001       882 CCCCTTTGCGGAACACTCCAACCAGCTGTGGAACATCAGTGCTGTCCCCT    931

EMBOSS_001      1100 CCTGGTCTAAAGTGAACCAGGGCCTCATTCGAATGTATAAGGCAGAGTGC   1149
                     ||||||||||||||||||||||||||||||||||||||||||||||||||||
EMBOSS_001       932 CCTGGTCTAAAGTGAACCAGGGCCTCATTCGAATGTATAAGGCAGAGTGC    981

EMBOSS_001      1150 CTGGAGAAGTTCCCTGTGATCCAGCACTTCAAGTTCGGGGAGCCTGCTGCC   1199
                     ||||||||||||||||||||||||||||||||||||||||||||||||||||
EMBOSS_001       982 CTGGAGAAGTTCCCTGTGATCCAGCACTTCAAGTTCGGGGAGCCTGCTGCC   1031

EMBOSS_001      1200 CATCCATCCCGTCACATCAGGC---------TAGGAGAGGCTGAACTACC   1240
                     ||||||||||||||||||||||         |.|
EMBOSS_001      1032 CATCCATCCCGTCACATCAGGCGCATGCATGTCG----------------   1065

EMBOSS_001      1241 AGAGCCACCCTGGCCAGGTTCCTGTGCTCTCTGTGACCCAGCACCCCTCC   1290

EMBOSS_001      1066 --------------------------------------------------   1065

EMBOSS_001      1291 CGCCCACCTTCTGTTCTTTCTGTTTGATGAGAGGCTGTTTACTGAGATGG   1340

EMBOSS_001      1066 --------------------------------------------------   1065

EMBOSS_001      1341 GTGCTAAGCAGGGCCTGAGTTGGGGGAATTGACCACAGTGTGCCCAGTTT   1390

EMBOSS_001      1066 --------------------------------------------------   1065

EMBOSS_001      1391 TTGACTGTCCTCCGTCTGGTGGCCGAGTAAGAAGAGAGGGGCCTGGACGT   1440
```

```
EMBOSS_001      1066 ----------------------------------------------------   1065

EMBOSS_001      1441 GGTCCCCGGCCCTGCCCATCCCTGTGCTCCTGCTTCCTCCCACGGTCAGG   1490 - 3'

EMBOSS_001      1066 ----------------------------------------------------   1065 - 3'
```

6.7.2. Colony Number 2

Alignment was performed using Emboss Needle Alignment tool. Upper Sequence is *Ptpa* wild-type mRNA. *Ptpa* coding sequence in reference sequence is marked in orange. In T2C6 mRNA one base pair (A) is deleted at position 356, marked in red, resulting in a frameshift and premature stop after 41 amino acids. PCR was performed using PTPA C1 contr1_s (forward) and PTPA 323aa SphI_R (reverse) primers. Wild-type amino acid sequence is indicated in green, amino acid sequence that arises from frameshift in **blue**. The wild-type sequence is provided as long as necessary, to show the result of the frameshift. Full-length amino acid sequence is not provided here.

```
EMBOSS_001      5'- 1 GGCGCCCCGCACCAAGATGGCCGCTGCCTCGGTCGGCGCGGCCGCCGCGA     50

EMBOSS_001      5'- 1 ----------------------------------------------------      0

EMBOSS_001        51 GACGGCCGTTGGTGGGCATGCTCCCTGAGTGCCTCGCACCGGCATGGCTG    100

EMBOSS_001         1 ----------------------------------------------------      0

EMBOSS_001       101 CCGCCTTCGCGCGAGTGACTGTAATTCTCGGCTTCCGGTCCTAGCCAGTC    150
                       ..||||||||||||||||||||||||||||||||||||||||||||||||
EMBOSS_001         1 ----GATCGCGCGAGTGACTGTAATTCTCGGCTTCCGGTCCTAGCCAGTC     46

EMBOSS_001       151 AGCGCTCATTTCCCTGCTGGAAGCTTGGCGGAGCCGGGGGAGAGCTGCGGG    200
                     ||||||||||||||||||||||||||||||||||||||||||||||||||||||
EMBOSS_001        47 AGCGCTCATTTCCCTGCTGGAAGCTTGGCGGAGCCGGGGGAGAGCTGCGGG     96

EMBOSS_001       201 GTGAACATTGAGAGGGACCGGCGAGCATCCGCTCCGGCTCCTCACGGAG-    249
                     |||||||||||||||||||||||||||||||||||||||||||||||||||||
EMBOSS_001        97 GTGAACATTGAGAGGGACCGGCGAGCATCCGCTCCGGCTCCTCACGGAGA    146

                    1     M  A  E  G  E  R  Q  P  P  P  D  S  S  E  E  T    16
EMBOSS_001       250 AAGATGGCCGAGGGCGAGCGGCAGCCGCCGCCAGATTCTTCAGAAGAGAC    299
                     ||||||||||||||||||||||||||||||||||||||||||||||||||||||
EMBOSS_001       147 AAGATGGCCGAGGGCGAGCGGCAGCCGCCGCCAGATTCTTCAGAAGAGAC    196
                    1     M  A  E  G  E  R  Q  P  P  P  D  S  S  E  E  T    16

                   17   P  P  T  T  Q  N  F  I  I  P  K  K  E  I  H  T    32
EMBOSS_001       300 CCCTCCAACTACTCAGAACTTTATCATTCCAAAAAAGGAGATCCACACAG    349
                     ||||||||||||||||||||||||||||||||||||||||||||||||||||||
EMBOSS_001       197 CCCTCCAACTACTCAGAACTTTATCATTCCAAAAAAGGAGATCCACACAG    246
                   17   P  P  T  T  Q  N  F  I  I  P  K  K  E  I  H  T    32

                   33 V  P  D   M  G  K  W  K  R  S  Q  A  Y  A  D  Y  I    49
EMBOSS_001       350 TTCCAGAT-ATGGGCAAATGGAAGCGCTCTCAGGCATATGCTGACTACAT    398
                     |||||||| ||||||||||||||||||||||||||||||||||||||||||||
EMBOSS_001       247 TTCCAGATAATGGGCAAATGGAAGCGCTCTCAGGCATATGCTGACTACAT    296
                   33 V  P  D  N  G  Q  M  E  A  L  S  G  I  C STOP       46

EMBOSS_001       399 TGGCTTCATCCTTACCCTCAATGAAGGTGTGAAGGGGAAGAAGCTGACCT    448
                     ||||||||||||||||||||||||||||||||||||||||||||||||||||||
EMBOSS_001       297 TGGCTTCATCCTTACCCTCAATGAAGGTGTGAAGGGGAAGAAGCTGACCT    346

EMBOSS_001       449 TCGACTACAAAGTCTCTGAGGCCATCGAGAAGCTGGTGGCACTTCTTGAT    498
                     ||||||||||||||||||||||||||||||||||||||||||||||||||||||
EMBOSS_001       347 TCGACTACAAAGTCTCTGAGGCCATCGAGAAGCTGGTGGCACTTCTTGAT    396

EMBOSS_001       499 ACGCTGGATAGGTGGATTGATGAAACCCCGCCAGTGGACCAGCCTTCCCG    548
                     ||||||||||||||||||||||||||||||||||||||||||||||||||||||
EMBOSS_001       397 ACGCTGGATAGGTGGATTGATGAAACCCCGCCAGTGGACCAGCCTTCCCG    446
```

```
EMBOSS_001       549 GTTTGGGAACAAAGCCTACAGAACCTGGTATGCCAAACTTGATCAGGAAG    598
                     ||||||||||||||||||||||||||||||||||||||||||||||||||||
EMBOSS_001       447 GTTTGGGAACAAAGCCTACAGAACCTGGTATGCCAAACTTGATCAGGAAG    496

EMBOSS_001       599 CAGAAAACTTGGTGGCCACAGTGGTCCCCACCCACCTGGCTGCTGCTGTG    648
                     ||||||||||||||||||||||||||||||||||||||||||||||||||||
EMBOSS_001       497 CAGAAAACTTGGTGGCCACAGTGGTCCCCACCCACCTGGCTGCTGCTGTG    546

EMBOSS_001       649 CCTGAAGTGGCAGTTTACCTGAAGGAGGCTGTGGGGAACTCCACACGAAT    698
                     ||||||||||||||||||||||||||||||||||||||||||||||||||||
EMBOSS_001       547 CCTGAAGTGGCAGTTTACCTGAAGGAGGCTGTGGGGAACTCCACACGAAT    596


EMBOSS_001       699 TGACTATGGCACAGGGCATGAGGCTGCCTTTGCTGCTTTCCTCTGTTGTC    748
                     ||||||||||||||||||||||||||||||||||||||||||||||||||||
EMBOSS_001       597 TGACTATGGCACAGGGCATGAGGCTGCCTTTGCTGCTTTCCTCTGTTGTC    646

EMBOSS_001       749 TCTGCAAGATTGGTGTACTCCGGGTGGACGACCAGGTGGCTATTGTCTTC    798
                     ||||||||||||||||||||||||||||||||||||||||||||||||||||
EMBOSS_001       647 TCTGCAAGATTGGTGTACTCCGGGTGGACGACCAGGTGGCTATTGTCTTC    696

EMBOSS_001       799 AAGGTGTTTGATAGGTATCTTGAGGTTATGCGGAAGTTGCAGAAGACATA    848
                     ||||||||||||||||||||||||||||||||||||||||||||||||||||
EMBOSS_001       697 AAGGTGTTTGATAGGTATCTTGAGGTTATGCGGAAGTTGCAGAAGACATA    746

EMBOSS_001       849 CAGGATGGAGCCTGCAGGCAGCCAGGGCGTATGGGGTCTGGATGACTTCC    898
                     ||||||||||||||||||||||||||||||||||||||||||||||||||||
EMBOSS_001       747 CAGGATGGAGCCTGCAGGCAGCCAGGGCGTATGGGGTCTGGATGACTTCC    796

EMBOSS_001       899 AGTTCCTGCCCTTCATCTGGGGCAGCTCACAGCTCATAGACCACCCCCAC    948
                     ||||||||||||||||||||||||||||||||||||||||||||||||||||
EMBOSS_001       797 AGTTCCTGCCCTTCATCTGGGGCAGCTCACAGCTCATAGACCACCCCCAC    846

EMBOSS_001       949 CTGGAGCCCAGACATTTCGTGGATGAGAAGGCGGTGAGCGAGAACCACAA    998
                     ||||||||||||||||||||||||||.||||||||||||||||||||||||
EMBOSS_001       847 CTGGAGCCCAGACATTTCGTGGATGAAAAGGCGGTGAGCGAGAACCACAA    896

EMBOSS_001       999 GGACTACATGTTTCTCCAGTGCATCCTGTTCATCACTGAGATGAAGACTG   1048
                     ||||||||||||||||||||||||||||||||||||||||||||||||||||
EMBOSS_001       897 GGACTACATGTTTCTCCAGTGCATCCTGTTCATCACTGAGATGAAGACTG    946

EMBOSS_001      1049 GCCCCTTTGCGGAACACTCCAACCAGCTGTGGAACATCAGTGCTGTCCCC   1098
                     ||||||||||||||||||||||||||||||||||||||||||||||||||||
EMBOSS_001       947 GCCCCTTTGCGGAACACTCCAACCAGCTGTGGAACATCAGTGCTGTCCCC    996

EMBOSS_001      1099 TCCTGGTCTAAAGTGAACCAGGGCCTCATTCGAATGTATAAGGCAGAGTG   1148
                     ||||||||||||||||||||||||||||||
EMBOSS_001       997 TCCTGGTCTAAAGTGAACCAGGGCCTCATT----------------------   1026

EMBOSS_001      1149 CCTGGAGAAGTTCCCTGTGATCCAGCACTTCAAGTTCGGGAGCCTGCTGC   1198

EMBOSS_001      1027 --------------------------------------------------   1026

EMBOSS_001      1199 CCATCCATCCCGTCACATCAGGCTAGGAGAGGCTGAACTACCAGAGCCAC   1248 - 3′

EMBOSS_001      1027 --------------------------------------------------   1026 - 3′
```

6.7.3. Colony Number 3

Alignment was performed using Emboss Needle Alignment tool. Upper Sequence is *Ptpa* wild-type mRNA. *Ptpa* coding sequence in reference sequence is marked in orange. In T2C6 mRNA a fragment of 106 base pairs from position 250 to 356 (-bp upstream of ATG) is deleted, marked in red. PCR was performed using PTPA C1 contr1_s (forward) and PTPA 323aa SphI_R (reverse) primers. The start of the wild-type amino acid sequence is provided in green.

```
EMBOSS_001     5'- 1 GGCGCCCCGCACCAAGATGGCCGCTGCCTCGGTCGGCGCGGCCGCCGCGA     50

EMBOSS_001     5'- 1 --------------------------------------------------       0

EMBOSS_001        51 GACGGCCGTTGGTGGGCATGCTCCCTGAGTGCCTCGCACCGGCATGGCTG    100
                                                                     |
EMBOSS_001         1 ----------------------------------------------------G      1

EMBOSS_001       101 CCGCCTTCGCGCGAGTGACTGTAATTCTCGGCTTCCGGTCCTAGCCAGTC    150
                     |.|   .||||||||||||||||||||||||||||||||||||||||||||||
EMBOSS_001         2 CAG--ATCGCGCGAGTGACTGTAATTCTCGGCTTCCGGTCCTAGCCAGTC     49

EMBOSS_001       151 AGCGCTCATTTCCCTGCTGGAAGCTTGGCGGAGCCGGGGAGAGCTGCGGG    200
                     ||||||||||||||||||||||||||||||||||||||||||||||||||||
EMBOSS_001        50 AGCGCTCATTTCCCTGCTGGAAGCTTGGCGGAGCCGGGGAGAGCTGCGGG     99

EMBOSS_001       201 GTGAACATTGAGAGGGACCGGCGAGCATCCGCTCCGGCTCCTCACGGAGA    250
                     ||||||||||||||||||||||||||||||||||||||||||||||||||||
EMBOSS_001       100 GTGAACATTGAGAGGGACCGGCGAGCATCCGCTCCGGCTCCTCACGGAGA    149

                       1    M  A  E  G  E  R  Q  P  P  P  D  S  S  E  E  T    16
EMBOSS_001       251 AGATGGCCGAGGGCGAGCGGCAGCCGCCGCCAGATTCTTCAGAAGAGACC    300
                     |
EMBOSS_001       150 A----------------------------------------------------    150

EMBOSS_001       301 CCTCCAACTACTCAGAACTTTATCATTCCAAAAAAGGAGATCCACACAGT    350

EMBOSS_001       151 ----------------------------------------------------    150

EMBOSS_001       351 TCCAGATATGGGCAAATGGAAGCGCTCTCAGGCATATGCTGACTACATTG    400
                           |||||||||||||||||||||||||||||||||||||||||||||
EMBOSS_001       151 -------ATGGGCAAATGGAAGCGCTCTCAGGCATATGCTGACTACATTG    193

EMBOSS_001       401 GCTTCATCCTTACCCTCAATGAAGGTGTGAAGGGGAAGAAGCTGACCTTC    450
                     ||||||||||||||||||||||||||||||||||||||||||||||||||||
EMBOSS_001       194 GCTTCATCCTTACCCTCAATGAAGGTGTGAAGGGGAAGAAGCTGACCTTC    243

EMBOSS_001       451 GACTACAAAGTCTCTGAGGCCATCGAGAAGCTGGTGGCACTTCTTGATAC    500
                     ||||||||||||||||||||||||||||||||||||||||||||||||||||
EMBOSS_001       244 GACTACAAAGTCTCTGAGGCCATCGAGAAGCTGGTGGCACTTCTTGATAC    293

EMBOSS_001       501 GCTGGATAGGTGGATTGATGAAACCCCGCCAGTGGACCAGCCTTCCCGGT    550
                     ||||||||||||||||||||||||||||||||||||||||||||||||||||
EMBOSS_001       294 GCTGGATAGGTGGATTGATGAAACCCCGCCAGTGGACCAGCCTTCCCGGT    343

EMBOSS_001       551 TTGGGAACAAAGCCTACAGAACCTGGTATGCCAAACTTGATCAGGAAGCA    600
                     ||||||||||||||||||||||||||||||||||||||||||||||||||||
EMBOSS_001       344 TTGGGAACAAAGCCTACAGAACCTGGTATGCCAAACTTGATCAGGAAGCA    393

EMBOSS_001       601 GAAAACTTGGTGGCCACAGTGGTCCCCACCCACCTGGCTGCTGCTGTGCC    650
                     ||||||||||||||||||||||||||||||||||||||||||||||||||||
EMBOSS_001       394 GAAAACTTGGTGGCCACAGTGGTCCCCACCCACCTGGCTGCTGCTGTGCC    443

EMBOSS_001       651 TGAAGTGGCAGTTTACCTGAAGGAGGCTGTGGGGAACTCCACACGAATTG    700
                     ||||||||||||||||||||||||||||||||||||||||||||||||||||
EMBOSS_001       444 TGAAGTGGCAGTTTACCTGAAGGAGGCTGTGGGGAACTCCACACGAATTG    493

EMBOSS_001       701 ACTATGGCACAGGGCATGAGGCTGCCTTTGCTGCTTTCCTCTGTTGTCTC    750
                     ||||||||||||||||||||||||||||||||||||||||||||||||||||
EMBOSS_001       494 ACTATGGCACAGGGCATGAGGCTGCCTTTGCTGCTTTCCTCTGTTGTCTC    543
```

```
EMBOSS_001       751 TGCAAGATTGGTGTACTCCGGGTGGACGACCAGGTGGCTATTGTCTTCAA    800
                     ||||||||||||||||||||||||||||||||||||||||||||||||||
EMBOSS_001       544 TGCAAGATTGGTGTACTCCGGGTGGACGACCAGGTGGCTATTGTCTTCAA    593

EMBOSS_001       801 GGTGTTTGATAGGTATCTTGAGGTTATGCGGAAGTTGCAGAAGACATACA    850
                     ||||||||||||||||||||||||||||||||||||||||||||||||||
EMBOSS_001       594 GGTGTTTGATAGGTATCTTGAGGTTATGCGGAAGTTGCAGAAGACATACA    643

EMBOSS_001       851 GGATGGAGCCTGCAGGCAGCCAGGGCGTATGGGGTCTGGATGACTTCCAG    900
                     ||||||||||||||||||||||||||||||||||||||||||||||||||
EMBOSS_001       644 GGATGGAGCCTGCAGGCAGCCAGGGCGTATGGGGTCTGGATGACTTCCAG    693

EMBOSS_001       901 TTCCTGCCCTTCATCTGGGGCAGCTCACAGCTCATAGACCACCCCCACCT    950
                     ||||||||||||||||||||||||||||||||||||||||||||||||||
EMBOSS_001       694 TTCCTGCCCTTCATCTGGGGCAGCTCACAGCTCATAGACCACCCCCACCT    743

EMBOSS_001       951 GGAGCCCAGACATTTCGTGGATGAGAAGGCGGTGAGCGAGAACCACAAGG   1000
                     ||||||||||||||||||||||||||||||||||||||||||||||||||
EMBOSS_001       744 GGAGCCCAGACATTTCGTGGATGAGAAGGCGGTGAGCGAGAACCACAAGG    793

EMBOSS_001      1001 ACTACATGTTTCTCCAGTGCATCCTGTTCATCACTGAGATGAAGACTGGC   1050
                     ||||||||||||||||||||||||||||||||||||||||||||||||||
EMBOSS_001       794 ACTACATGTTTCTCCAGTGCATCCTGTTCATCACTGAGATGAAGACTGGC    843

EMBOSS_001      1051 CCCTTTGCGGAACACTCCAACCAGCTGTGGAACATCAGTGCTGTCCCCTC   1100
                     ||||||||||||||||||||||||||||||||||||||||||||||||||
EMBOSS_001       844 CCCTTTGCGGAACACTCCAACCAGCTGTGGAACATCAGTGCTGTCCCCTC    893

EMBOSS_001      1101 CTGGTCTAAAGTGAACCAGGGCCTCATTCGAATGTATAAGGCAGAGTGCC   1150
                     ||||||||||||||||||||||||||||||||||||||||||||||||||
EMBOSS_001       894 CTGGTCTAAAGTGAACCAGGGCCTCATTCGAATGTATAAGGCAGAGTGCC    943

EMBOSS_001      1151 TGGAGAAGTTCCCTGTGATCCAGCACTTCAAGTTCGGGAGCCTGCTGCCC   1200
                     ||||||||||||||||||||||||||||||||||||||||||||||||||
EMBOSS_001       944 TGGAGAAGTTCCCTGTGATCCAGCACTTCAAGTTCGGGAGCCTGCTGCCC    993

EMBOSS_001      1201 ATCCATCCCGTCACATCAGG--------------------CTAGGAGAGG   1230
                     ||||||||||||||||||||                    ||||.|||
EMBOSS_001       994 ATCCATCCCGTCACATCAGGCGCATGCATGTCGATCTTTTCTAGAAGA--    1041

EMBOSS_001      1231 CTGAACTAC------CAGAGCCACCCTGGCCA----GGTTCCTGTGCTCT   1270
                      |...||||      |..|||..||.|||..|    |
EMBOSS_001      1042 -TCTCCTACAATATTCTCAGCTGCCATGGAAAAATCG-------------   1077

EMBOSS_001      1271 CTGTGACCCAGCACCCCTCCCGCCCACCTTCTGTTCTTTCTGTTTGATGA   1320

EMBOSS_001      1078 ---------------------------------------------------   1077

EMBOSS_001      1321 GAGGCTGTTTACTGAGATGGGTGCTAAGCAGGGCCTGAGTTGGGGGAATT   1370 - 3′

EMBOSS_001      1078 ---------------------------------------------------   1077 - 3′
```

6.8. Vector Maps

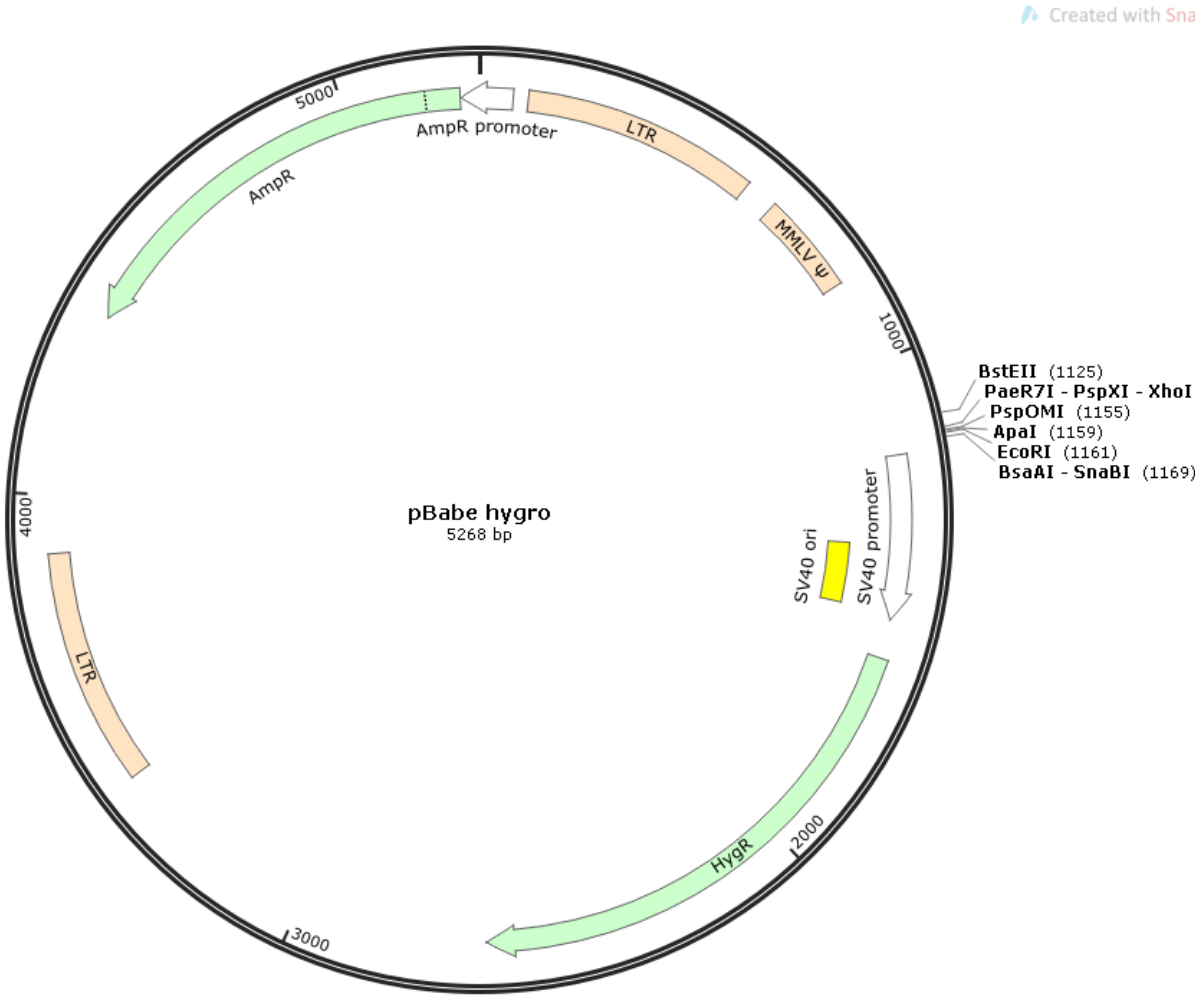

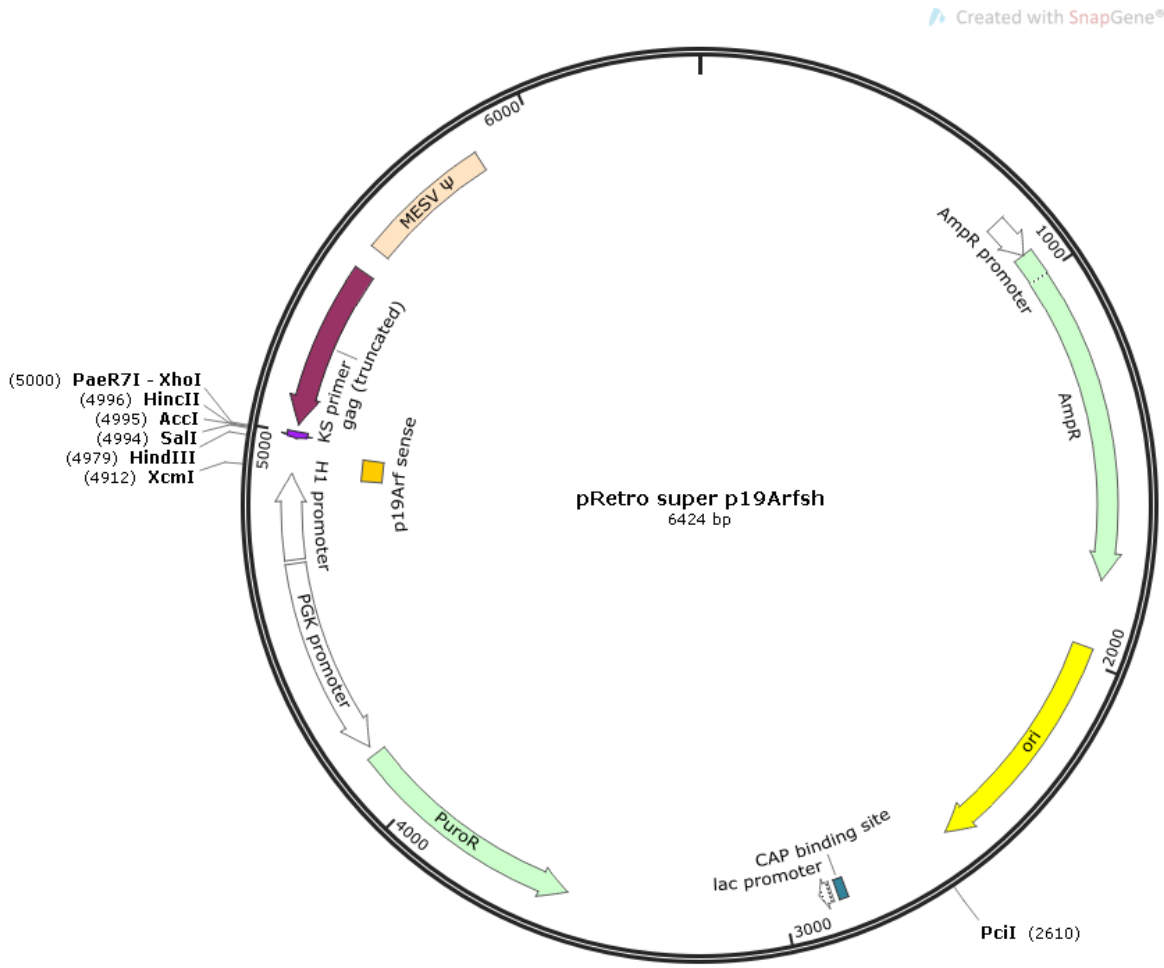

Supplementary Figure 5 Vector map used for immortalization of B6 MEFs. Plasmid carries an ampicillin and puromycin restistance. P19Arfsh (sense) is indicated in organe. Ori = Origin of replication; MESV = murine embryonic stem cell virus (packaging signal). Vector map was created using Snapgene Viewer 4.3.10.

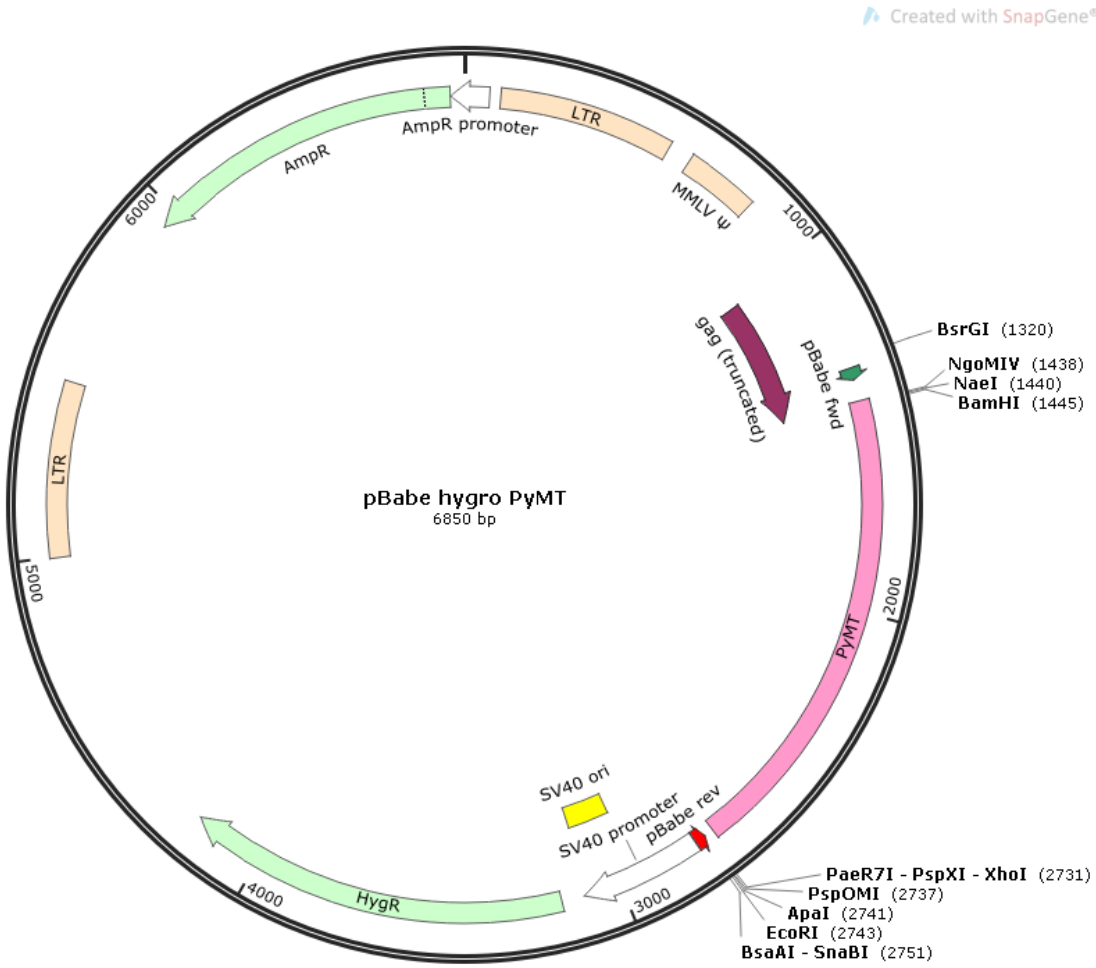

Supplementary Figure 6 Vector Map of pBabe hygro and pBabe hygro carrying PyMT used for transfection of PyMT into B6 cells. Plasmid carries an ampicillin and hygromycin resistance. LTR = long terminal repeat; ori = origin of replication; MMLV = Moloney Murine Leukemia Virus (packaging signal). Vector map was created using Snapgene Viewer 4.3.10.

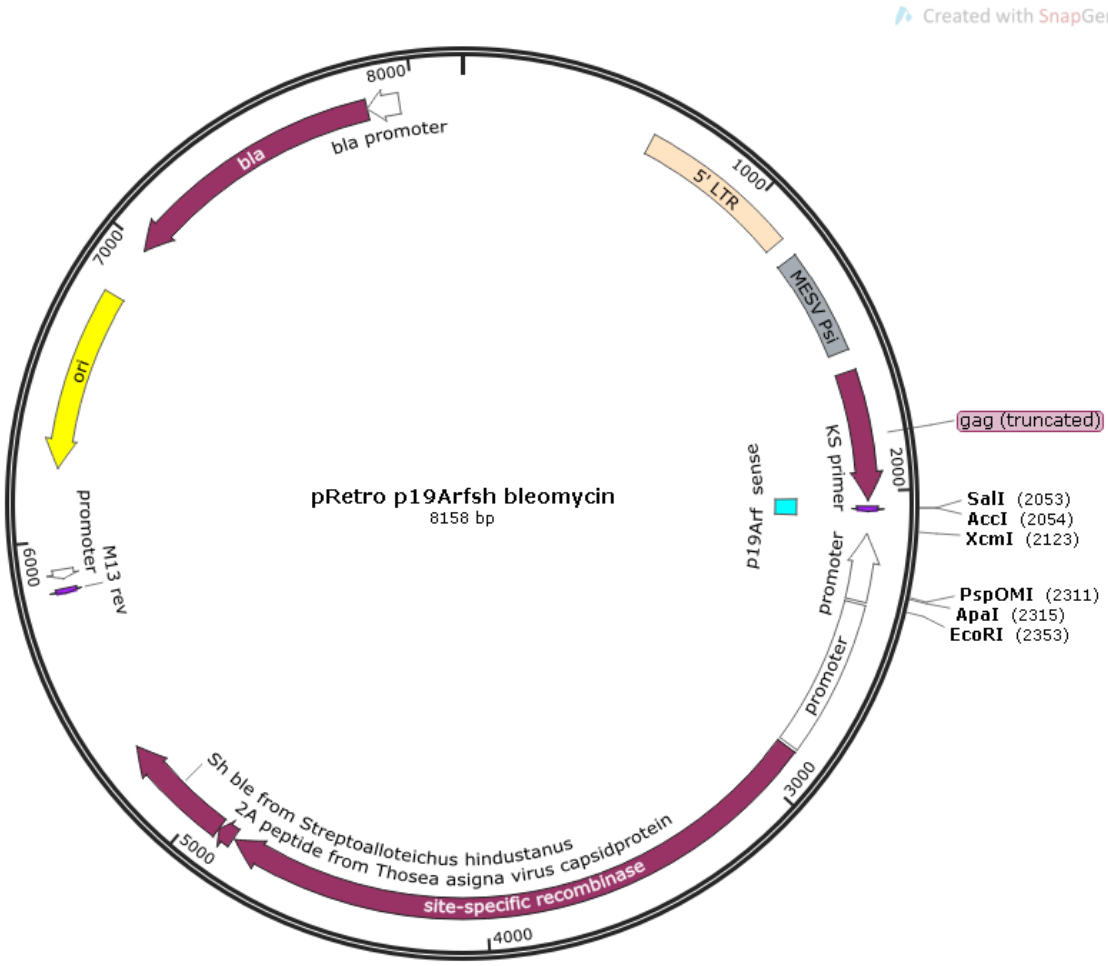

Supplementary Figure 7 Vector map of plasmid used to immortalize (p19Arfsh) 326 # 7 MEFs. Same plasmid carries Cre recombinase fused over a cleavable T2A linker to a bleomycin resistance. bla codes for ampicillin resistance. LTR = long terminal repeat; ori = origin of replication; MESV = murine embryonic stem cell virus (packaging signal). Vector map was created using Snapgene Viewer 4.3.10.

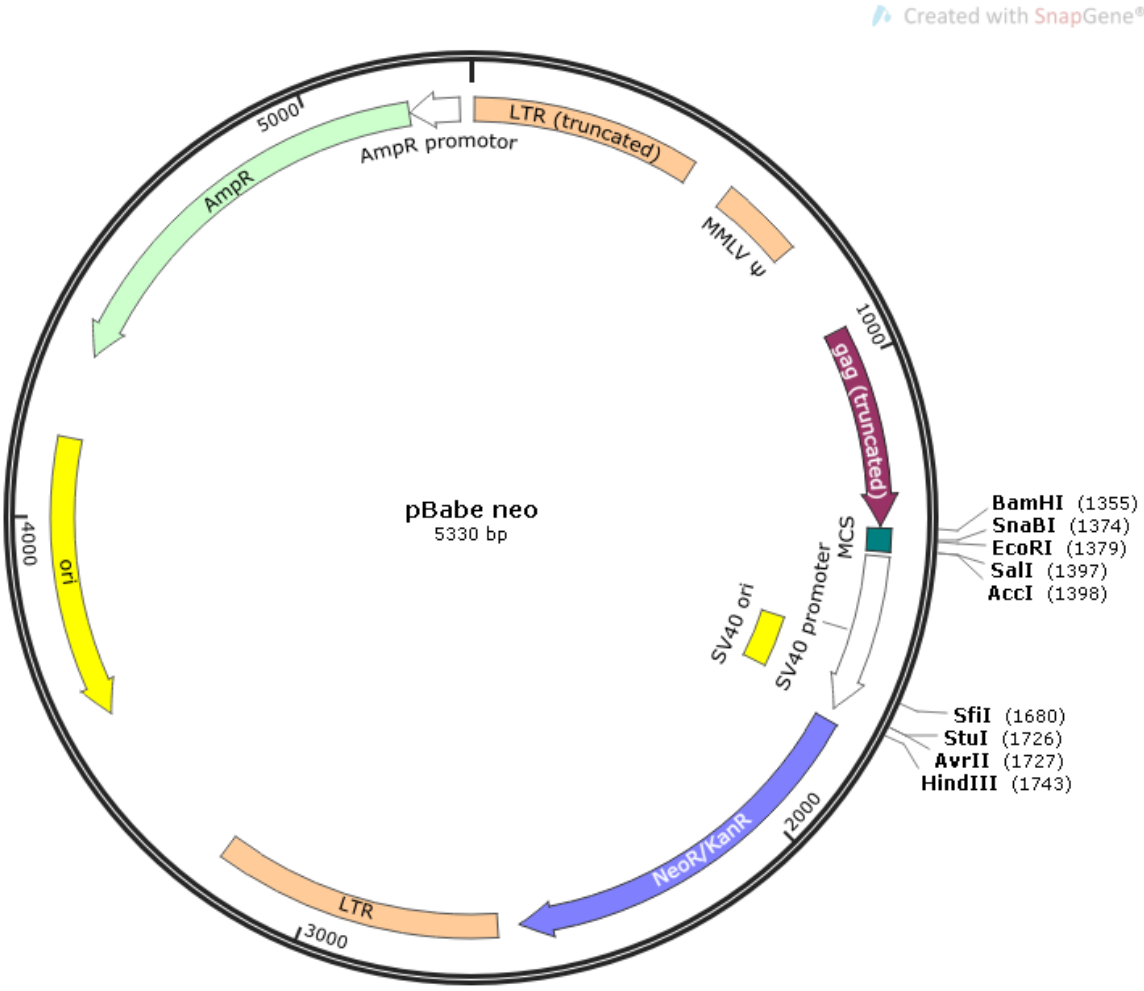
Created with SnapGene®
pBabe neo
5330 bp
5000
AmpR
AmpR promotor
LTR (truncated)
MMLV Ψ
1000
gag (truncated)
MCS
BamHI (1355)
SnaBI (1374)
EcoRI (1379)
SalI (1397)
AccI (1398)
SV40 promoter
SV40 ori
SfiI (1680)
StuI (1726)
AvrII (1727)
HindIII (1743)
2000
NeoR/KanR
LTR
3000
ori
4000

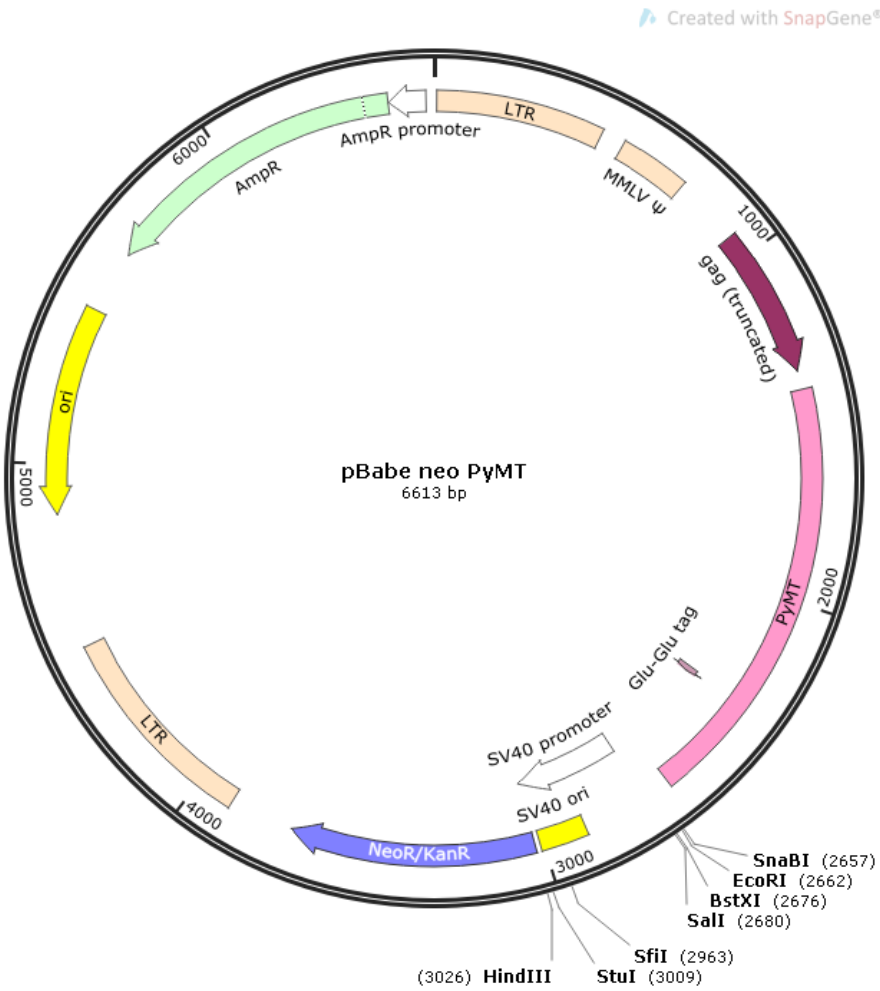

Supplementary Figure 8 Vector Map of pBabe neo and pBabe neo carrying PyMT used for transfection of PyMT into 326 # 7 MEFs. Plasmid carries an ampicillin and neomycin/kanamycin resistance. LTR = long terminal repeat; ori = origin of replication; MMLV = Moloney Murine Leukemia Virus (packaging signal); MCS = multiple cloning site. Vector map was created using Snapgene Viewer 4.3.10.

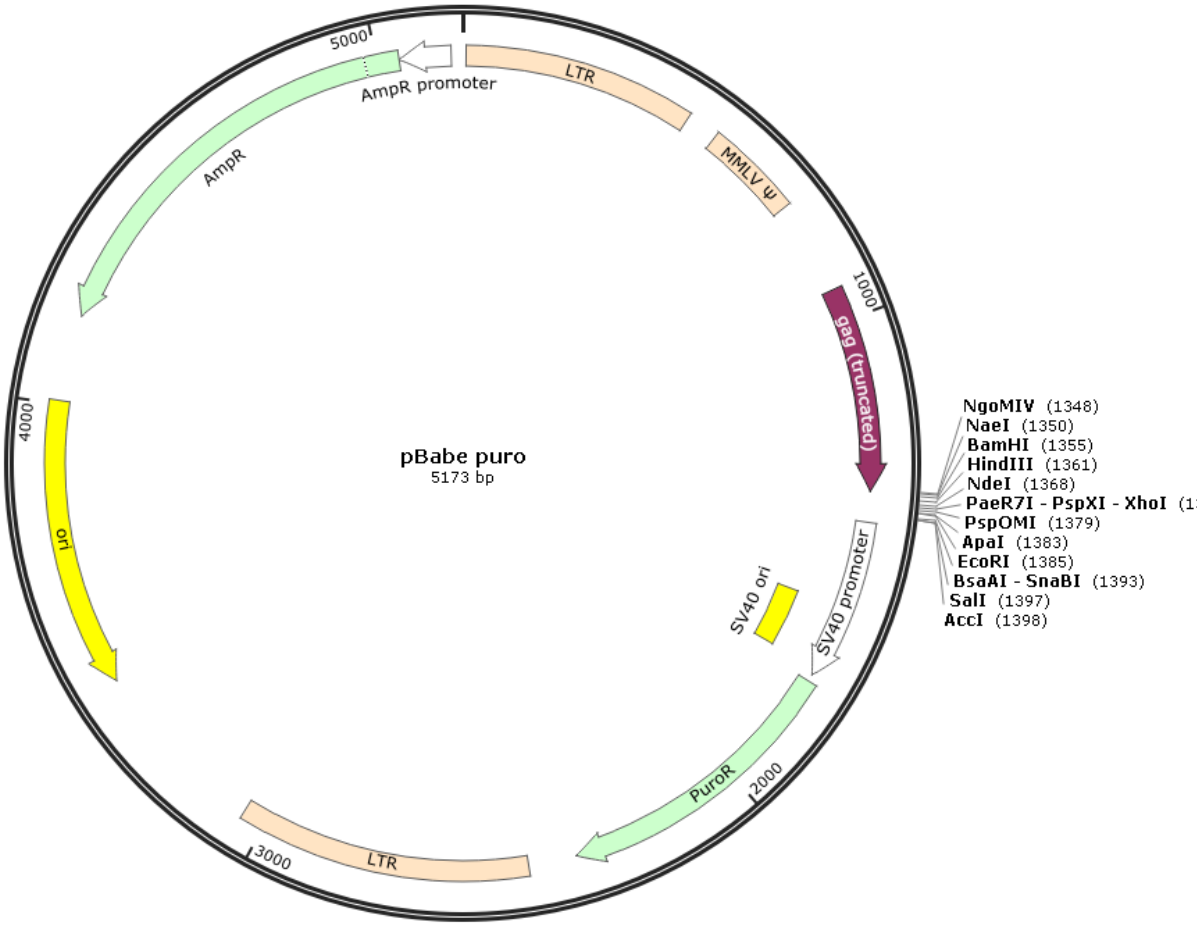

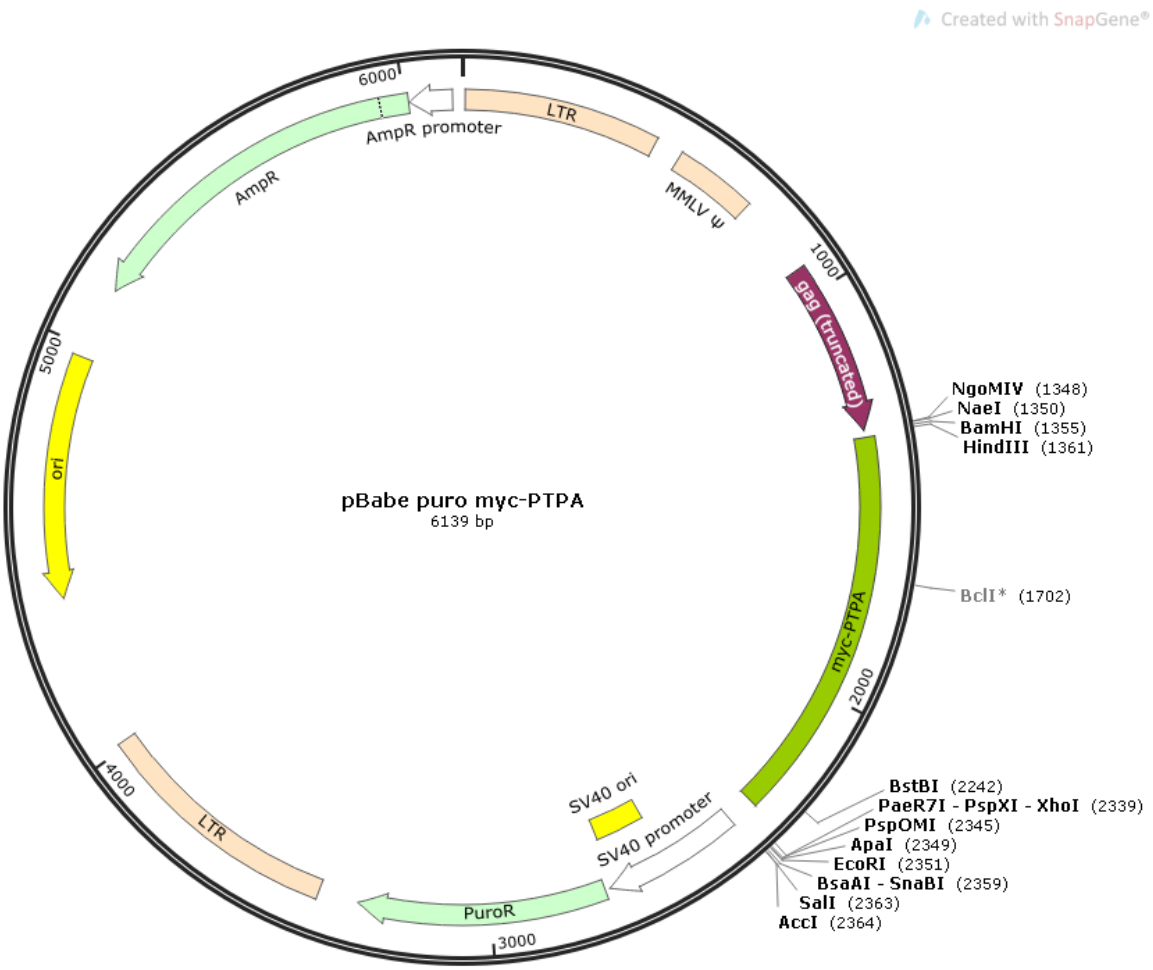

Supplementary Figure 9 Vector Map of pBabe puro and pBabe puro carrying myc-PTPA used for transfection of myc-PTPA into 326 # 7 MEFs and τ2C3C1 neo cells. Plasmid carries an ampicillin and puromycin resistance. LTR = long terminal repeat; ori = origin of replication; MMLV = Moloney Murine Leukemia Virus (packaging signal). Vector map was created using Snapgene Viewer 4.3.10.

.

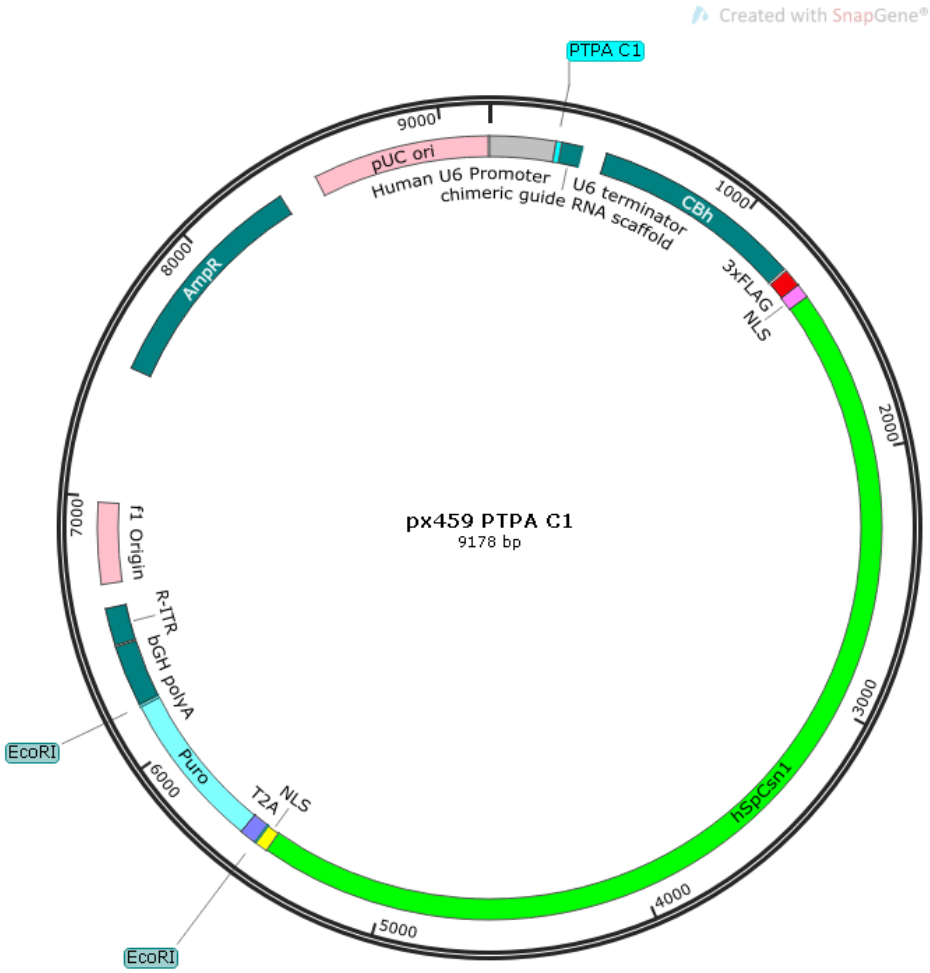
Created with SnapGene®
PTPA C1
9000
pUC ori
Human U6 Promoter
chimeric guide
U6 terminator
RNA scaffold
1000
CBh
3xFLAG
NLS
2000
3000
hSpCsn1
4000
5000
6000
T2A
NLS
Puro
bGH polyA
R-ITR
EcoRI
EcoRI
7000
f1 Origin
8000
AmpR
px459 PTPA C1
9178 bp

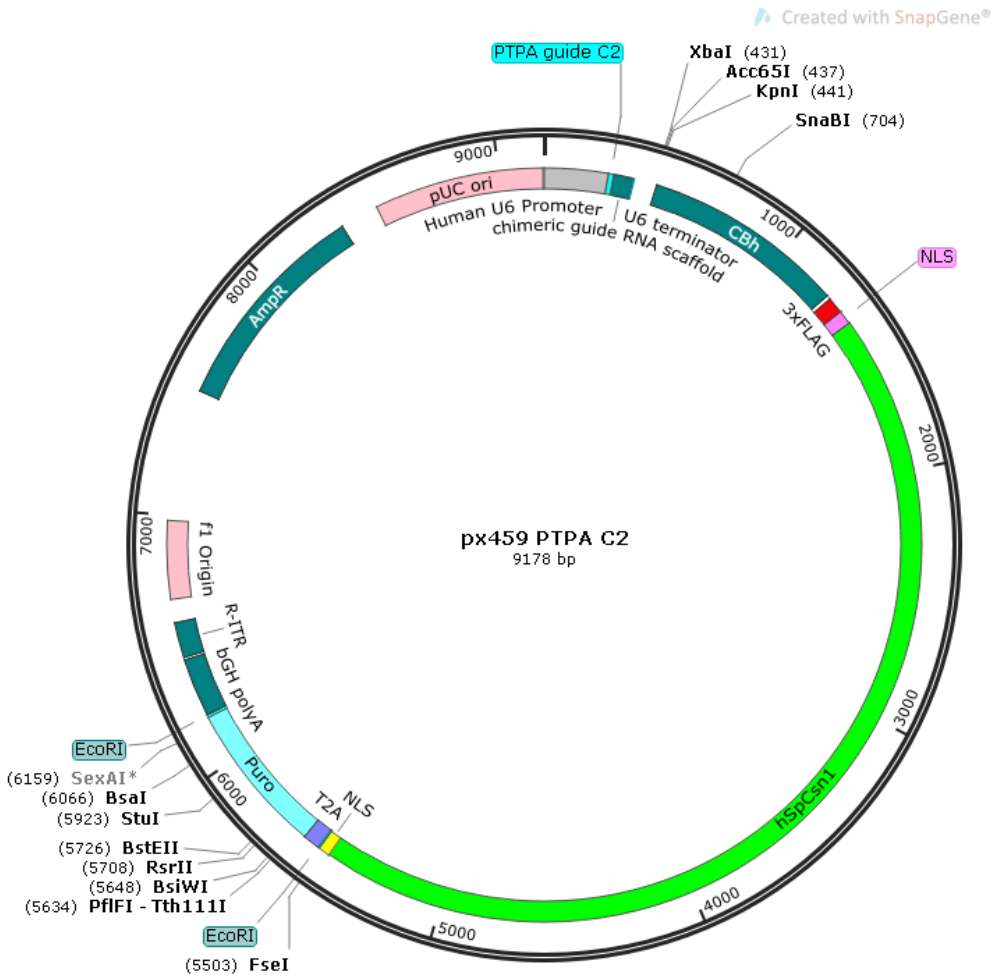

Supplementary Figure 10 Vector maps of plasmids used for CRISPR/Cas9 transfections. CBh is the promotor for Cas9. hspCsn1 codes for Cas9 and is fused to puromycin resistance over a cleavable T2A linker. PTPA guide RNAs are indicated. NLS = nuclear localisation signal; ori = origin of replication. Vector map was created using Snapgene Viewer 4.3.10.